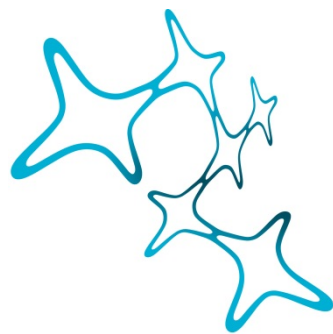


ALS-Associated Mutations in the FUS Nuclear
Localization Signal in Mice Alter the Cytosolic Protein
and RNA Interactome of FUS

Hilary Wunderlich



Graduate School of
Systemic Neurosciences
LMU Munich



Dissertation at the
Graduate School of Systemic Neurosciences
Ludwig-Maximilians-Universität München

May 31st, 2019

This Ph.D. thesis was conducted and written under the supervision of Dr. Dorothee Dormann at the BioMedical Center (BMC) of the Ludwig Maximilians University Munich, Germany, in the time from the 15th June 2015 to the 31st May 2019.

1st examiner and supervisor:
Dorothee Dormann, Ph.D.
Ludwig Maximilians University (LMU) Munich
BioMedical Center (BMC), Department of Cell Biology (Anatomy III)
Großhaderner Str. 9
82152 Planegg-Martinsried
Germany

Dissertation Review Committee:

Dr. Dorothee Dormann
Dr. Stefan Lichtenthaler
Dr. David Housman

Oral Defense Committee:

Dr. Dorothee Dormann
Dr. Stefan Lichtenthaler
Dr. Bettina Schmid
Dr. Wolfgang Wurst

Date of Defense: 23 September 2019

ABBREVIATION INDEX

ALS	Amyotrophic Lateral Sclerosis
CNS	Central Nervous System
FTD	Frontotemporal Dementia
FUS	Fused in Sarcoma (aka TLS)
IP	Immunoprecipitation
KO	Knockout
LC or LCD	Low Complexity (Domain)
MS	Mass spectrometry
NLS	Nuclear Localization Signal
NMJ	Neuromuscular Junction
P-body or PB	Processing Body
RBP	RNA Binding Protein
RGG	Arginine-Glycine-Glycine
RNP	Ribonuclearprotein
RRM	RNA Recognition Motif
SG	Stress Granule
UTR	Untranslated Region

INDEX

ABSTRACT	6
I. INTRODUCTION	8
1. Amyotrophic Lateral Sclerosis and Frontotemporal Dementia	8
1.1 Clinical Presentation and Causes of Amyotrophic Lateral Sclerosis	8
1.2 Clinical Presentation and Causes of Frontotemporal Dementia	9
1.3. Overlap between ALS and FTD	10
1.4 Current Treatments	11
2. RNA Binding Proteins in ALS and FTD	12
2.1 FUS (Fused in Sarcoma) protein	12
3. The Life of an RNA in Neurons	14
3.1. Transcription, Capping and Splicing	14
3.2. mRNP Granules and Low Complexity Domains	15
3.2.1. Stress Granules	17
3.2.2. RNA Transport Granules	19
3.3. The Role of FUS in RNA Processing in Neurons	21
4. FUS-ALS Mouse Models	25
5. Aims of this thesis	27
II. RESULTS	28
1. Establishment of FUS RNP granule isolation from mouse brain	28
1.1. FUS Antibody Testing	29
1.2. Fractionation of mouse cortex into nuclear and cytosolic fraction	33
1.3. Optimization of FUS Immunoprecipitation Procedure	34
1.3.1. Testing different FUS antibodies in immunoprecipitation	34
1.3.2. Optimizing elution from beads	38
1.4. Testing Different Methods to Enrich FUS RNP Granules	40
1.4.1. Density gradient centrifugation	40
1.4.2. Differential centrifugation at 20,000 x g / 100,000 x g	42
2. Test-IP followed by mass spectrometry and RNA-sequencing and further optimization of the workflow	43
3. FUS Immunoprecipitation from FUS^{ANLS/+} vs wild type mouse cortices, followed by Western blot, RNAseq and MS analysis	47
3.1 Western blot analysis	47
3.2. RNA sequencing to identify differential RNAs in FUS ^{ANLS/+} vs wild type FUS RNPs	49
3.2.1 FUS ^{ANLS/+} RNP granules contain reduced <i>Ric3</i> and <i>Chrn2</i> mRNAs, involved in nicotine receptor signaling	51
3.2.2. Alternative splicing in FUS ^{ANLS/+} mouse cortex	52
3.2.2.1 Alternatively spliced transcripts in the cytosolic fraction	52
3.2.2.2 Alternatively Spliced transcripts in the FUS IPs	54
3.3. Changes in the protein composition of FUS-RNPs in FUS^{ANLS/+} mice	59
4. FUS^{ANLS/+} target and interactome validation	62
4.1. Attempts to Establish Primary Neuronal Cultures from FUS ^{ANLS/+} mice	62
4.2 Analyzing candidates from the MS analysis in a FUS WT vs. FUS ^{ANLS} expressing cell line	64
4.2.1 FUS and Septin Interactions	64
4.2.2. FUS 514X and recruitment into stress granules following heat shock	68
4.2.3. Investigation into the interaction between FUS and the Proteasome	71
III. Discussion	73
1. The FUS RNA and Protein Interactome	73
1.1. Conclusions from RNAseq	73

1.1.1. Changes in RNA Expression and Splicing in FUS ^{ΔNLS/+} mice.....	73
1.1.2. Comparison with published RNASeq data from aged Fus ^{ΔNLS} mouse line	74
1.1.3. Involvement of FUS in the nicotinic signaling pathway	76
1.1.4. RNAs that show differential binding to cytosolic Fus ^{ΔNLS/+} vs. FUS-WT	77
1.1.5. Alternative splicing changes in Fus ^{ΔNLS/+} mice cortices.....	77
1.1.6. RNASeq Follow Up.....	79
1.2. Changes in the cytosolic FUS protein interactome in Fus ^{ΔNLS/+} mice	80
1.2.1 Comparison to other interactome studies	81
1.2.2. Overlap with unmethylated FUS interactors	81
1.2.3. Fus and the proteasome.....	83
1.2.4. FUS and the Septins	85
2. Conclusion	86
IV. EXPERIMENTAL PROCEDURES	87
1. Mouse breeding and genotyping.....	87
2. Subcellular Fractionation of Adult Mouse Cortices	88
3. FUS Immunoprecipitation (IP)	88
4. RNAseq library preparation and RNA Sequencing analysis	89
5. Mass spectrometry.....	90
5.1 Sample preparation for mass spectrometry	90
5.2 LC-MS/MS analysis	91
5.3 LC-MS/MS data analysis and label free quantification.....	92
6. SDS-PAGE and Immunoblotting.....	93
7. Optiprep Gradient and High Speed Centrifugation.....	94
8. Cell Culture	95
9. Primary Neuronal Culture.....	95
10. Immunostaining.....	96
11. Fluorescence Microscopy.....	96
12. Antibodies	97
V. REFERENCES.....	98
VI. ACKNOWLEDGEMENTS	113
VIII. DECLARATION OF COPYRIGHT AND CONTRIBUTIONS.....	114

ABSTRACT

Amyotrophic Lateral Sclerosis (ALS) and Frontotemporal Dementia (FTD) are neurodegenerative diseases affecting motor neurons and neurons in the frontal/temporal lobes of the cortex, respectively. A pathological hallmark of both ALS and FTD patients are neuronal and glial proteinaceous inclusions in the affected brain regions. In a subset of patients, these inclusions contain the RNA-binding protein (RBP) Fused in Sarcoma (FUS). Although most cases are sporadic, there are familial cases in which several causal genes have been identified for both diseases. In a subset of ALS patients, several ALS-causing mutations in the *FUS* gene have been identified. Disease-associated *FUS* mutations are found primarily in the nuclear localization signal (NLS) of FUS. NLS mutations impair nuclear import of FUS and hence result in increased cytosolic accumulation of FUS.

As FUS is primarily localized in the nucleus and plays important roles in transcription, alternative splicing, DNA damage repair and miRNA biogenesis, most studies have focused on the nuclear role of FUS. In recent years, a cytoplasmic role for FUS has become more evident, e.g. in the regulation of mRNA stability or mRNA transport. In ALS and FTD patients, FUS is partially lost from the nucleus and found in cytoplasmic aggregates, resulting in loss of the nuclear function of FUS as well as toxic gain-of-function by cytosolic FUS aggregates.

This leads to the question as to the effect of the cytosolic mislocalization of FUS. In order to determine if this mislocalization results in an altered FUS interactome, I aimed to isolate FUS mRNP complexes from a FUS mutant mouse model and identify both RNA and protein interactors. The *Fus*^{ΔNLS/+} mouse model was created by removing the FUS NLS, causing FUS cytoplasmic mislocalization and resulting in an early cortical and a late motor phenotype. Using the cytosolic fraction from the cortices of 50 day old *Fus*^{ΔNLS/+} mice, I performed immunoprecipitation (IP) of FUS followed by mass spectrometry (MS) and RNA sequencing (RNASeq). I identified an altered FUS interactome, both on an RNA

and protein level. Differentially bound RNAs included those whose proteins are involved in transcription, proteasomal activity, nicotinic signaling and RNA binding. I found changes in alternatively spliced mRNAs present in the cytoplasm of these mice, including *Ddhd1* and *Ptpvf1*. This could indicate a nuclear loss-of-function of FUS and hence missplicing of FUS target genes. Differential protein interactors included those important to synapse function and RNA regulation. The altered FUS interactome caused by FUS cytosolic mislocalization may not only result in expression of alternative isoforms, but also perhaps affect RNA stability and localization resulting in impaired neuronal function. This study provides new insights into the pathomechanisms of FUS-associated neurodegeneration.

I. INTRODUCTION

1. Amyotrophic Lateral Sclerosis and Frontotemporal Dementia

Amyotrophic Lateral Sclerosis (ALS) and Frontotemporal Dementia (FTD) are devastating neurodegenerative diseases. Although they affect different brain regions and therefore present with different phenotypes, they overlap both genetically and neuropathologically.

1.1 Clinical Presentation and Causes of Amyotrophic Lateral Sclerosis

ALS involves the degeneration of upper and lower motor neurons responsible for voluntary muscle movements, such as walking, talking and chewing. The upper motor neurons send signals to the lower motor neurons in the spinal cord. These neurons in turn send signals to the appropriate muscle. Without signal from the neurons, the muscle becomes denervated and eventually atrophies. Typical onset occurs between 55-75 years of age, and occurs initially either in the arms or legs (limb onset) or in the mouth (bulbar onset). Symptoms include muscle spasms, weakness, tightness, and spasticity. Muscle atrophy then spreads to the rest of the body. Most people die of respiratory failure within 3-5 years of symptom onset (van Es MD et al. 2017; van Langenhove, van der Zee, and van Broeckhoven 2011; Taylor, Brown, and Cleveland 2016). ALS is typically diagnosed based on a patient's symptoms, medical history and electromyography (EMG).

Approximately 90% of ALS cases are sporadic, the remaining cases are genetic, more than a dozen genes have been identified (Taylor, Brown, and Cleveland 2016). Although some speculation has been made regarding the possible environmental influences, nothing definitive has been found. Mutations in several key genes have been identified. The first gene to be discovered to be associated with ALS was *SOD1* (Rosen et al. 1993). Since then, *ANG*, *VCP*, *TARDBP*, *FUS*, *hnRNPA1*, and *C9orf72* are some among several that have been added to the

growing list (Ghasemi and Brown 2018). The cause of sporadic ALS is unknown, while several genome-wide association studies have identified various associated loci, many were not reproducible (Ajroud-Driss and Siddique 2014). A few genes have been confirmed in a larger cohort to mediate susceptibility and/or modulate survival, such as *UNC13A*, *ELP3* and *ATXN2* (van Blitterswijk et al. 2014; M.-D. Wang et al. 2017).

Several studies have identified problems in RNA processing in ALS, which should not be surprising as a large number of the implicated genes encode for RNA binding proteins, e.g. TDP-43, FUS, hnRNPA1. Additionally post-mortem pathology shows accumulation of TDP-43 and FUS in aggregates (Neumann et al. 2006; Vance et al. 2009; Kwiatkowski et al. 2009). This pathology will be described further in the overlap of FTD and ALS section.

1.2 Clinical Presentation and Causes of Frontotemporal Dementia

Frontotemporal Dementia is the second most common presenile dementia, it occurs 10-15 per 100,000 individuals aged 45-65 (Rademakers, Neumann, and Mackenzie 2012). Mutations are found in approximately 50% of patients with a family history (Ling, Polymenidou, and Cleveland 2013), resulting in degeneration of the frontal, temporal and insular lobes of the cortex. Rather than just one disease, FTD is actually a group of conditions divided into the following categories: Behavioral variant frontotemporal dementia (bvFTD), semantic variant primary progressive aphasia (svPPA), and non-fluent/agrammatic variant primary progressive aphasia (nfvPPA) (Bang, Spina, and Miller 2015). These different forms lead to slightly different behaviors and language symptoms depending on the region of the brain that degenerates.

Initial symptoms generally include a gradual change in behavior, language dysfunction and possibly physical weakness. For example, patients may have increased impulsivity and apathy, as well as loss of sympathy and poor insight. The language dysfunction involved in one of the language variants of FTD results

in difficulty expressing oneself, although the memory is intact (Bang, Spina, and Miller 2015).

Thus far, a handful of genes have been identified to cause FTD: microtubule-associated protein Tau (*MAPT*) (Hutton et al. 1998) and progranulin (*PRGN*) (Baker et al. 2006; Cruts et al. 2006) and *C9ORF72* (Renton et al. 2011; DeJesus-Hernandez et al. 2011). In very rare cases, mutations in *TARDBP* and *FUS* cause FTD (Borrioni et al. 2009; Benajiba et al. 2009).

1.3. Overlap between ALS and FTD

Approximately 15% of FTD or ALS patients reach the criteria for the other disease (Ringholz et al. 2005; Wheaton et al. 2007). FTD and ALS overlap genetically, pathologically and clinically. The hexanucleotide expansion in *C9ORF72* has been found to be a common genetic cause for both ALS and FTD (Renton et al. 2011; DeJesus-Hernandez et al. 2011). Mutations in other genes, such as *UBQLN2* can cause either ALS or FTD (Figure 1).

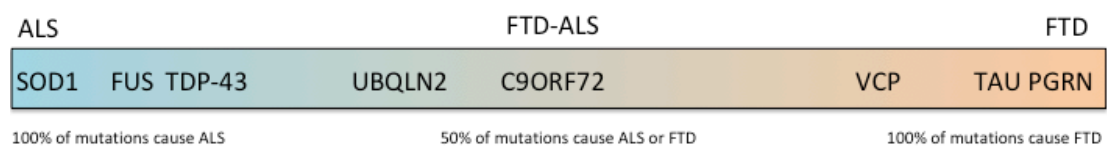


Figure 1. Genetic overlap between ALS and FTD. Mutations in genes such as *SOD1* or *PGRN* only cause ALS or FTD, respectively, while the hexanucleotide repeat expansion in *C9ORF72* can cause either or both ALS and FTD.

The neuropathological presentation of the diseases is also very similar. While usually affecting different parts of the nervous system, both ALS and FTD can contain either TDP-43 or FUS inclusions. These inclusions not only occur in familial cases of ALS and FTD, but also in sporadic (Neumann et al. 2006). In most ALS cases and approximately 50% of FTD cases, TDP-43 loss from the

nucleus occurs and cytosolic aggregates are present, and in rare cases intranuclear aggregates are found (Ling, Polymenidou, and Cleveland 2013). In even rarer cases of ALS, but slightly more often in FTD, FUS is mislocalized and aggregated (Neumann et al. 2009; Kwiatkowski et al. 2009; Vance et al. 2009). Since these RNA-binding proteins are important in multiple steps in RNA metabolism, it is believed that RNA processing errors may play a large role in ALS and FTD pathogenesis. Several groups have shown that mutations in either TDP-43 or FUS result in differential RNA expression. Not only are mRNA levels altered, but alternate splice variants are also produced. Further, complete loss of either TDP-43 or FUS results in dramatic changes to the transcriptome. Additionally, there is some overlap of the affected transcripts between TDP-43 and FUS (Lagier-Tourenne et al. 2012; Polymenidou et al. 2011).

Aside from RNA binding proteins, other classes of genes that have been found to be mutated are those of autophagy and cytoskeleton/transport. Autophagy or proteasome-related genes such as *UBQLN2*, *p62/SQSTM1*, *TBK1*, *VCP* and cytoskeletal genes such as *MAPT* and *TUBA4A* are among the growing list of the genes associated with ALS and/or FTD (reviewed in (Nguyen, van Broeckhoven, and van der Zee 2018)).

1.4 Current Treatments

Currently there is no cure for either ALS or FTD. There are a few drugs for both diseases that slightly slow the progression and alleviate symptoms. Riluzole, a compound that blocks tetrodotoxin-sensitive sodium channels, kainate and NMDA receptors, may increase survival of ALS patients by a few months (Bensimon, Lacomblez, and Meininger 1994). Edaravone, an anti-oxidant, has been shown to improve daily function for individuals with ALS (Takei et al. 2017). At this moment, there is no way to slow the progression of FTD. Most commonly, patients are given antidepressants and antipsychotics. Both treatment approaches may reduce behavioral problems in some patients.

2. RNA Binding Proteins in ALS and FTD

As previously mentioned, several RNA binding proteins (RBPs) have been implicated in the disease pathogenesis of ALS and FTD. Mutations in genes encoding for *TDP-43*, *FUS*, *TAF15*, *EWSR1*, *hnRNPA1*, *hnRNPA2B1* and *TIA1* have all been reported to cause ALS or FTD, while an intermediate expansion in *ATXN2* is associated with an increased risk for ALS. TDP-43 was initially isolated from the inclusions found in the CNS of ALS and FTD patients. ALS-associated mutations in TDP-43 alter axonal morphology and mRNA transport. Expression of mutant TDP-43 in both zebrafish larvae and mice in the CNS results in neuromuscular junction (NMJ) defects and impaired transmission (Arnold et al. 2013; Armstrong and Drapeau 2013). Not only do TDP-43 mutations affect axons, but also dendritic morphology and RNA transport. Expression of mutant TDP-43 in either mouse or rat neurons results in mislocalization of TDP-43 to the cytosol, abnormally small neuritic processes and larger, less mobile, TDP-43 containing granules (Han et al. 2013; Liu-Yesucevitz et al. 2014).

2.1 FUS (Fused in Sarcoma) protein

FUS (also called TLS), a FET protein family member, is a 526 amino acid protein that was originally identified as a proto-oncogene in liposarcomas, as a fusion protein caused by translocation of the prion-like domain of FUS with CHOP (Croizat et al. 1993). FUS is comprised of an N-terminal prion-like low complexity (LC) domain, three RGG domains, an RNA binding (RRM) domain, a zinc finger domain (ZnF) and finally a nuclear localization signal (NLS) (Figure 2).

FUS

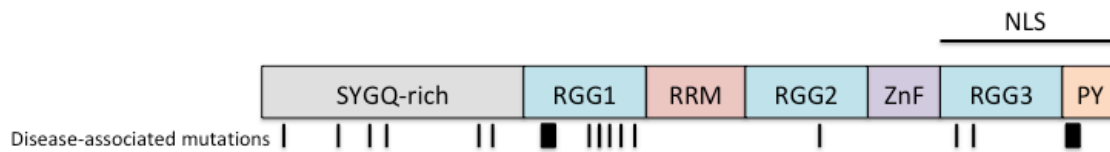


Figure 2. The domain structure and disease-associated mutations of FUS. FUS is made up of an N-terminal LC domain (grey), 3 RGG domains (blue), an RRM domain (red), a ZnF (purple) and a C-terminal PY-NLS (orange). Black lines indicate identified disease-associated mutations.

The low complexity N-terminal domain, comprised primarily of serines, tyrosines, glycines and glutamines, is thought to mediate aggregation (Burke et al. 2015; Murakami et al. 2015; Patel et al. 2015; S. Sun et al. 2015) and acts as a transcriptional activation domain (Rabbitts et al. 1993; Crozat et al. 1993). Mutations in this domain promote liquid-to-solid phase transition and aggregation (Patel et al. 2015). The nucleic acid binding domains, consisting of an RRM, three RGG and a ZnF domain, mediate protein-RNA interactions, as well as protein-protein interactions. Finally, the non-classical proline-tyrosine (PY)-NLS (Lee et al. 2006) plus the RGG3 domain make up the NLS for FUS (Dormann et al. 2012). TNPO1 binds the FUS NLS, mediating import from the cytosol into the nucleus (Lee et al. 2006). Mutations in the NLS decrease TNPO1 binding therefore disrupting nuclear import.

Most of the ALS-associated FUS mutations, such as R521G, R522G, R524S and P525L, occur in the RGG3-PY domain of FUS (Kwiatkowski et al. 2009; Dormann and Haass 2013; Vance et al. 2009), resulting in various degrees of cytosolic mislocalization; the higher degree of cytosolic mislocalization, the quicker the disease progression (Dormann et al. 2010).

3. The Life of an RNA in Neurons

3.1. Transcription, Capping and Splicing

The life of any eukaryotic RNA begins with transcription in the nucleus. As soon as the pre-mRNA emerges from the RNA polymerase, it is modified by several RNA binding proteins. The following modifications occur: capping, splicing, addition of a poly(A) tail and RNA editing. Capping occurs co-transcriptionally and consists of a terminal 7-methylguanosine group; the 5' cap is required for ribosomal recognition and protection against RNAses. Splicing, a process that removes introns and joins exons together, also occurs in the nucleus, either during or directly after transcription. Splicing allows for genes to express different isoforms, which can create different proteins products (or even trigger the resulting RNA for degradation). Several factors regulate RNA splicing, such as FUS. For example, the microtubule-associate protein Tau (MAPT) has six alternative isoforms expressed in the human brain. Alternative splicing of exon 10 results in isoforms with varied amount of microtubule binding repeats. This alternative splicing is thought to lead to tauopathies seen in neurodegeneration and dementia. Although, most alternative splicing is not pathological, but rather is attuned to the cells needs. Depending on cell type or conditions, different isoforms of the same protein may be required. For example, the alternative splicing of the extracellular domain of the AMPA receptors yields to variants, known as flip and flop (Pei et al. 2009). In the case of GluR2, the flop variant desensitizes faster than the flip variant, the two variants also display different kinetics. In this case, the different isoforms tailor synaptic response.

An additional RNA editing variable, more specific to neurons, is 3' UTR length and composition. Neuronal mRNAs frequently possess multiple 3' UTR isoforms, this allows transcripts' localization and stability to be more highly regulated. Transcripts with a tendency to be localized, such as those encoding for synaptic or neuritic proteins, tend to have a longer 3' UTR (Tushev et al. 2018).

3.2. mRNP Granules and Low Complexity Domains

Messenger ribonucleoprotein particles (mRNPs) are defined as a complex of RNA binding proteins (RBPs) and mRNAs. Many mRNP components are added co-transcriptionally and aid in mRNA splicing (Moore and Proudfoot 2009). As the mRNP exits the nucleus, some components are removed while others, such as FUS, may remain associated into the cytoplasm. Once in the cytoplasm, the mRNPs may undergo further restructuring. The addition and removal of various mRNP components determines the localization, stability and translation of the RNA. Some mRNPs need to be delivered to particular subcellular regions, such as axons and dendrites, for local translation (Doyle and Kiebler 2011). In order to achieve this, particular components are necessary and the RNA must be maintained in a translationally-repressed state. These translationally-inactive RNPs are able to assemble into larger structures, called mRNP granules. Examples of mRNP granules include: 1) processing bodies (P-bodies; PB), 2) stress granules (SGs), 3) P granules in germ cells, and finally 4) RNA transport granules in neurons, also called RNA granules.

While all of these granule types are distinct, they have several things in common. First, they transiently store silenced mRNA for transport or storage (Erickson and Lykke-Andersen 2011; Mitchell and Parker 2014). Second, they are dynamic entities that interact with each other (Kedersha et al. 2005; Buchan, Muhlrad, and Parker 2008). This interaction allows for exchange of some components, such as G3BP. G3BP is a key component of stress granules but is also found in neuronal transport granules (Atlas et al. 2004). Additionally, several RNA transport granule components, such as Staufen and Pumilio 2, in response to cellular stress, can be found in dendritic SGs (Thomas et al. 2005; Vessey et al. 2006). These observations suggest that each granule type is not separate, but rather part of a continuum (Buchan and Parker 2009).

An additional and important similarity between different mRNP granules is the manner in which they are assembled. All translationally-silenced mRNP granules form by liquid-liquid demixing or liquid phase separation (LLPS) (Weber and

Brangwynne 2012). mRNP granules behave like condensed liquid phases and show droplet-like attributes, they flow when in a streaming fluid and fuse with one another to form larger droplets/granules (Patel et al. 2015; Shin and Brangwynne 2017) giving them their dynamic behavior. The weak interactions between low complexity domains (LCDs) drive liquid-liquid demixing and therefore formation of mRNP granules (Holehouse and Pappu 2015; Shin and Brangwynne 2017). LC domains are naturally disordered, have low amino acid diversity, and often contain repetitive sequences (J. Wang et al. 2018; Tompa et al. 2014). TIA-1, as essential component of SG assembly, was the first protein containing an LC domain demonstrated to be vital for mRNP granule assembly (Gilks et al. 2004).

LLPS and aggregation of FUS are likely largely driven by the N-terminal SYGQ-rich domain and occurs in a concentration dependent manner (Burke et al. 2015; Kato et al. 2012; Murakami et al. 2015; Patel et al. 2015; Z. Sun et al. 2011). Disease-associated mutations in FUS accelerate the transition between liquid and solid state (Patel et al. 2015). Additionally, it has been shown that the C-terminal RGG3-PY domain and the arginines are integral for phase separation (Hofweber et al. 2018). As formation of these solid state aggregates are dependent on concentration, it is easy to see how a mutation in the NLS, causing increased amounts of cytosolic FUS, would promote aggregation and aberrant interactions.

Studies have shown that LC domains are particularly abundant in RBPs linked to protein aggregation diseases, especially in FTD and ALS (J. Wang et al. 2018). FUS and other LC domain containing RBPs undergo a concentration-dependent LLPS, and form liquid-like protein droplets. Over time FUS and other RBP droplets undergo a liquid-to-solid-phase transition resulting in the formation of solid condensates (Molliex et al. 2015; Patel et al. 2015; Lin et al. 2015). These solid condensates are much less dynamic and inhibit exchange of components, thus promoting aggregation.

3.2.1. Stress Granules

Stress granules are present in the cytoplasm, they are composed of poly (A) RNA and RNA binding proteins. SGs form in response to stress, in order to protect the cell; they sequester non-essential RNAs, allowing stress-protective RNAs (such as heat shock proteins) to be preferentially translated (Buchan, Capaldi, and Parker 2012). SGs can also recruit proteins, such as those involved in apoptosis (thereby preventing cell death) and mTORC1, protecting the cells from DNA damage (Takahara and Maeda 2012). Core SG components include the 48S pre-initiation complex, PABP-1, TIAR and G3BP (Kedersha et al. 2005; Anderson and Kedersha 2006). The latter three proteins promote SG assembly and serve as common SG markers. Under acute stress, elongating ribosomes run off the mRNA and SG nucleation begins by the recruitment of proteins such as TIAR and G3BP thus promoting the aggregation of mRNPs (Anderson and Kedersha 2008). During recovery from stress, the SG proteins dissociate, allowing progression of translation.

Several ALS/FTD-associated RBPs are recruited to SGs (e.g. TDP-43, FUS, EWS, TAF15, ATXN2, hnRNP A/B family) and some of them have been shown to regulate SG dynamics (Aulas et al. 2015). Two of the most well-studied RBPs are TDP-43 and FUS. FUS knockdown or overexpression does not affect SG formation, however TDP-43 directly regulates G3BP levels (Aulas, Stabile, and Vande Velde 2012; Aulas et al. 2015; Blechingberg et al. 2012), therefore affecting SG-PB interactions. Under most stress conditions, only small amounts of TDP-43 and FUS can be found in SGs, however, the hyperosmolar stressor sorbitol induces a large cytosolic distribution and SG localization of both wild type TDP-43 and FUS (Meyerowitz et al. 2011; Sama et al. 2013; Walker et al. 2013). Point mutations located in the NLS leading to cytosolic mislocalization of both TDP-43 and FUS strongly increase SG association (Dormann et al. 2010; Bentmann et al. 2012) and were found to affect the binding of other SG-associated proteins such as TIA-1 and G3BP resulting in an increased number and size of SGs (Baron et al. 2013; Vance et al. 2013). These observations suggest that disease-associated mutations in the NLS of FUS cause aberrant protein

interactions, possibly recruiting additional proteins into SGs, resulting in altered SG size and dynamics.

High local concentrations of RBPs, such as FUS, in the cytoplasm, may cause liquid-to-solid phase transition resulting in SG solidification, therefore forming irreversible, non-dynamic aggregates over time (Figure 3). Evidence supporting this has been shown by the colocalization of SG markers with pathological FUS inclusions in FTD and ALS patients (Fujita et al. 2008; Bäumer et al. 2010; Dormann et al. 2010). FUS proteinopathies are not the only examples of pathological SGs: full-length TDP-43 inclusions were also shown to co-localize with the SG marker PABP-1 (Bentmann et al. 2012; Liu-Yesucevitz et al. 2010). Additionally, FTD-Tau and Alzheimer's patients show co-localization of SG markers and Tau aggregates (Vanderweyde et al. 2012).

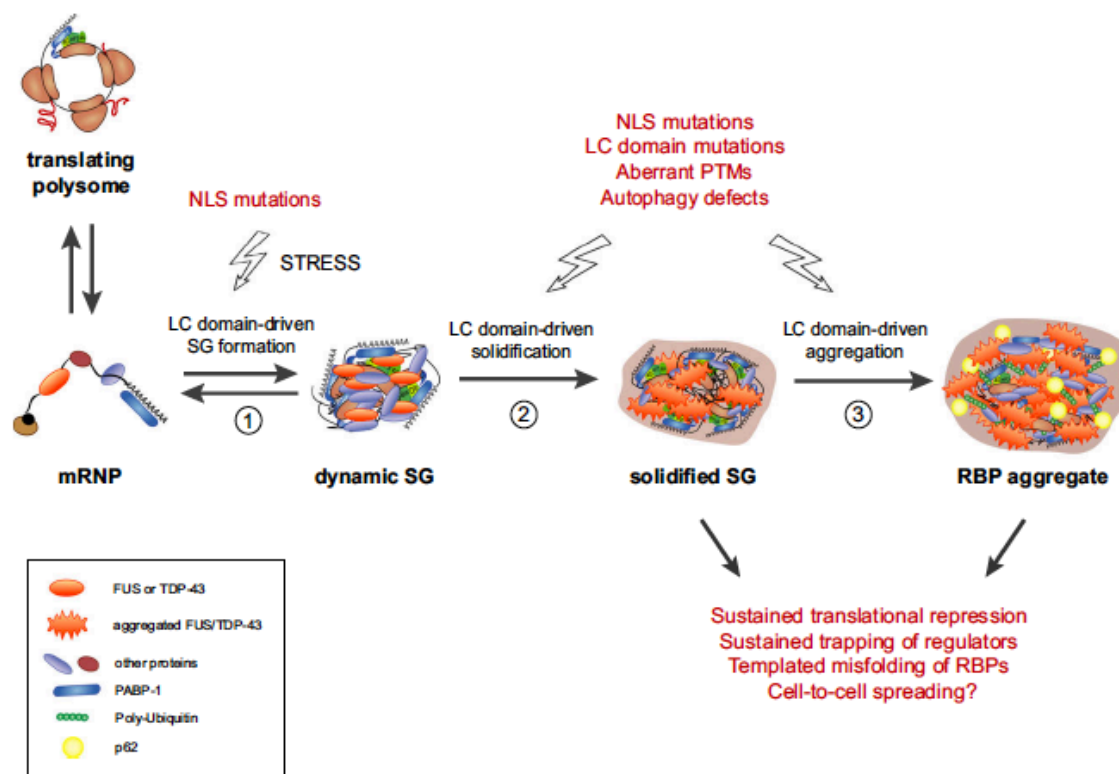


Figure 3: LC domain driven stress granule formation and pathological aggregate formation (adapted from (Bowden and Dormann 2016)). In response to cellular stress, mRNA translation is paused and transcripts and inactive mRNPs are transiently sequestered (step 1). The LC domains of some RBPs, such as G3BP and TIA1 drive this formation. FUS may be sequestered via its mRNA targets. Solidified SGs may be formed by LC domain driven pathological liquid-to-solid phase transition, triggered by disease-associated mutations or post-translational modifications (PTMs) (step 2). Finally, this may lead to development of irreversible RBP aggregates (step 3), which may promote neurodegeneration by sustained translational repression and/or trapping of RBPs. Wiley-Blackwell holds the copyright (2016) for this article published in Journal of Neurochemistry and permits the usage of figures in this dissertation.

3.2.2. RNA Transport Granules

Neurons are polarized cells, extending from the cell body are axons and dendrites. Largely, the proteins present in the axon and dendrites are synthesized in the cell body and transported into the neurites (Kennedy and Ehlers 2006). Local protein synthesis can also be triggered to take place along the axon or dendrites, away from the cell body (Hengst and Jaffrey 2007; Doyle

and Kiebler 2011). In order for local protein synthesis to occur, translationally silenced mRNAs must be transported via RNA transport granules into axons and dendrites. In response to particular signals, the mRNAs can be released from their translationally inactive state and then translated into protein. Local protein synthesis allows the neuron to amplify specific signaling pathways quickly and acutely in a location-specific manner. mRNA transport and local translation has been visualized for several transcripts in vitro in live neurons, some of the first transcripts imaged were beta-actin mRNA bound by ZBP1 (Buxbaum, Wu, and Singer 2014; H. Y. Park et al. 2014).

Neuronal RNA granules have been extensively purified and studied. The first indication that the bound mRNAs are in a translationally inactive state came from a cell fractionation followed by sucrose gradient from cultured rat neurons. The authors found that while the granules were enriched in ribosomes and Staufen, they lacked eIF4E, eIF4G and tRNAs (Krichevsky and Kosik 2001). A few years later, Kanai and colleagues isolated a large detergent-resistant, RNase-sensitive granule from mouse brain found to bind mouse kinesin (KIF5). Most of the major protein components were found to be RBPs: Pur-alpha, hnRNP-U, PSF/Splicing factor proline/glutamine-rich (SFPQ) and Staufen 1, all of which are vital for CamKIIalpha mRNA dendritic localization. FUS was also identified as a major component of neuronal RNA granules (Kanai, Dohmae, and Hirokawa 2004).

mRNA localization and translation play an essential role in axonal path finding in the developing nervous system. Axons are guided to their final destination through the plasticity of their growth cones enabled by local protein synthesis (Hengst and Jaffrey 2007). Local translation in axons seems to be primarily occurring in developing axons, however nerve injury or neurodegeneration results in the reappearance of machinery necessary for local translation (Baleriola et al. 2015). This may also occur in FTD/ALS patients, as both TDP-43 and FUS have been identified at pre-synaptic sites of axon terminals in neurons (Narayanan et al. 2013; Schoen et al. 2015).

In the mature CNS, local translation is important in dendritic spines. Upon neuronal stimulation, dendritic spines can be removed, morphologically altered or new spines can appear (Lang et al. 2004). Activity-induced local protein synthesis at synapses contributes to these changes and is crucial for synaptic plasticity, the cellular basis for learning and memory (Doyle and Kiebler 2011; Puthanveetil et al. 2008). Local translation begins with the binding of RBPs to cis-acting localization elements, usually located in the 3'UTR (Doyle and Kiebler 2011). Largely occurring in the nucleus, RBPs come into contact with the native transcripts and mRNPs are assembled. The mRNP is then exported from the nucleus to the cytoplasm, where additional RBPs, such as Staufen, can bind and remodel them. These mRNPs, in a translationally repressed state, are then assembled into larger granules, known as RNA transport granules (Kiebler and Bassell 2006; Mitchell and Parker 2014). Subsequently, molecular motors, such as kinesins, are recruited to the granules and transport them along microtubules to their final destination (Hirokawa 2006). RNA transport granules are then anchored at or near synapses or they cruise back and forth within dendrites awaiting a signal (Bramham and Wells 2007; Doyle and Kiebler 2011). In the final step, upon synaptic activation, mRNPs are recruited into dendritic spines via actin filaments or microtubules (Yoshimura et al. 2006; Jaworski et al. 2009). The transcripts are then released from the mRNPs for translation to occur (Hüttelmaier et al. 2005). The mechanism by which these mRNAs are released is not yet completely understood. Post-translational modification of RBPs (Ostareck-Lederer et al. 2002; Hüttelmaier et al. 2005) or a prion-like switch in protein conformation, as what occurs with CPEB and its *Drosophila* homolog Orb2 (Si et al. 2010; Khan et al. 2015), are two possible explanations as to the mechanism.

3.3. The Role of FUS in RNA Processing in Neurons

FUS is a primarily nuclear protein, where it tends to bind long introns and regulate splicing (Polymenidou et al. 2011; Ishigaki et al. 2012; Lagier-Tourenne et al. 2012; Rogelj et al. 2012; Zhou et al. 2013) as well as regulate transcription by binding to promoters (Tan et al. 2012; Yang et al. 2014). Due to its largely

nuclear presence, its cytosolic roles have been poorly studied until more recently. Using super-resolution microscopy, Schoen and colleagues recently found that FUS is also present in axon terminals of mature hippocampal neurons, very closely localized to synaptophysin, a pre-synaptic vesicle protein, and adjacent to the active zone protein, Bassoon (Schoen et al. 2015). Although these findings are still preliminary, they imply that FUS may play more of a role in axons than previously thought, and that further investigation of this important issue is warranted.

Even more evidence suggests there is a vital role for FUS in dendrites. FUS has been identified in somatic and dendritic punctae (Belly et al. 2005; Fujii et al. 2005). In both human and mice, FUS-positive neuropil granules have been identified in MAP2-positive dendrites in the cortex, brainstem and spinal cord (Aoki et al. 2012). Upon synaptosomal fractionation FUS can be detected mostly in the post-synaptic density (PSD) fraction. In hippocampal neurons, FUS is found in dendrites and occasionally in PSD95-positive dendritic spines (Belly et al. 2005; Fujii et al. 2005). These FUS-positive dendritic granules show bidirectional movement, but within spines become stationary. This movement can be abolished with actin or microtubule destabilizing compounds (Fujii 2005). The kinesin, KIF5, a microtubule motor protein, binds directly to FUS-containing granules and transports them along microtubules (Kanai, Dohmae, and Hirokawa 2004). Myosin-Va, an actin based motor protein delivers FUS further into the dendritic spines (Yoshimura et al. 2006).

There is mounting evidence that neuronal stimulation recruits FUS into dendritic spines. Treatment of mouse hippocampal neurons with 3,5-dihydroxyphenylglycine (DHPG), a group I mGluR agonist, causes FUS-positive granules in dendrites and dendritic spines to increase, while other post-synaptic proteins (PSD95, Homer-1c and Shank) remain unchanged (Fujii et al. 2005). Using a combination of a chemically-induced long-term potentiation (cLTP) protocol combined with BDNF to stimulate rat cortical neurons led to an increase in several RBPs, including FUS, in the postsynaptic densities (Zhang, Neubert, and Jordan 2012). Additionally, FUS has been found to be associated

with N-methyl-D-aspartate (NMDA) receptor complexes isolated from mouse brain (Husi et al. 2000).

FUS is a known RNA binding protein, it is present in neurites and responds to dendritic stimulation. But what about its RNA targets in neurons? The Takumi lab has shown that *Nd1-L* mRNA, which encodes for an actin stabilizing protein, co-immunoprecipitates with FUS. In neurons treated with DHPG, there is an increase in β -actin and *Nd1-L* mRNA in dendrites. This activity-dependent recruitment of *Nd1-L* mRNA into dendrites is lost in FUS knockout mice and further rescued upon re-expression of FUS. Primary cortical neurons from FUS knockout mice not only have a decrease in the number of spines, but also decrease in the ratio of mature to immature spines. This dendritic spine abnormality can be rescued by over-expression of *Nd1-L*. Thus, one manner in which FUS may regulate spine morphology and synaptic transmission is through the delivery of *Nd1-L* mRNA to synapses (Fujii 2005). Furthermore, a dominant negative mutant or knockdown of myosin Va inhibits activity-dependent FUS relocalization, demonstrating this relocalization is mediated by the actin cytoskeleton (Yoshimura et al. 2006).

Not only has FUS been shown to mediate RNA transport, but it has also been shown to stabilize some of its mRNA targets. Examples of such are *GluA1*, a glutamate receptor, and *SynGAP* α 2, a protein essential for spine maturation (Udagawa et al. 2015; Yokoi et al. 2017). *GluA1* mRNA encodes for a subunit of alpha amino-3-hydroxy-5-methylisoxazole-4-propionate (AMPA) receptors and is vital for spine maturation and synaptic transmission. FUS binds the *GluA1* 3' UTR and, by controlling poly(A)-tail length, FUS regulates its stability in the cytosol. Knockdown of FUS, by introduction of FUS shRNA in the mature mouse hippocampus *in vivo*, results in a decrease in mature spines and an increase in filopodia-like spines. This causes a change in synaptic transmission of hippocampal neurons and FTD-like behavioral abnormalities, including disinhibition, hyperactivity and social interaction defect. These cellular and behavioral defects can partially be attributed to down-regulation of *GluA1* mRNA and protein levels resulting from the knockdown of FUS. Re-expression of

GluA1, in the context of a FUS knockdown, rescues synaptic transmission, spine maturation defects and some of the behavioral abnormalities (Udagawa et al. 2015).

Synaptic Ras GTPase-activating protein 1 (SynGAP1) is a Ras activating protein critical for cognition and synapse function, localizing to the PSD, it negatively regulates the Ras/Rap pathway (Kim et al. 1998; Carlisle et al. 2008; Jeyabalan and Clement 2016) and has previously been shown to be associated with autism spectrum disorders and epilepsy (Mignot et al. 2016). Heterozygous knockout of SynGAP in mice causes an increase in the number of mature spines (Kim et al. 2003; Clement et al. 2012; C.-C. Wang, Held, and Hall 2013). However, it is important to note that there are several isoforms of SynGAP with opposing effects on synaptic transmission. For example, SynGAP α 1 overexpression decreases mEPSC amplitude, whereas SynGAP α 2 overexpression increases mEPSC amplitude (McMahon et al. 2012). The inclusion of exon 19 in the α 1 isoform causes a frameshift mutation resulting not only in a shorter protein product than that of α 2, but also a longer 3'UTR in α 2. It is this longer 3'UTR of SynGAP α 2 that has been shown to be bound by FUS. In conjunction with ELAVL4, FUS mediates stable *SynGAP* α 2 mRNA expression, in the absence of FUS, ELAVL1 binds and *SynGAP* α 2 mRNA is destabilized and degraded. FUS knockout mice have decreased levels of SynGAP α 2 and supplementation of SynGAP α 2 ameliorates the behavioral abnormalities seen in FUS knockout mice (Yokoi et al. 2017).

Thus, some of the identified mRNA targets of FUS, such as Nd1-L, GluA1 and SynGAP α 2, are all major players in dendritic spine dynamics. Therefore alteration of FUS levels, either by knockdown or overexpression can affect spine morphology and synaptic transmission. A summary of its role in neurons can be seen in Figure 4 (Bowden and Dormann 2016).

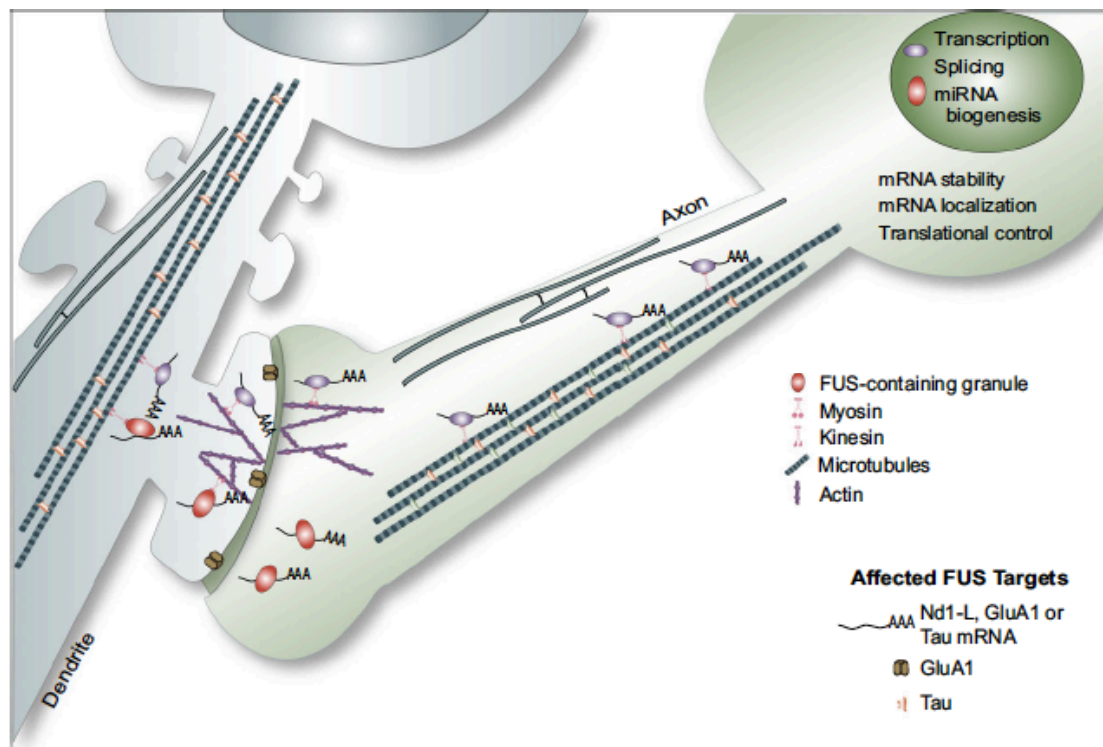


Figure 4: The physiological role of FUS in neuritic mRNA metabolism (modified from (Bowden and Dormann 2016))¹¹. FUS regulates splicing of *Tau* mRNA and transports the mRNA of *Nd1-L* into dendrites. FUS also regulates the stability of *GluA1* mRNA. Impaired synaptic function may occur upon misregulation of these targets. Wiley-Blackwell holds the copyright (2016) for this article published in Journal of Neurochemistry and permits the usage of figures in this dissertation.

4. FUS-ALS Mouse Models

ALS-associated FUS mutations, resulting in higher concentrations of FUS in the cytosol (Dormann and Haass 2013), also cause aberrant dendritic morphology and changes in local protein synthesis in dendrites. Several mouse models have been created and demonstrate this aberrant local proteome, spine morphology and synaptic transmission. Transgenic mice expressing human FUS-R521G show reduced dendritic arbors and mature spines compared to non-transgenic or FUS-WT mice (Sephton et al. 2014).

More recently, the Shneider lab created three mouse lines expressing human FUS: wild type, R521C and P525L from the *MAPT* locus. Although the mRNA levels are equal, mutant FUS protein is expressed at higher levels than FUS wild

type in the brain and spinal cords of the mice. FUS was found to be cytosolically mislocalized and all Tau-expressing cells underwent progressive degeneration. Both mutant lines also experienced progressive and early degeneration of neuromuscular junctions (NMJs.) Postnatal knockout of endogenous FUS from motor neurons confirmed that it was not simply loss of function that resulted in motor degeneration (Sharma et al. 2016).

In 2017, the Fisher lab created the FUSDelta14 mouse model in which they introduced a human frameshift mutation in the mouse FUS locus. This frameshift mutation causes the skipping of exon 14 and out of frame translation of exon 15. Heterozygous FUSDelta14 mice were found to have diffuse nuclear and cytosolic FUS staining (without complete depletion of FUS from the nucleus), RNA expression changes, progressive motor, NMJ and motor neuron degeneration (Devoy et al. 2017).

The Dupuis lab created the mouse model utilized for these studies. A mutant FUS mouse line, Fus^{ANLS} , was made by removing the NLS from endogenous FUS. Using homologous recombination, they inserted a floxed stop cassette following exon 14, preventing transcription of the NLS-encoding exon 15 (Scekic-Zahirovic et al. 2016). The Fus^{ANLS} mice show a dramatic relocalization of FUS from the nucleus to the cytosol, resulting in RNA expression changes, motor neuron loss, as well as aberrant protein localization. Mice homozygous for Fus^{ANLS} die upon birth due to respiratory insufficiency. Heterozygous ($Fus^{ANLS/+}$) mice demonstrate hyperactive behavior around 1-2 months of age, further behavioral defects (primarily in social interaction) are evident around 4 months of age. $Fus^{ANLS/+}$ mice do not show an overt motor phenotype until approximately 10 months of age, which is accompanied by brain atrophy. By 22 months, the motor deficit is more pronounced as observed in tasks such as the inverted grid and catwalk. Electromyography and ChAT immunohistochemistry reveal denervation of NMJs and degeneration of motor neurons. The $Fus^{ANLS/+}$ mice seem to recapitulate early stages of ALS, although they do not have cytosolic FUS or p62 inclusions, but they do have significant ubiquitin pathology. The resulting molecular and behavioral phenotype appears to be a result of a gain of cytosolic function of FUS,

rather than a loss of nuclear function of FUS. Reversal of the $Fus^{\Delta NLS}$ mutation (by expression of Cre recombinase) in motor neurons prevents motor neuron degeneration and delays motor deficits, implying both a cell autonomous and non-cell autonomous mechanism of degeneration (Scekic-Zahirovic et al. 2017; Scekic-Zahirovic et al. 2016).

5. Aims of this thesis

As the cytosolic and neuritic roles of FUS are not yet fully understood, I decided to unravel the FUS cytosolic interactome, both on an RNA and protein level and examine how these interactions are altered by ALS-associated mutations. It is clear from preliminary studies of the cytosolic targets of FUS, that its role in the cytosol and processes is vital. In disease, FUS can be found in cytosolic aggregates, thereby removing FUS from its normal duties. In addition to the nuclear loss of function, perhaps there is a toxic cytosolic gain of function. More specifically, some protein interactors may be lost or gained, altering RNP composition. This altered RNP composition, in combination with altered RNA target binding may result in disturbed cytosolic mRNA processing.

In order to evaluate the effect of disease-associated mutations on the FUS interactome and downstream processes, we obtained the $Fus^{\Delta NLS}$ mouse model described above. Using the heterozygous $Fus^{\Delta NLS/+}$ mice I aimed to:

- (i) purify cytosolic FUS mRNP complexes from the cortices of $Fus^{\Delta NLS/+}$ mice,
- (ii) identify RNA and protein interactors of FUS,
- (iii) identify the differentially bound RNA targets and protein interactors between FUS WT and $Fus^{\Delta NLS}$ mice and finally
- (iv) confirm some of the significantly different interactors in cell culture.

I hypothesize that abnormal cytosolic localization of FUS causes both a toxic gain and loss of function in its interactions with targets and other proteins.

II. RESULTS

DECLARATION OF CONTRIBUTIONS

cDNA library preparation and RNA Sequencing was performed by Laboratory for Functional Genome Analysis (LAFUGA) at the Gene Center Munich. RNA Sequencing Analysis was performed in collaboration with Tobias Straub of the Biomedical Center, LMU. Stephan Mueller of the Lichtenthaler lab, DZNE Munich, performed the Mass Spectrometry and requisite sample preparation and prepared Figure 33.

1. Establishment of FUS RNP granule isolation from mouse brain

To properly evaluate changes in the FUS interactome in wild type versus mutant mice, I first needed to establish a protocol to enrich for the cytosolic compartment of mouse cortex and then immunoprecipitate (IP) FUS with a high degree of specificity. Therefore, I began by testing different FUS antibodies in both native and denaturing conditions. The final workflow of the procedure can be seen Figure 5.

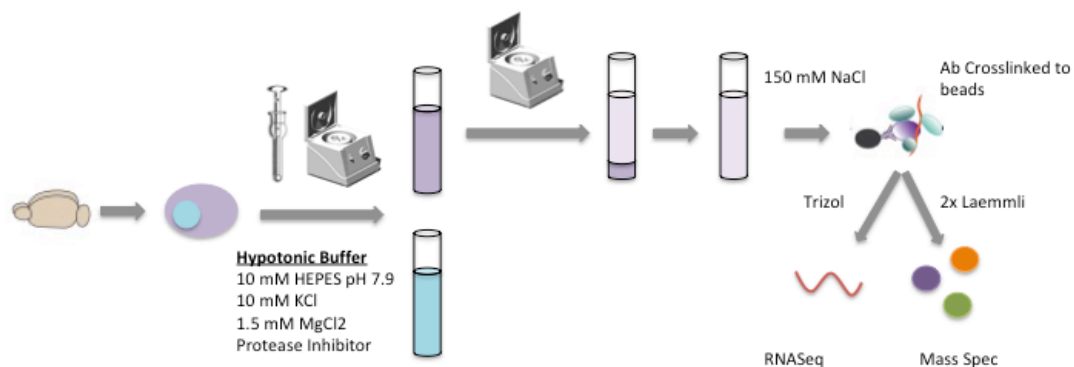


Figure 5: Schematic of the optimized workflow for isolating cytosolic FUS-RNPs from mouse cortex. Following hypotonic lysis, the cytosolic fraction of mouse cortices was centrifuged at 14,000 x g to remove heavier membrane components and debris. The samples were then IP'd with a FUS antibody or mouse IgG, both of which were covalently-crosslinked to magnetic beads. Following washes in the same buffer, the samples were eluted with 2x Laemmli (for SDS-PAGE and MS analysis) or Trizol (for RNA-sequencing).

1.1. FUS Antibody Testing

In order to analyze FUS localization properly, I first needed to confirm antibody specificity. A table of the antibodies used throughout this thesis is presented in Table 1.

Antibody	Company	Epitope	Species	Application Specificity
4H11	Santa Cruz	C-terminus, but N-terminal of aa. 466	Mouse	IF, WB, IP
A300-302	Bethyl	N-terminus (aa. 1-50)	Rabbit	IF, WB
A300-294	Bethyl	far C-terminus (aa. 500 - 526)	Rabbit	WB, IP
19B2	Ruepp Lab	middle	Mouse	IF, WB
Ruepp Lab	Ruepp Lab	N-terminus (aa. 1-286)	Rabbit	WB
11570-1-AP	Proteintech	N-terminus	Rabbit	
9G6	Helmholtz Antibody Core Facility	Asymm. Dimethylated FUS-RGG3 domain (aa. 473 - 503)	Rat	

Table 1: FUS antibodies used throughout this thesis. The antibody name/catalog number, along with the source, epitope and species in which it was produced are listed. Applications in which each antibody was found to be FUS-specific are listed under application specificity.

I first began by confirming FUS reactivity in western blot (Figure 6). I tested the following antibodies: Santa Cruz anti-FUS 4H11 (mouse), Bethyl A300-302 (rabbit), and two home-made antibodies from a collaborator, one produced in mouse (19B2) and one produced in rabbit. I performed subcellular fraction on mouse brain and ran the cytosolic and nuclear fractions on an SDS-PAGE followed by western blot. While the molecular weight of FUS is approximately 55 kD, it usually runs around 75 kD on SDS-PAGE. While all tested antibodies had the appropriate-sized band present at approximately 75 kD, the two home-made

antibodies from a collaborator had additional bands, suggesting nonspecific reactivity.

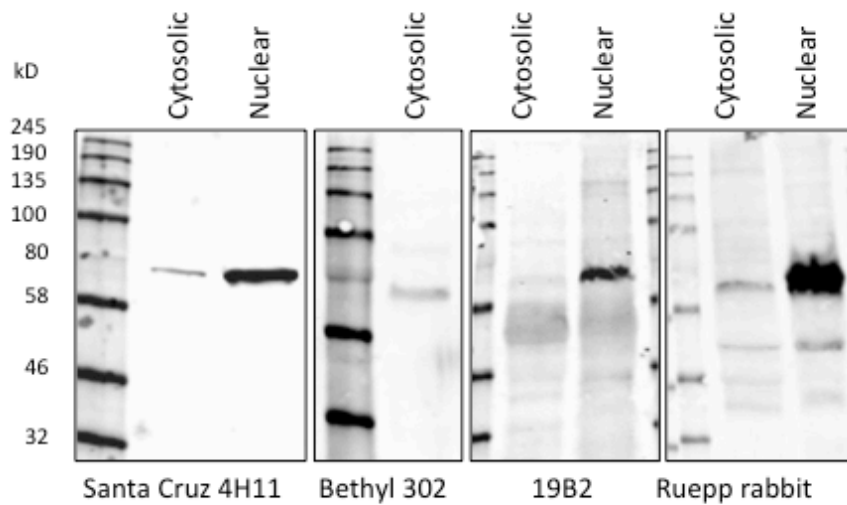


Figure 6: Testing of FUS antibodies, Santa Cruz 4H11, Bethyl 302, Ruepp Lab 19B2 and Ruepp Lab Rabbit by western blot on fractionated mouse brain. All antibodies show bands at the correct size, although some show more background bands than others.

To further confirm antibody specificity, I stained two different human cell lines, HeLa and SH-SY5Y, for which we had a FUS knockout (KO) line available from a collaborator (Dr. Marc-David Ruepp). In the first test, I stained for FUS in HeLa FUS KO and in the parental wild type cell line (Figure 7). Santa Cruz 4H11, 19B2 and Bethyl 302 all showed a strong nuclear staining in the wild type cells with a very weak background staining in the Fus KO line. While the Abcam, Bethyl 294 and 9G6 antibodies also showed a nuclear staining, the staining in the FUS KO line had much higher background. I found that the 4H11 (Santa Cruz) and the A300-302 (Bethyl) had satisfactory signal to noise ratios.

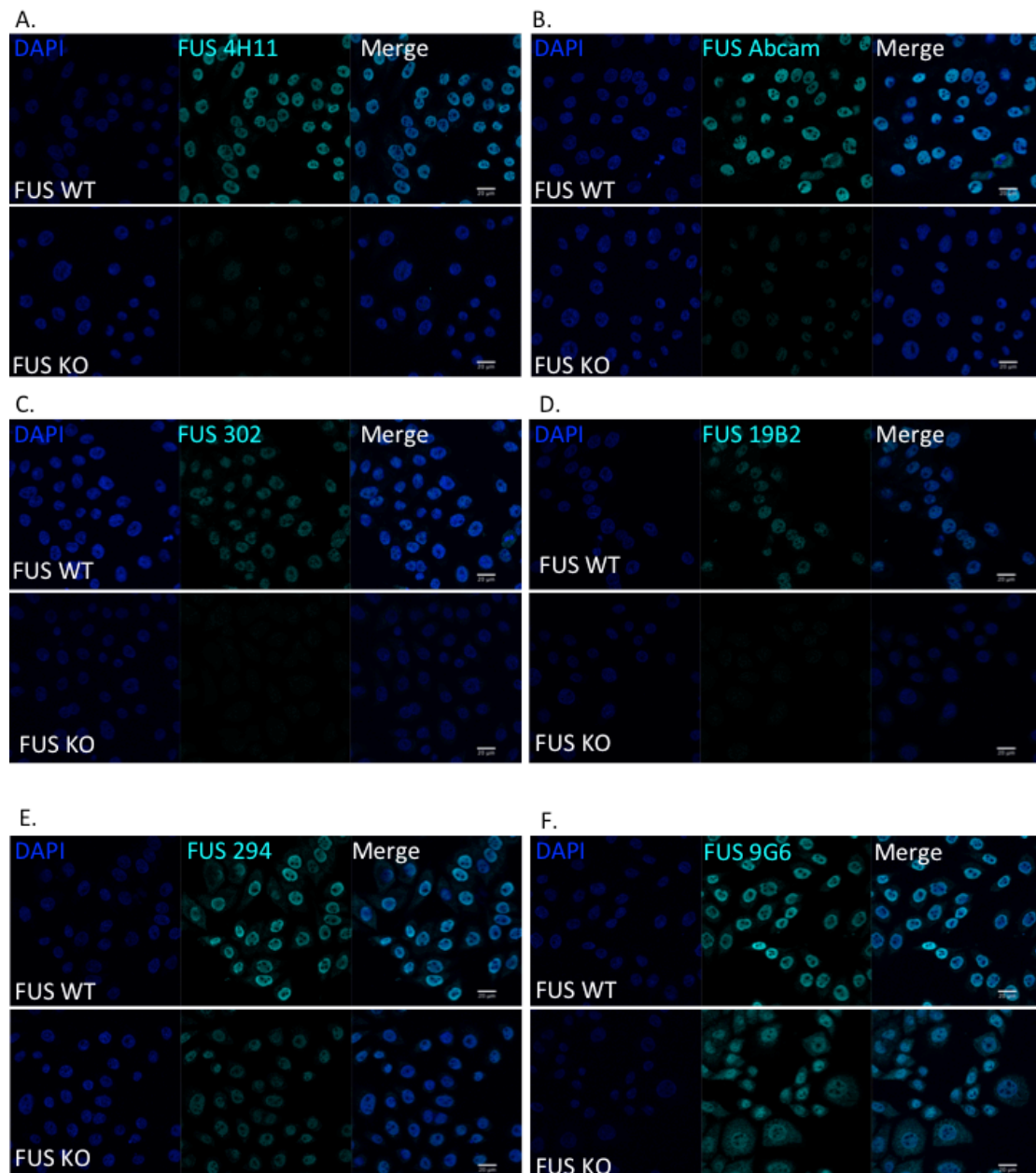


Figure 7: Immunostaining in HeLa WT or FUS KO with different FUS antibodies: A. Santa Cruz 4H11 (1:1000), B. Abcam (1:500), C. Bethyl A300-302 (1:500), D. Ruepp Lab 19B2 (1:1000), E. Bethyl A300-294 (1:500) and F. 9G6 (1:2). Cells were fixed in 4% formaldehyde and permeabilized with 0.5% Triton in PBS. Blocking and antibody incubations were performed in 5% milk in PBS-Tween (T). All washes were done with PBS-T.

As every cell type is different and as I would ultimately like to stain primary neuronal cultures, I proceeded to examine FUS antibody reactivity in the human neuronal-like SH-SY5Y cell line. As demonstrated in Figure 8, all antibodies,

excluding 11570-1-AP (Proteintech) produced a FUS-specific signal in the parental SH-SY5Y cell line compared to the FUS KO line.

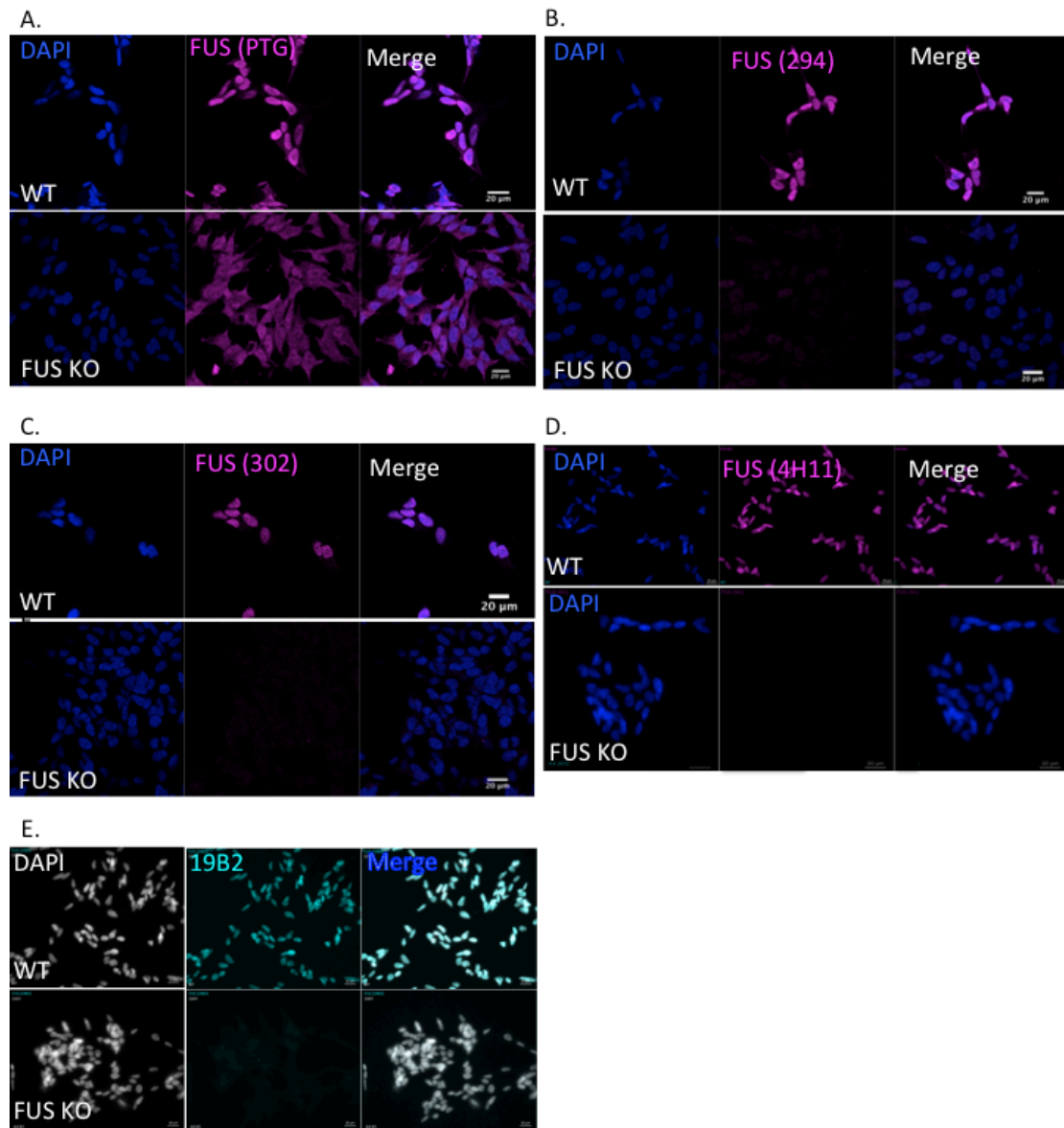


Figure 8: Staining of FUS in either WT or FUS KO SH-SY5Y cells using A. Proteintech (PTG) 11570-1-AP (1:500), **B.** Bethyl A300-294 (1:500), **C.** Bethyl A300-302 (1:500), **D.** Santa Cruz 4H11 (1:1000) or **E.** Ruepp Lab 19B2 (1:1000). Cells were fixed in 4% formaldehyde and permeabilized with 0.5% Triton in PBS. Blocking and antibody incubations were performed in 5% milk in PBS-Tween (T). All washes were done with PBS-T.

1.2. Fractionation of mouse cortex into nuclear and cytosolic fraction

As the aim of this these is to identify differential cytosolic FUS protein interactors, following initial antibody tests, the next step is then to optimize the subcellular fractionation protocol (Figure 9). I initially tried various HEPES-based buffers and cytosolic fractionation kits (NE-PER from Invitrogen) but found high amounts of the nuclear contamination in the cytosolic fraction. I eventually tried a classical hypotonic lysis buffer without detergent, which causes the cells to swell, and then rupture them. The initial basic workflow of the nuclear/cytosolic fractionation can be seen in Figure 9.

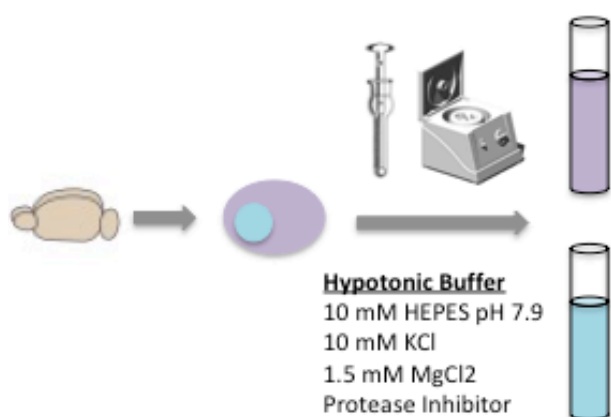


Figure 9: The initial subcellular fractionation workflow. Cortices from young adult mice were removed and flash frozen. Immediately upon removal of cortices from the -80°C freezer, cortices were put into a dounce homogenizer with hypotonic buffer (10 mM HEPES pH 7.9, 10 mM KCl, 1.5 mM MgCl₂ and protease inhibitor). Brains were gently dounced and then left on ice for 10 minutes. Following this incubation, the suspension was then either vortexed or dounced again, followed by centrifugation at 3,000 x g for 10 minutes. The supernatant was collected as the cytosolic fraction (purple) and pellet as the nuclear fraction (blue).

FUS is mostly nuclear and only small amounts of FUS are present in the cytosol under physiological conditions (Scekic-Zahirovic et al. 2017). Therefore, the next step after obtaining a cytosolic fraction was to confirm that FUS is in fact present at detectable levels for further enrichment by immunoprecipitation. Western blotting demonstrated that FUS is present at expected ratios between the cytosol and nucleus (Figure 10). Antibodies against histone H3, a nuclear marker, and GAPDH, a cytosolic marker, were used to confirm enrichment of the cytosolic fraction. Although there is some GAPDH contamination in the nuclear fraction,

likely representing unbroken cells, the cytosolic fraction is clear of obvious nuclear contamination.

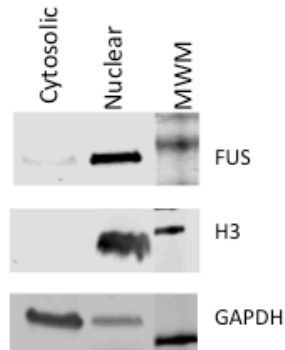


Figure 10: Successful Subcellular Fraction of wild type mouse brain.

Following subcellular fractionation, fractions were immunoblotted FUS (4H11), Histone H3 (Abcam), to identify nuclear enrichment and depletion from the cytosolic fraction and GAPDH (Helmholtz) as a cytosolic marker. The blot shows a nice cytosolic enrichment.

1.3. Optimization of FUS Immunoprecipitation Procedure

1.3.1. Testing different FUS antibodies in immunoprecipitation

As previously shown, we have several FUS-specific antibodies to detect FUS by IF or Western blot (see Table 1 above). I next wanted to test which of these antibodies also was suitable for immunoprecipitation (IP) of FUS. As the nuclear fraction contains much more FUS than the cytosolic fraction, I initially used the nuclear fraction of mouse brain to test the different antibodies in IP. I first tested three rabbit polyclonal antibodies (two from Bethyl Labs and a third made by the Ruepp Lab) bound to Sepharose A beads performed the immunoprecipitation in hypertonic buffer (10 mM HEPES, pH 7.9, 10 mM KCl, 1.5 mM MgCl₂, 150 mM NaCl, 0.5% NP-40, protease inhibitor) plus 10% glycerol. After 3 washes in hypertonic buffer, I eluted bound protein by boiling in 2x Laemmli buffer.

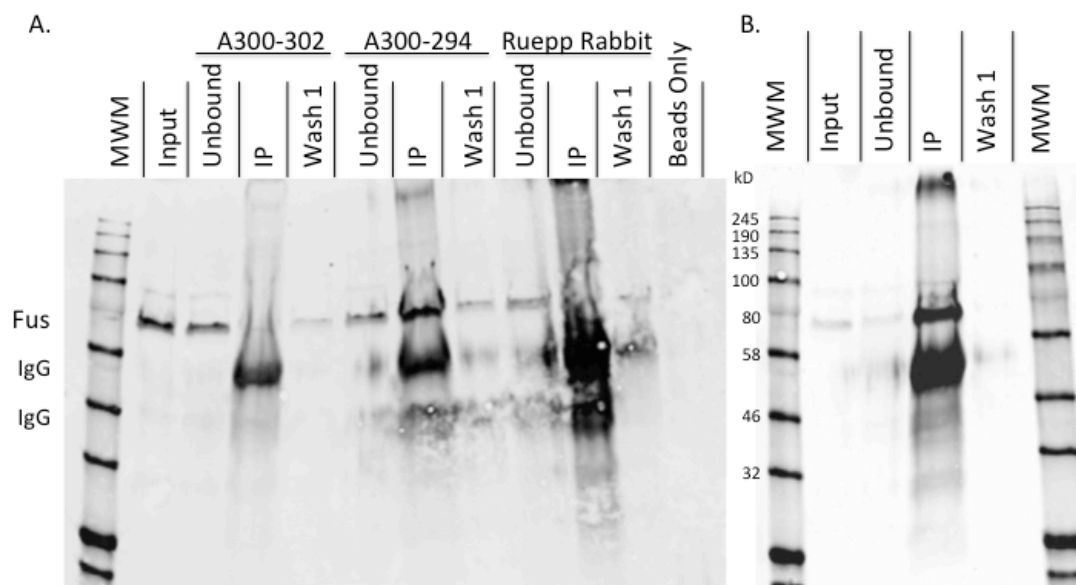


Figure 11: Testing of FUS antibodies in immunoprecipitation. **A.** Antibody-bound beads were incubated with the nuclear fractions from wild type mouse brains in a hypertonic buffer. Following washes, protein was eluted in 2x Laemmli and run on a 10% SDS-PAGE, transferred to nitrocellulose and developed using mouse monoclonal FUS-specific antibody 4H11 from Santa Cruz. **B.** The cytosolic fraction of wild type mouse brains was applied to A300-294 bound beads, run on SDS-PAGE and then western blotted for FUS.

As shown in Figure 11A, the A300-294 antibody from Bethyl appeared to work best to immunoprecipitate FUS under these conditions, while no efficient IP was seen for Bethyl antibody A300-302 and the Ruepp lab rabbit antibody. Next, I tested the Bethyl A300-294 antibody in the cytosolic brain fraction, which contains lower amounts of FUS than the nuclear fraction. The IP of FUS from the cytosolic fraction with A300-294 also worked well with the above-described protocol (Figure 11B).

In addition, I tested the Proteintech rabbit antibody (11570-1-AP) which recognizes the N-terminus of FUS (Figure 12). Although the rabbit IgG yielded background FUS binding, the antibody appeared to immunoprecipitate FUS.

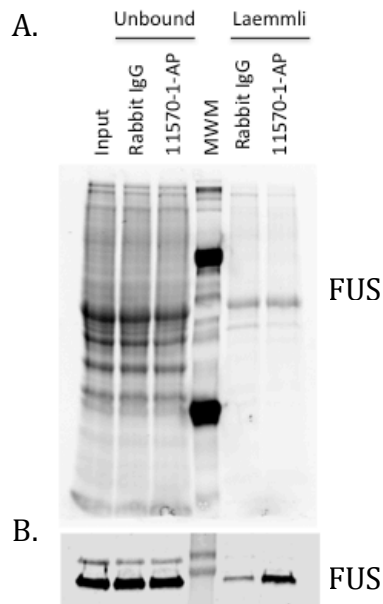


Figure 12: Immunoprecipitation of FUS by an N-terminal Proteintech antibody (11570-1-AP). Although there appears to be background binding of FUS to rabbit IgG, the antibody immunoprecipitates FUS as shown in the Bio-Rad Stain-Free gel (A) and by immunoblotting with Bethyl A300-302 (B).

While FUS was specifically immunoprecipitated with the A300-294 antibody, but not the control rabbit IgG, a known cytosolic interaction partner of FUS, Aly/Ref (Kanai, Dohmae, and Hirokawa 2004), only showed a weak signal in both the IgG and the A300-294 IP samples (Figure 13). FUS was previously shown to be in complex with kinesins and Aly/Ref, so perhaps this interaction would be seen with greater intensity if the granules were more enriched for motor protein interactions (Kanai, Dohmae, and Hirokawa 2004). Our results could indicate that either only a small portion of FUS is binding Aly/REF in the cytosol or perhaps the interaction itself is not stable under our experimental conditions.

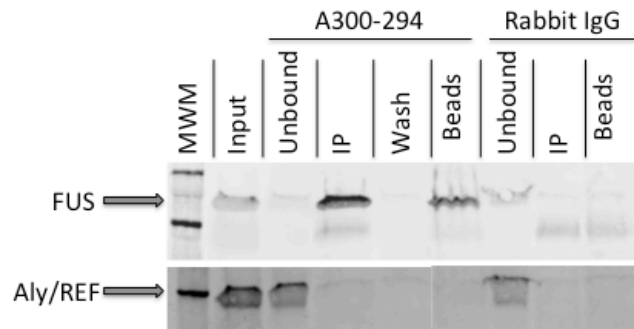


Figure 13: FUS from cytosolic mouse brain fractions was immunoprecipitated with the A300-294 antibody and eluted with glycine pH 2.2. Prior to the IP, BSA and tRNA were added to the beads to prevent nonspecific binding of protein and RNA to the beads. Aly/REF, a known FUS cytosolic interaction partner, showed no or only a very weak signal in both the FUS and control-IP.

As the antibody that worked best in IP, Bethyl A300-294, is directed against the C-terminal PY-NLS of FUS (aa. 500 -526), which is largely truncated in the Fus^{ANLS} mouse model that I wanted to include in my analysis, I tried an additional antibody, a mouse monoclonal antibody from Santa Cruz (4H11), which recognizes a more N-terminal epitope (Table 1). 4H11 also efficiently immunoprecipitated FUS out of the cytosolic fraction, as well as some of its known interaction partners, Aly/REF and PABP1 (Figure 14, (Kanai, Dohmae, and Hirokawa 2004)). Some FUS did remain bound to the beads following the glycine elution.

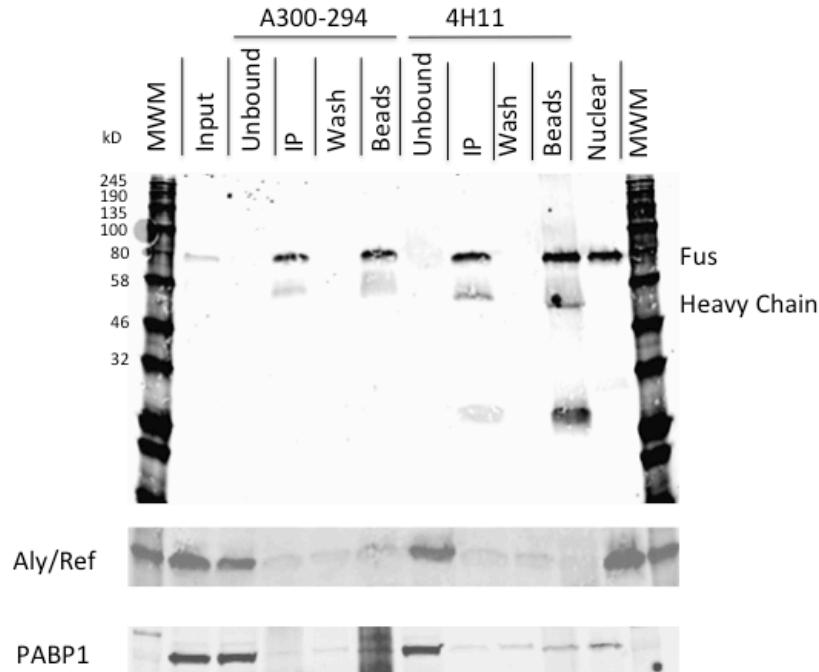


Figure 14: Immunoprecipitation of FUS complexes with Bethyl and Santa Cruz antibodies. FUS from cytosolic mouse brain fractions (Input) was immunoprecipitated with either the rabbit Bethyl antibody A300-294 or the mouse monoclonal 4H11 antibody (IP). Samples were then blotted for FUS (4H11 antibody) and potential complex partners, Aly/Ref and PABP1. The nuclear fraction was loaded as a positive control (right lane). Both antibodies immunoprecipitated FUS and its interaction partners equally well.

1.3.2. Optimizing elution from beads

Low pH glycine elution from beads is a gentle way to remove bound protein while minimizing antibody contamination. In order to fine tune a low pH glycine elution (pH 3, 0.2M glycine) I then returned to the nuclear fraction. As the glycine appeared to cause the DNA in the nuclear fraction to precipitate (assessed by the presence of a white precipitate), I tested the IP with and without DNase I treatment (performed prior to IP). Additionally, to have a negative control for the FUS antibody, I also incubated the nuclear fraction with rabbit IgG-bound beads. Two sequential glycine elutions were performed, followed by an elution with 2x Laemmli buffer to see how much FUS remained on the beads (Figure 15).

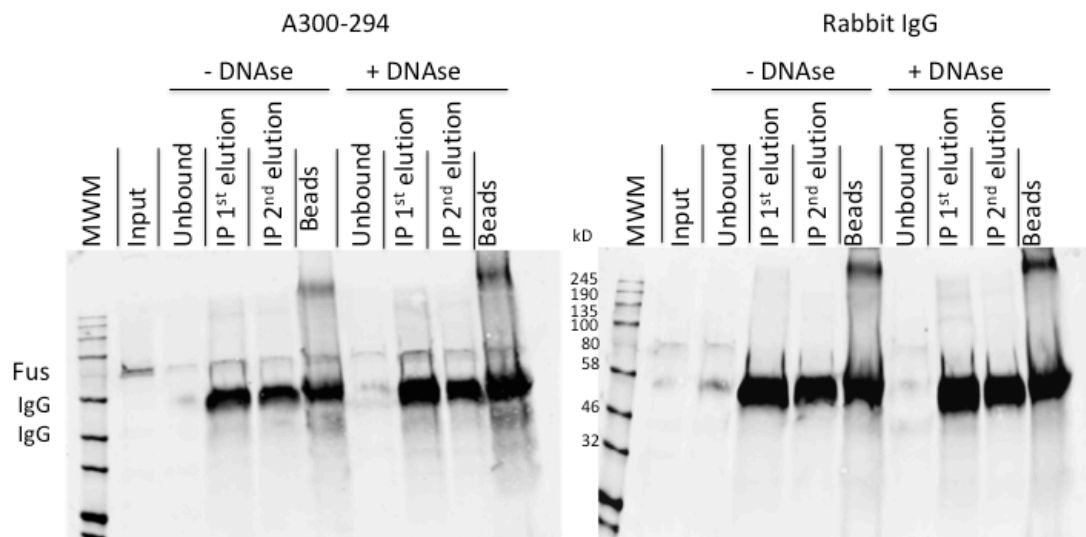


Figure 15: Immunoprecipitation of FUS with Bethyl A300-294. Nuclear fractions immunoprecipitated with the A300-294 were eluted with sequential glycine pH 3 elutions. Finally, beads were boiled in Laemmli to examine how much FUS remained after the glycine elution. DNase I was added to the nuclear fraction in order to test the effect of the presence of DNA on the elution. A rabbit IgG control antibody was used as a negative control.

There did not appear to be a major difference between DNase-treated and untreated samples, and FUS only was immunoprecipitated by the Bethyl A300-294 antibody, but not the rabbit IgG negative control. Although, it did appear that the glycine elution was not entirely efficient, as some FUS remained on the beads, therefore for the following IP, I lowered the pH of the glycine to pH 2.2. Additionally, to prevent any nonspecific binding to the beads, I added a blocking step for the beads, which included 0.125 mg/ml yeast tRNA and 1 mg/ml BSA.

Additionally, as we also wanted to examine RNAs in the FUS-IPs by RNA sequencing (Figure 5), I tested the elution efficiency of Trizol (Figure 16). I found that Trizol eluted as efficiently as Laemmli buffer. Low FUS signal in the input is likely due to limited antibody sensitivity.

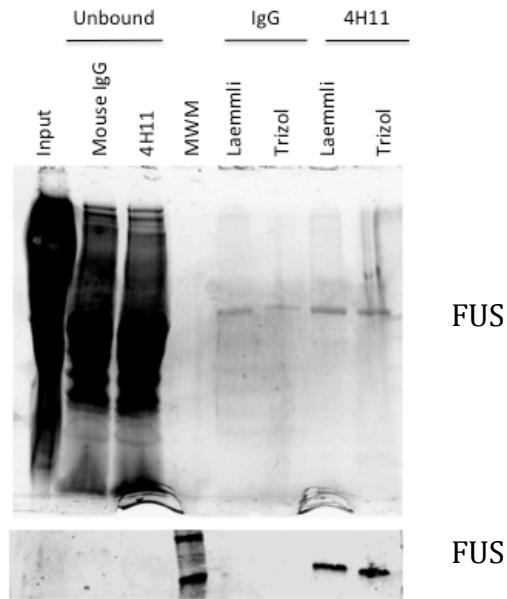


Figure 16: Successful elution of the FUS complexes with Trizol and Laemmli.
A. A Bio-Rad Stain Free gel and **B.** western blot of FUS using Bethyl A300-302.

At this point, I wanted to confirm that FUS RNP complexes were still intact in the cytosolic fraction and additionally, attempt to enrich for these FUS RNP granules.

1.4. Testing Different Methods to Enrich FUS RNP Granules

After successful nuclear/cytosolic fractionation and immunoprecipitation, I next wanted to test whether I could further enrich for FUS RNP granules by density gradient centrifugation or stepwise centrifugation.

1.4.1. Density gradient centrifugation

Density centrifugation provides us with the opportunity separate protein complexes to enrich RNP granules. Fortunately, the Kiebler lab in our department had previously established an Optiprep protocol to specifically isolate Stau2 and Btz-containing mRNP granules from rat brains. Briefly, soluble lysate was generated from rat brain followed by application of these lysates to a 15-30% Optiprep gradient. The gradient allows for separation of mRNP granules

from the main protein peak and from the endoplasmic reticulum. Furthermore, co-segregation of the Stau2 and Btz-containing granules with PABP1 and treatment of the soluble lysate prior to density gradient centrifugation with RNase, leading to a shift of the Stau2 and Btz to lighter fractions, confirmed the presence of intact RNP particles (Fritzsche et al. 2013).

In short, I treated half of the cytosolic fraction with an RNase I mixture, during this time a 15-30% Optiprep density gradient was prepared. The samples were gently pipetted on top of the gradient and then centrifuged at 197,500 x g, following centrifugation, 12 fractions were collected beginning with the lightest fraction (Figure 17). Afterwards, I performed a chloroform/methanol precipitation to precipitate the proteins present in the individual fractions and analyzed them by Western blotting with a FUS-specific antibody, PABPC1 was used as a control to confirm that granules were intact.

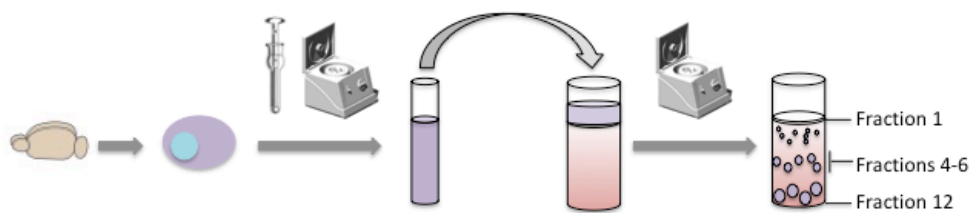


Figure 17: The basic workflow of an optiprep density gradient. Cytosolic fraction of cortex was prepared as previously described and applied to a 15-30% Optiprep density gradient. High-speed centrifugation at 197,500 x g was performed and 12 fractions were collected. RNP granules are expected to be found in fractions 4-6.

Interestingly, I found FUS present in all fractions but primarily concentrated in the lower to middle density fractions, indicating that FUS is both diffuse and present in various-sized higher order complexes (Figure 18). RNase I treatment resulted in a shift of FUS and PABPC1 to lower density fractions, suggesting that FUS is present in intact mRNP granules.

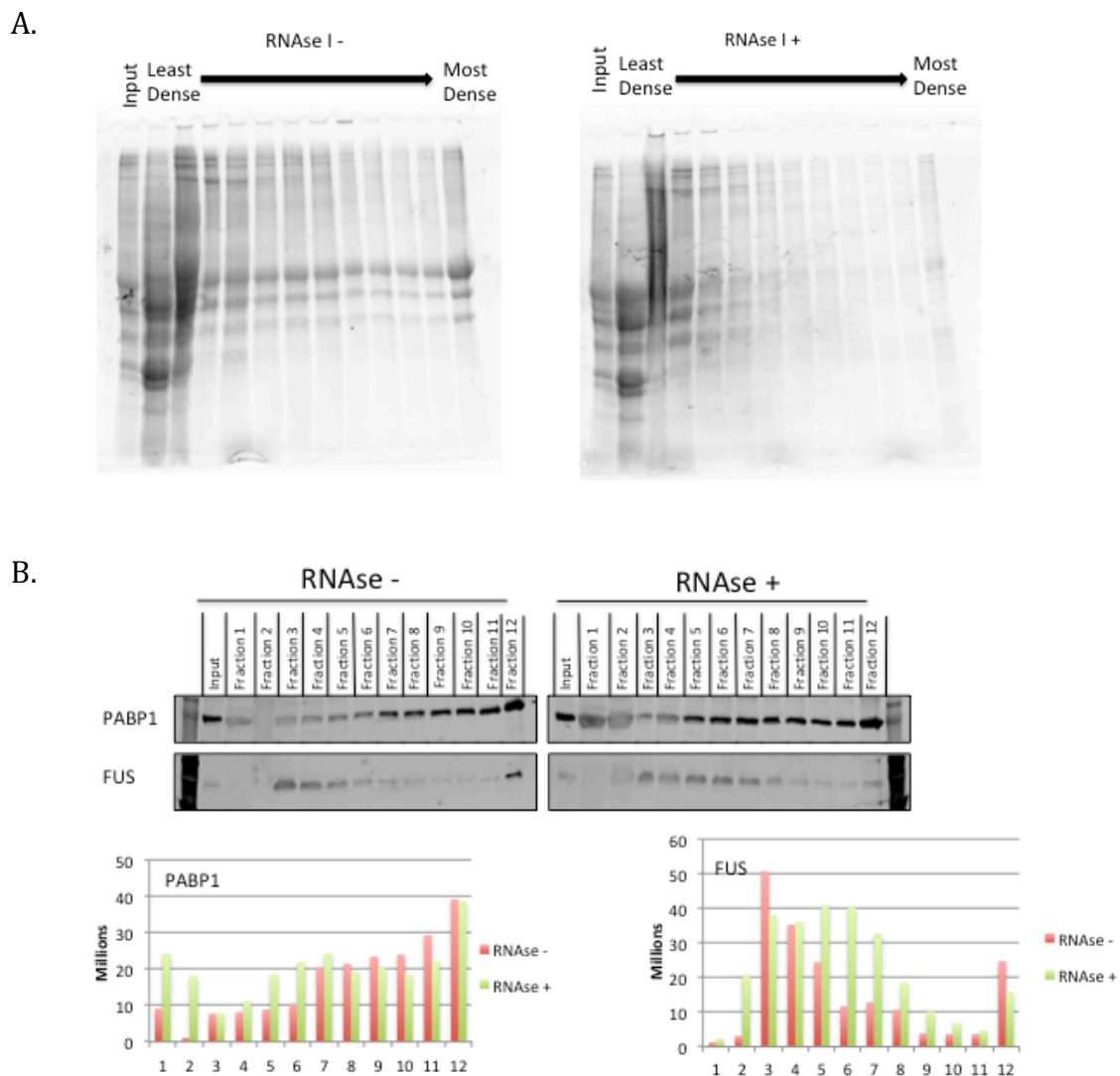


Figure 18: Optiprep density centrifugation of cytosolic mouse brain. Fractions collected following Optiprep centrifugation were loaded onto a 10% SDS-PAGE gel and **A.** stained with Coomassie or **B.** transferred to nitrocellulose and blotted for FUS and PABPC1. **C.** FUS and PABPC1 levels were quantified using ImageJ.

Overall, it can be concluded that FUS exists in complexes of different densities and no enrichment is seen in a particular fraction. Hence, this method did not seem to be suitable to further enrich for FUS RNP granules before immunoprecipitation.

1.4.2. Differential centrifugation at 20,000 x g / 100,000 x g

Next, I tried an alternative centrifugation method (two separate high-speed centrifugations at 20,000 x g and then 100,000 x g) in order to test in which fraction FUS was enriched and whether the complexes are sensitive to RNase (Figure 19). This demonstrated that most FUS pelleted at 100,000 x g, indicating that it may associate with cellular membranes or ribosomes (Mallardo et al. 2003). Only very little FUS was present in the S100 fraction, making it impossible to further purify FUS RNPs from the S100 fraction. Therefore, I decided to proceed by not using any pre-enrichment steps, but by using the entire cytosolic fraction and immunoprecipiating FUS complexes.

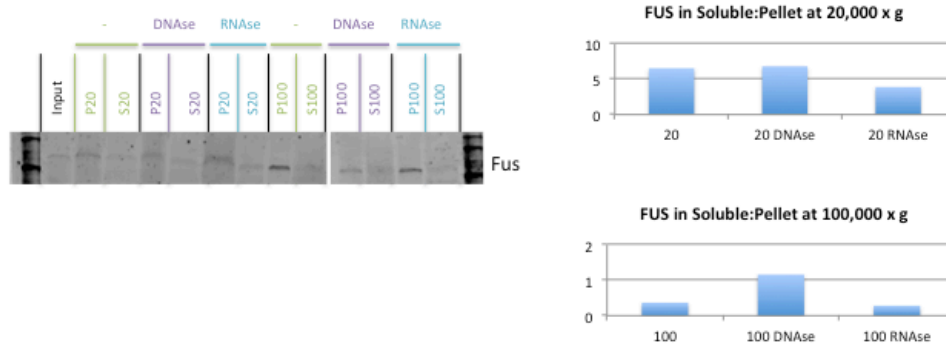


Figure 19: Differential centrifugation of cytosolic mouse brain. Cytosolic fractions were incubated with RNase I for 1h at 37°C, samples were then centrifuged at 20,000 x g and subsequently 100,000 x g. Supernatant and pellet from each centrifugation were loaded onto a 10% SDS-PAGE, transferred to nitrocellulose and subsequently blotted for FUS. All of the pellet fractions, 10% of the S20 fractions and 50% of the S100 fractions were loaded. Densitometry measurements were performed in ImageJ, then the ratio of the soluble to pellet fraction was calculated for each.

2. Test-IP followed by mass spectrometry and RNA-sequencing and further optimization of the workflow

Thus far, following cytosolic fraction, I have been able to successfully IP FUS and some of its known interaction partners. The next step is to do a test run for the mass spectrometry. First, I wanted to confirm that more expected interaction partners immunoprecipitated with FUS. I also wanted to know if different FUS antibodies yielded different interactions partners (perhaps due to epitope

availability) and finally, I needed to confirm that I had enough material in my sample to detect interaction partners.

Therefore, I decided to compare the FUS interaction partners that were co-immunoprecipitated with three different FUS antibodies in parallel by mass spectrometry. As A300-294 yielded promising results, I included it in this submission to examine the overlap between the antibodies. I also used the Santa Cruz 4H11 mouse monoclonal antibody, which recognizes an epitope slightly more N-terminal than the A300-294 and an antibody recognizing the N-terminus, Proteintech 11570-1-AP. In order to allow for better detection of FUS interaction partners and a greater depth in the mass spec analysis, by reducing antibody contamination in the samples, I covalently conjugated the antibodies to sepharose beads using dimethyl pimelimidate (DMP), a chemical cross-linker. Covalent conjugation of the antibody to the beads also allowed me to elute with Laemmli buffer and increase yield. I also removed the BSA and glycerol from the protocol, as they are known to interfere with the MS analysis.

As I only submitted one sample per antibody, I was unable to do statistical analysis on my results and therefore simply looked at the most enriched proteins. All antibodies showed enriched FUS in the FUS-IP relative to IgG control (Figure 20A), the highest enrichment was seen with the Bethyl antibody, followed by the Santa Cruz antibody and finally the Proteintech antibody. Cell compartment classification of the co-IP'd proteins yielded approximately the same results for all samples, with a primarily cytosolic enrichment, along with significant membrane and nucleus enrichment (Figure 20B). I found that the number of peptides identified was surprisingly high across all antibodies and IgG, indicating potentially high background. Setting the \log_2 fold change to a conservative cutoff of 1 resulted in some overlap between the antibodies (Figure 20C). Additionally, lowering the fold change threshold to a \log_2 fold change of .5 (fold change 1.4) for both Santa Cruz and Bethyl yielded an overlap of 84 proteins. The Proteintech antibody had the lowest amount of enriched protein with a 2 or more fold change and did not yield many RNA binding proteins. Upon submitting the results to gene ontology (GO) analysis across multiple platforms,

including Gorilla, Panther and DAVID, the Proteintech-IP did not yield any enriched GO categories. Both the Santa Cruz- and Bethyl-IP were enriched for categories related to transport (Figure 20D). Due to the possibility of altered epitope availability in different granules, the different epitopes between the two antibodies could explain the different interaction partners. As the Bethyl antibody does not recognize the FUS^{ANLS} mutant I planned to use, I chose to move forward with the Santa Cruz antibody

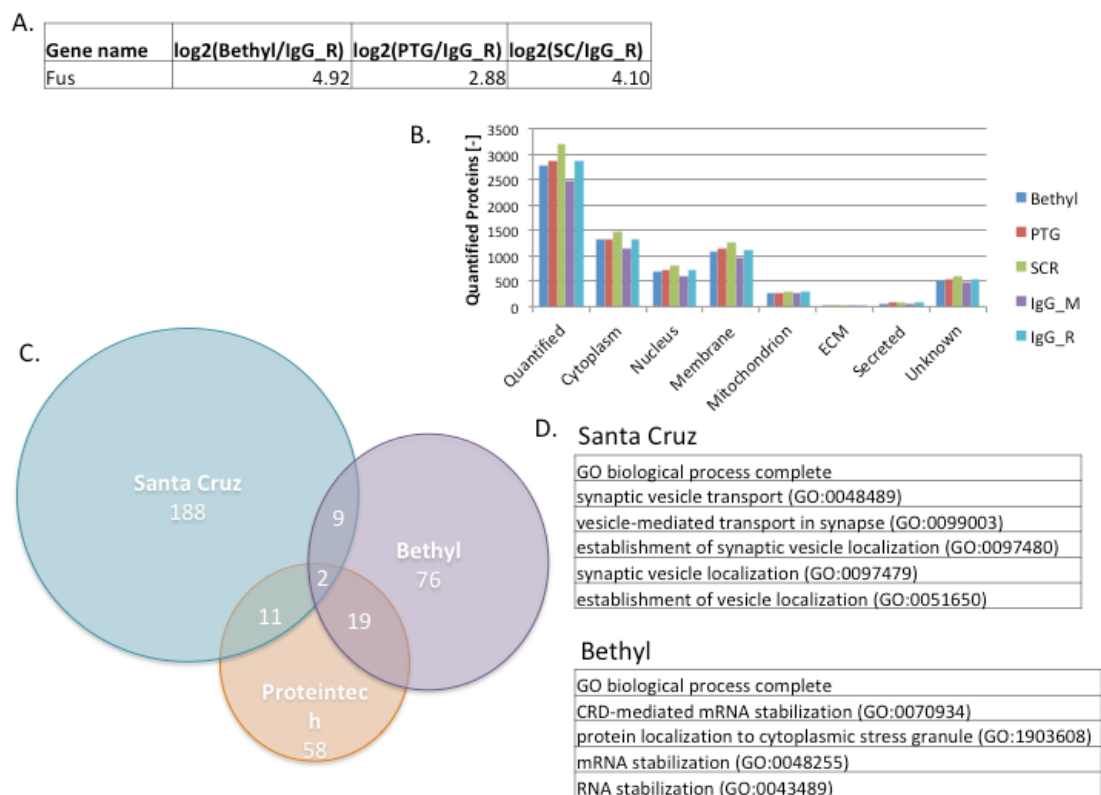


Figure 20: FUS IP MS Results. **A.** The relative enrichment of FUS protein for each tested antibody compared to IgG. **B.** The total number of quantified proteins and the quantification of the annotated cell compartment. **C.** The overlap of the proteins identified in the different IPs with a log₂ fold change cutoff of 1 (2-fold). **D.** GO enrichment for Santa Cruz and Bethyl antibodies using DAVID.

The next step was to confirm that the Santa Cruz antibody could in fact immunoprecipitate different RNA transcripts relative to IgG. I performed the IP in triplicate, eluted with Trizol and submitted the eluted RNA to the RNA Sequencing facility (LAFUGA, Gene Center). As there should not be much RNA present in the IgG control samples and the RNASeq involves a large amplification of cDNA, we spiked in control DNA (from another species) to all of the samples prior to amplification so that the amount of transcripts could be properly normalized between the FUS-IP and IgG control. Unfortunately, this first analysis did not yield differential transcript immunoprecipitation between IgG control and FUS antibody.

The high peptide number in the MS analysis and the non-differential immunoprecipitation of RNAs indicated a need to increase the specificity of the IP. Up until this point, although I had been blocking the beads with tRNA, I had been using sepharose beads, which have reportedly high background binding. I was also performing the immunoprecipitation in hypotonic buffer, followed by washes in a buffer containing 150 mM NaCl. It seemed possible that performing the IP in hypotonic buffer reduces the specificity and results in unspecific binding of proteins and RNAs to the beads. Therefore, I made some adjustments to the protocol: First, I performed an additional 14,000 x g centrifugation step after isolating the cytosolic fraction, to get rid of sticky membranes and debris. Second, I added 150 mM NaCl to the hypotonic 14,000 x g supernatant to reduce unspecific hydrophobic interactions in the IP. Finally, I used magnetic beads (Dynabeads) instead of sepharose beads (Figure 5).

Using this new protocol, I performed the IP, eluted and isolated the RNA from the FUS antibody or IgG-bound beads and then performed qPCR on two established FUS mRNA targets (*GluA1* and *Nd1-L*) and one negative control (*Park7*, (Lagier-Tourenne et al. 2012)). I found enrichment of both *GluA1* and *Nd1-L* in the FUS IP compared to IgG control, while the negative control, *Park7* was not enriched in the FUS-IP (Figure 21). In order to further examine enrichment of FUS binding to *GluA1* and *Nd1-L*, I normalized the expression of the bound transcripts to the cytosolic input.

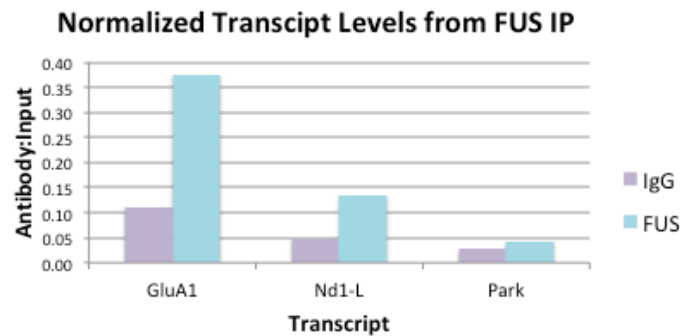


Figure 21: qPCR of RNA eluted from the FUS immunoprecipitation (using the 4H11 antibody) confirmed differential IP of FUS-specific targets. RNA eluted from the beads underwent reverse transcription followed by amplification for two confirmed FUS targets, *GluA1* and *Nd1-L* and a confirmed negative control, *Park*. RNA bound to beads was normalized to RNA in the input.

Finally, I needed to confirm that the new protocol works well with protein elution and subsequent mass spectrometry. I prepared two test samples, using both the Santa Cruz antibody and mouse IgG.. Rather than excising multiple fractions from the gel, one large fraction was submitted for a quick analysis by MS. The number of identified proteins was reduced by 22% in the FUS IP compared to the previous submission, FUS was enriched by a \log_2 fold change of 6 (64 fold change) and cytosolically localized proteins remained enriched. I decided to use this protocol for the quantitative comparison of the $FUS^{\Delta NLS/+}$ mice and their wild type littermates.

3. FUS Immunoprecipitation from $FUS^{\Delta NLS/+}$ vs wild type mouse cortices, followed by Western blot, RNAseq and MS analysis

3.1 Western blot analysis

As the $FUS^{\Delta NLS/+}$ mice were not yet available in our animal facility at the time, I obtained frozen cortices isolated from approximately 50 day old mice (5 $FUS^{\Delta NLS/+}$ mice and 5 wild type littermates, Table 2) from our collaborator Diana Wiesner (University of Ulm).

No	gender	genotype	age
1027	♂	het	49
1028	♂	wt	49
1041	♂	het	49
1042	♂	het	49
1043	♂	het	49
1047	♂	het	47
1048	♂	wt	47
1049	♂	wt	47
1050	♂	wt	47
1051	♂	het	47
1054	♂	wt	46
1055	♂	wt	46
1056	♂	wt	46
1057	♂	het	46

Table 2: Mice used for the FUS interactome studies. 5 male wild type and 5 male heterozygous mice were used for the main experiment. The remaining mice were used for confirmatory experiments.

The cortices were fractionated and FUS was immunoprecipitated according to the previously established procedure (Figure 5). To verify successful fractionation and immunoprecipitation, I took a small aliquot of the nuclear and cytosolic fractions as well as the IP fraction and analyzed them by Western blot with antibodies specific to FUS, GAPDH (as cytosolic marker) and histone H3 (as nuclear marker) (Figure 22). As expected, increased amounts of FUS were observed in the cytosolic fraction in the FUS^{ANLS/+} cortices whereas similar amounts of FUS were pulled down in the FUS-IP between the two genotypes (Figure 22, upper blot). Nuclear/cytosolic markers showed enrichment in their respective fractions.

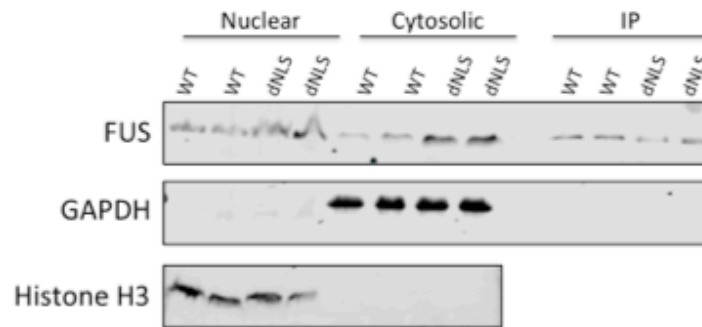


Figure 22: Western blot of the subcellular fractionation and subsequent cytosolic IP from wild type and FUS^{ΔNLS/+} mouse cortices. 2 mice are shown as example. Western blotting with a FUS-specific antibody (4H11, Santa Cruz) demonstrated increased cytosolic localization of FUS^{ΔNLS/+} and equal immunoprecipitation efficiency. Histone H3 and GAPDH antibodies were used to confirm successful preparation of a nuclear and cytosolic fraction

3.2. RNA sequencing to identify differential RNAs in FUS^{ΔNLS/+} vs wild type FUS RNPs

Single end HiSeq was performed using 100 base pair reads on both the cytosolic input and the FUS IP. The pipeline can be seen in Figure 23.



Figure 23: RNA Sequencing Pipeline. Following elution of the RNA from the magnetic beads with Trizol, RNA was purified with Zymo's Directzol RNA Miniprep Kit, reverse transcribed, multiplexed and amplified. They were then run through HiSeq using single end 100 base pair reads. These reads were then aligned to the genome using STAR, reads to each gene were quantified using Rsem, the IP was normalized to the input (cytosolic fraction before IP) and then differential RNA levels between FUS^{ΔNLS/+} and wild type was calculated.

Unfortunately, one sample from each genotype yielded poor quality and low read count in the RNASeq analysis, therefore we eliminated these samples from the analysis and performed the analysis with 4 wild-type and 4 FUS^{ΔNLS/+} samples. In the input (cytosolic fraction before IP), the levels of only two RNA transcripts significantly changed in mutant relative to wild type: Fus, with a log₂ fold change

(log₂FC) of 0.83 (i.e. ~ 1.8-fold higher in mutant vs. wild type) and Prkch, a protein kinase C family member, with a log₂FC of -1.53 (~ 3-fold lower in mutant vs. wild type). The reads obtained from the IP were then normalized to the input to account for slight changes in overall mRNA levels in the input sample. We obtained 307 significant changes with an adjusted p-value of 0.05 or lower. Of these 307 changes, 240 were decreased in mutant relative to wild type and 67 were increased, indicating that there may be a combination of loss-of-function and gain-of-function changes in cytoplasmic mRNA processing in FUS^{ΔNLS/+} mutant mice. Transcripts with a fold change of more than two, and a p-value of less than 0.01 are shown in Figure 24.

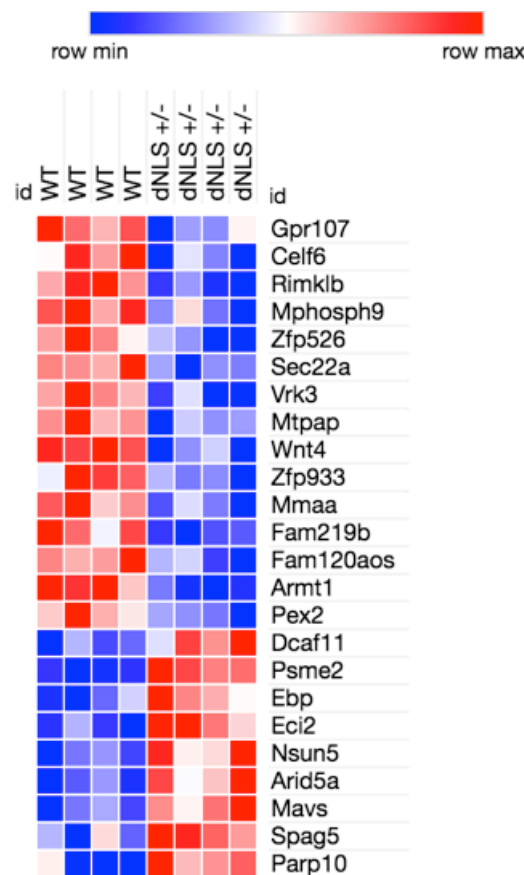


Figure 24: A heatmap of top differentially expressed transcripts. A heat plot of individual transcripts and biological replicates (4 / genotype) with a p-value of less than .01 and a fold change of more than 2 are shown.

When all of the significantly changed transcripts ($p < 0.05$) are subjected to gene ontology (GO) analysis by DAVID, enrichment is found in several categories (Figure 25), of which the top enriched terms are: transcription, RNA binding, lipid metabolism, proteasome, G-protein signaling and ion transport.

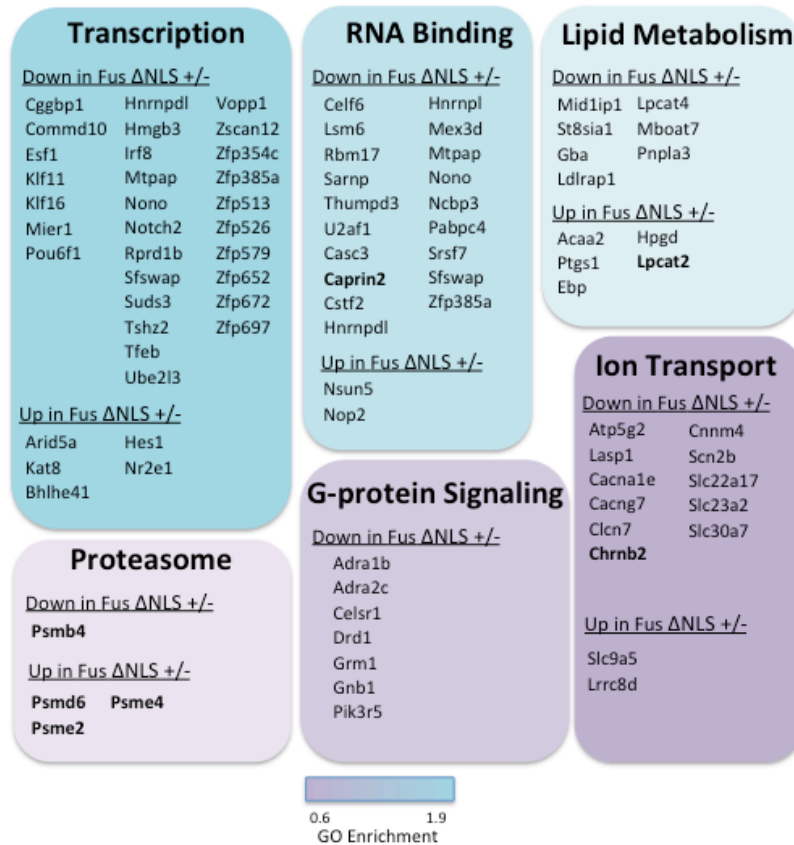


Figure 25: GO analysis of all significant transcript changes in the FUS^{ΔNLS/+} relative to wild type mice, with highest enrichment in transcription. Transcripts in bold are those I was interested in following up.

3.2.1 FUS^{ΔNLS/+} RNP granules contain reduced *Ric3* and *Chrn2* mRNAs, involved in nicotine receptor signaling

Our collaborator Luc Dupuis (Strasbourg) has recently shown that the FUS^{ΔNLS/+} mice appear to have aberrant nicotine signaling (personal communication, unpublished). Therefore, I parsed through our RNAseq results for transcripts that are related to nicotine receptor signaling by submitting the results to DAVID and String. Two candidates of interest include *Ric3* and *Chrn2*. *Ric3* mRNA showed a decrease binding to FUS in the heterozygous mice of a log₂ fold change of -1.12, i.e. a reduction of > 2-fold. The *Ric3* mRNA encodes a protein that promotes expression of nicotinic receptors. *Chrn2*, which showed a log₂ fold change of -0.56 (i.e. a reduction to 0.67) in FUS^{ΔNLS/+} /wild type, encodes a nicotinic acetylcholine receptor. This indicates that aberrant processing of *Ric3* and *Chrn2* mRNAs may be involved in the phenotype and aberrant nicotine signaling observed in FUS^{ΔNLS/+} mice.

3.2.2. Alternative splicing in FUS^{ΔNLS/+} mouse cortex

3.2.2.1 Alternatively spliced transcripts in the cytosolic fraction

I also analyzed whether the cytosolic fraction of FUS^{ΔNLS/+} cortices contains significant changes in alternatively spliced transcripts compared to wild-type cortices.

Our analysis in the program Rmats revealed 357 significant changes in splicing events between the FUS^{ΔNLS/+} and wild type cortices. Most of these changes were alterations in exon inclusion (Figure 26). Of the 237 skipped exon events, 132 (56%) led to increased exon inclusion in FUS^{ΔNLS/+} mice while the remaining events led to decreased exon inclusion in FUS^{ΔNLS/+} mice. The next most enriched categories were equally alternative 3 and 5' splice site usage, mutually exclusive exon, followed by retained intron.

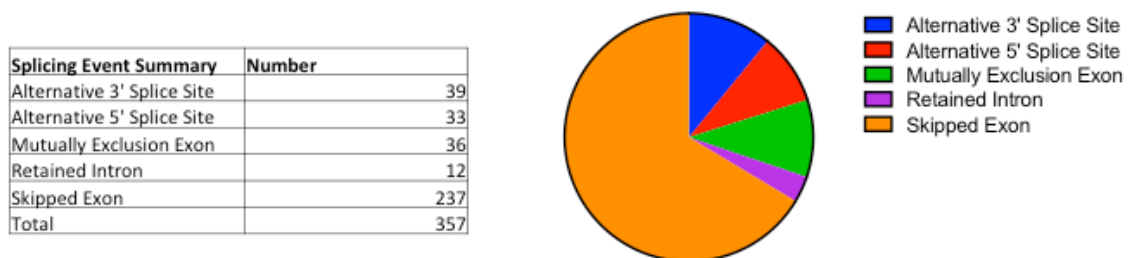


Figure 26: Alternative Splicing analysis of transcripts in the cytosolic fraction of FUS^{ΔNLS/+} vs. wild-type mice. The primary alternative splicing event that is affected in the FUS^{ΔNLS/+} mice is skipped exons, followed by alternative 3' and 5' splice site usage, mutually exclusion exon and finally retained intron.

For all splicing changes I used DAVID to perform GO and KEGG analysis (annotated pathway enrichment), and found significant enrichment in the categories poly(A) binding, transcription, proteasome, anterograde synaptic vesicle transport, lipid metabolism and dephosphorylation (Figure 27A). Interestingly, there was also enrichment in the RNA Degradation KEGG pathway (Figure 27B).

Looking through candidates with the largest splicing changes, I found a few transcripts of particular interest. *Ddhd1*, the gene that encodes for phospholipase A1 has increased inclusion of exon 3 in the *FUS^{ΔNLS/+}* mice (Figure 28A). Mutations in this gene have been associated with juvenile ALS and hereditary spastic paraplegia (C. Wu and Fan 2016; Liguori et al. 2014). *Ptprf*, encoding for LAR tyrosine phosphatase, has increased inclusion of an exon included in an isoform other than the canonical one which is part of a fibronectin type III domain (Figure 20B). Alterations in the fibronectin domains may affect extracellular binding partners. As LAR has been implicated in axon guidance, maintenance of excitatory synapses and cholinergic neuron size and number (Van Lieshout et al. 2001) perhaps this alternatively spliced isoform might contribute to defects in these areas in *FUS^{ΔNLS/+}* mice.

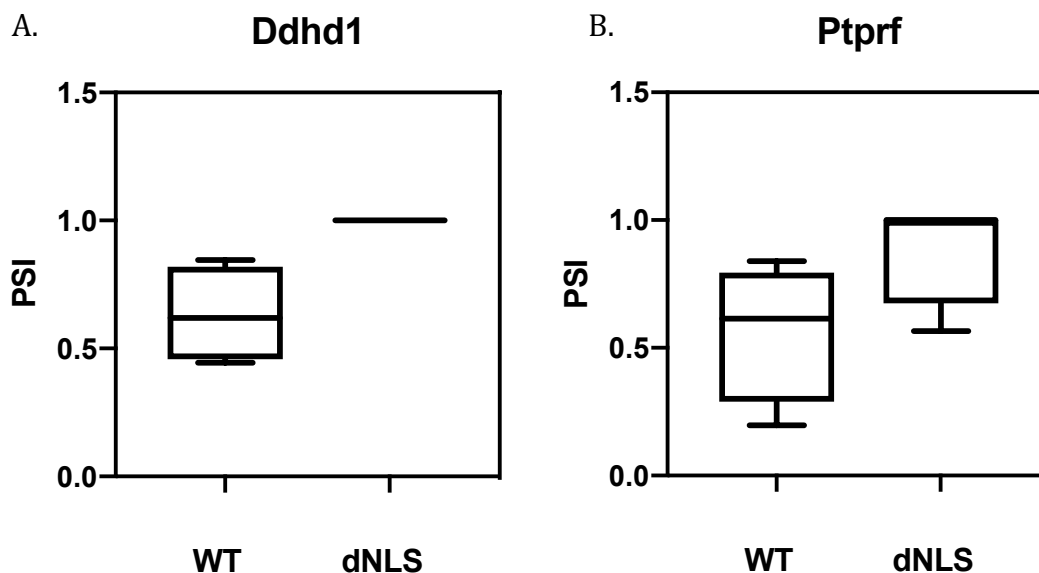


Figure 28: Box plots of showing exon inclusion differences between FUS wild type and mutant, PSI: percent spliced in. A. *Ddhd1* shows increased inclusion of exon 3 in the mutant. **B.** *Ptprf* has increased exon inclusion of exon 13 in the mutant.

3.2.2.2 Alternatively Spliced transcripts in the FUS IPs

Alternative splicing analysis of transcripts identified in the FUS-IPs yielded even more differences between the cortices of *FUS^{ΔNLS/+}* mice and wild type. In total, I found 471 changes between the two genotypes. As in the cytosolic fraction, most

changes (68.8%) were skipped exon events, followed by alternative 3' splice site, mutually exclusion exon, retained intron and finally alternative 5' splice site (Figure 29). This indicates that many alternatively spliced transcripts associate with mutant FUS in the cytoplasm of FUS^{ΔNLS/+} mutant cortices and hence could be misregulated in the mutant mice.

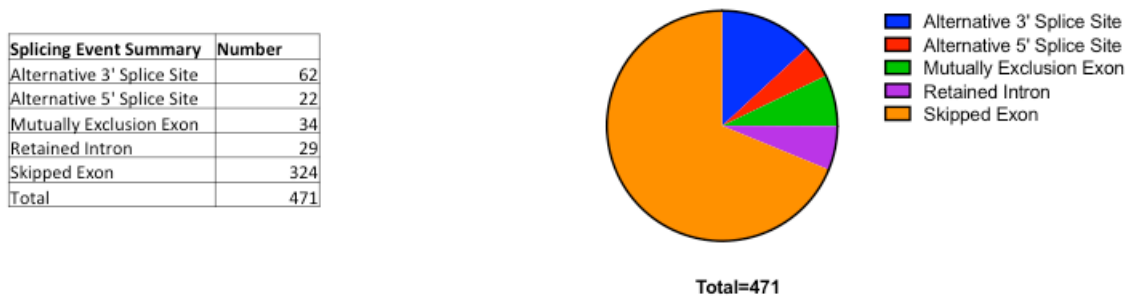
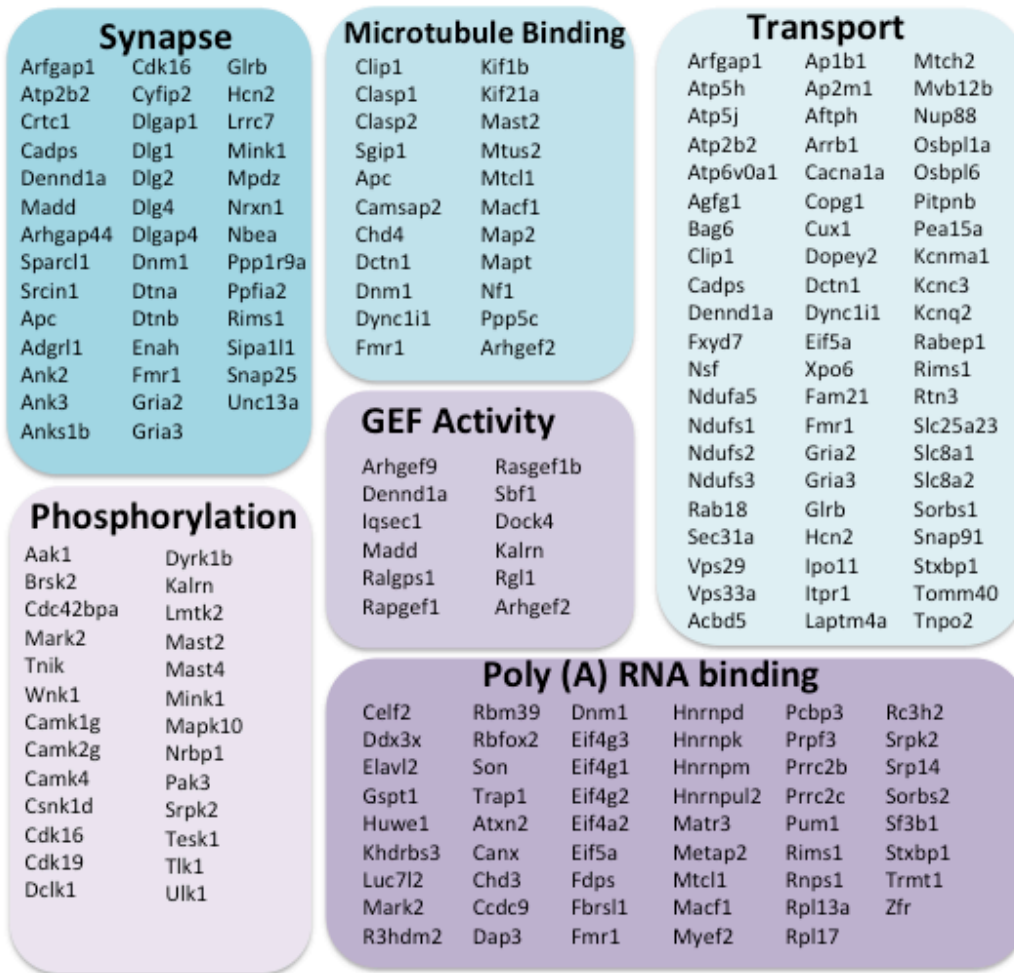


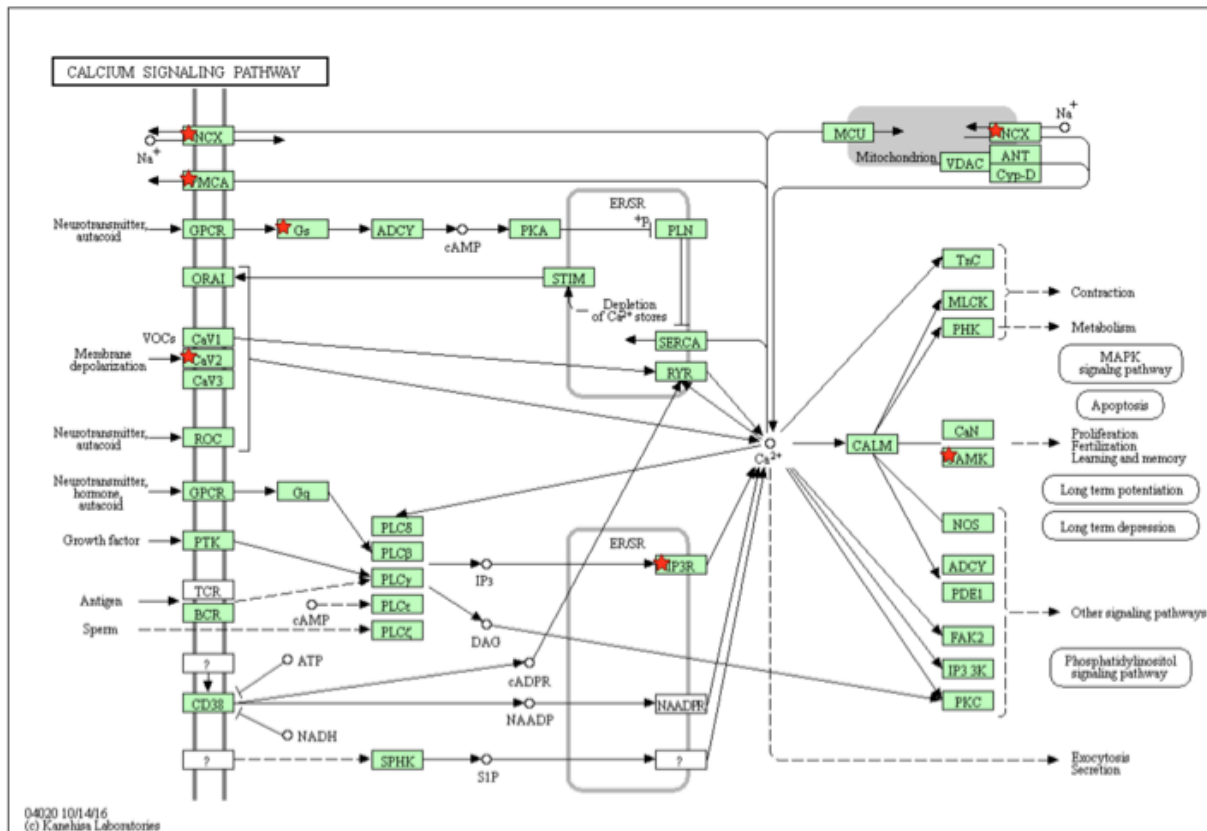
Figure 29: Summary of Alternatively Spliced Transcripts and FUS Motif Analysis. Alternative splicing analysis of the transcripts in the FUS-IPs of FUS^{ΔNLS/+} versus wild-type mice. The primary event change in mice is skipped exon, then alternative 3' usage, mutually exclusive exon, retained intron and finally alternative 5' splice site usage.

GO analysis by DAVID revealed extremely enriched categories, with the highest term, synapse, reaching an enrichment score of 10.9. The top enriched GO categories were synapse, microtubule binding, transport, phosphorylation, guanyl-nucleotide exchange activity and poly (A) RNA binding (Figure 30A). This high level of enrichment implies that mutation or relocalization of FUS has a large effect on the specified categories. KEGG pathways of interest include calcium signaling and long-term potentiation (LTP, Figure 30B and C).

A.



B.



C.

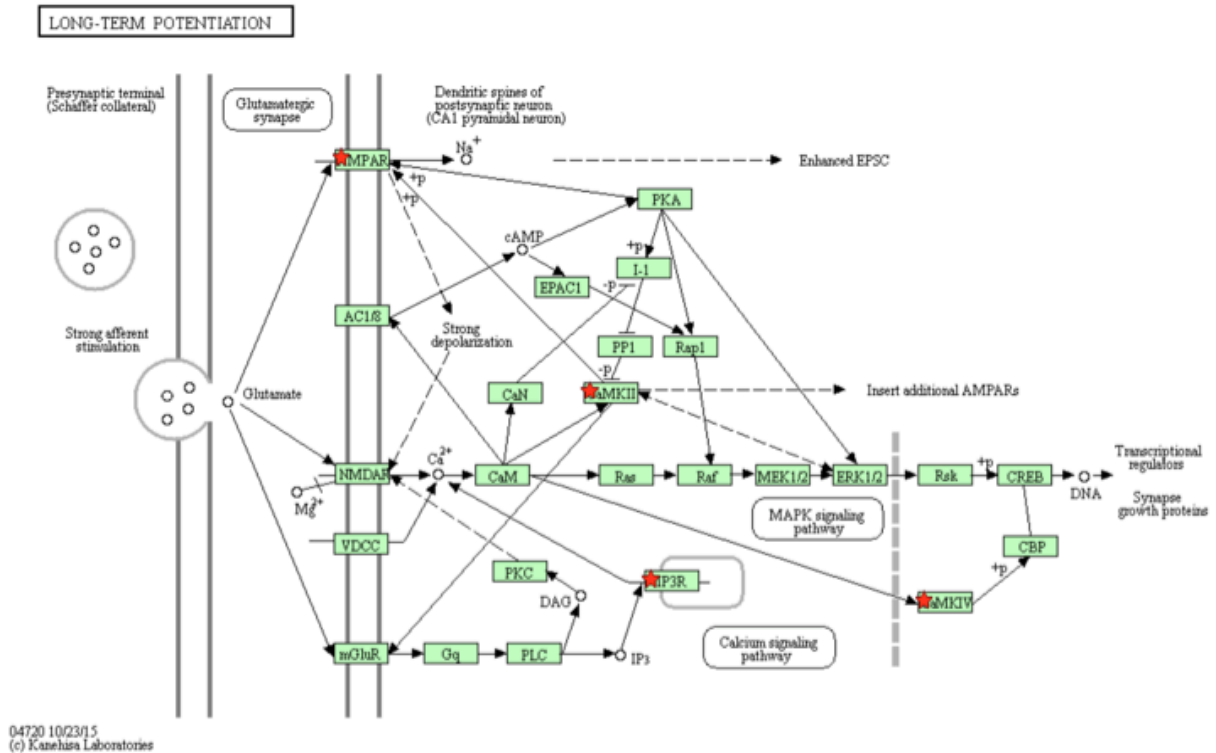


Figure 30: GO and KEGG analysis of alternatively spliced transcripts bound to FUS. A. GO enrichment analysis of the significantly different alternatively spliced RNA's in the FUS-IPs (FUS^{ΔNLS/+} vs. WT). **B.** Enrichment in the Calcium Signaling KEGG Pathway. **C.** Enrichment in the Long Term Potentiation KEGG Pathway. Alterations in these pathways and processes may point us in the direction of the upstream causes of aberrant neuronal signaling and function.

Some highly altered candidates relevant to nicotinic signaling also appeared in the IP data. Nrnx1, a cell surface receptor that is required for efficient neurotransmission and synaptic interactions (Pak et al. 2015), has a 25% increase in the inclusion of exon 7 of the canonical transcript (Figure 31A). Exon 7 makes up part of the second laminin G domain which is responsible for interactions with several partners such as, neuroligins and diacylglycerol (DAG). Macf1, a protein responsible for crosslinking actin to other cytoskeletal elements and also a microtubule binder, has a 35% increase of inclusion of an exon which makes up the microtubule-binding Gas2-related homology domain (GAR) domain of Macf1 in FUS^{ΔNLS/+} (Figure 31B). This change in isoforms could potentially affect microtubule localization or vesicle transport. *Apc*, whose protein product is involved in cell polarization, attachment and cholinergic synapse formation (Temburni 2004), shows that the mutant FUS-IP has decreased binding to an isoform which undergoes nonsense mediated decay

(Figure 31C). *Gria3*, encoding for an ionotropic glutamate receptor, shows a 40% change in inclusion of 14 (Figure 31C). This could potentially result in a change between the isoforms flip and flop, thereby altering the speed of glutamate receptor desensitization (Sommer et al. 1990; Pei et al. 2009).

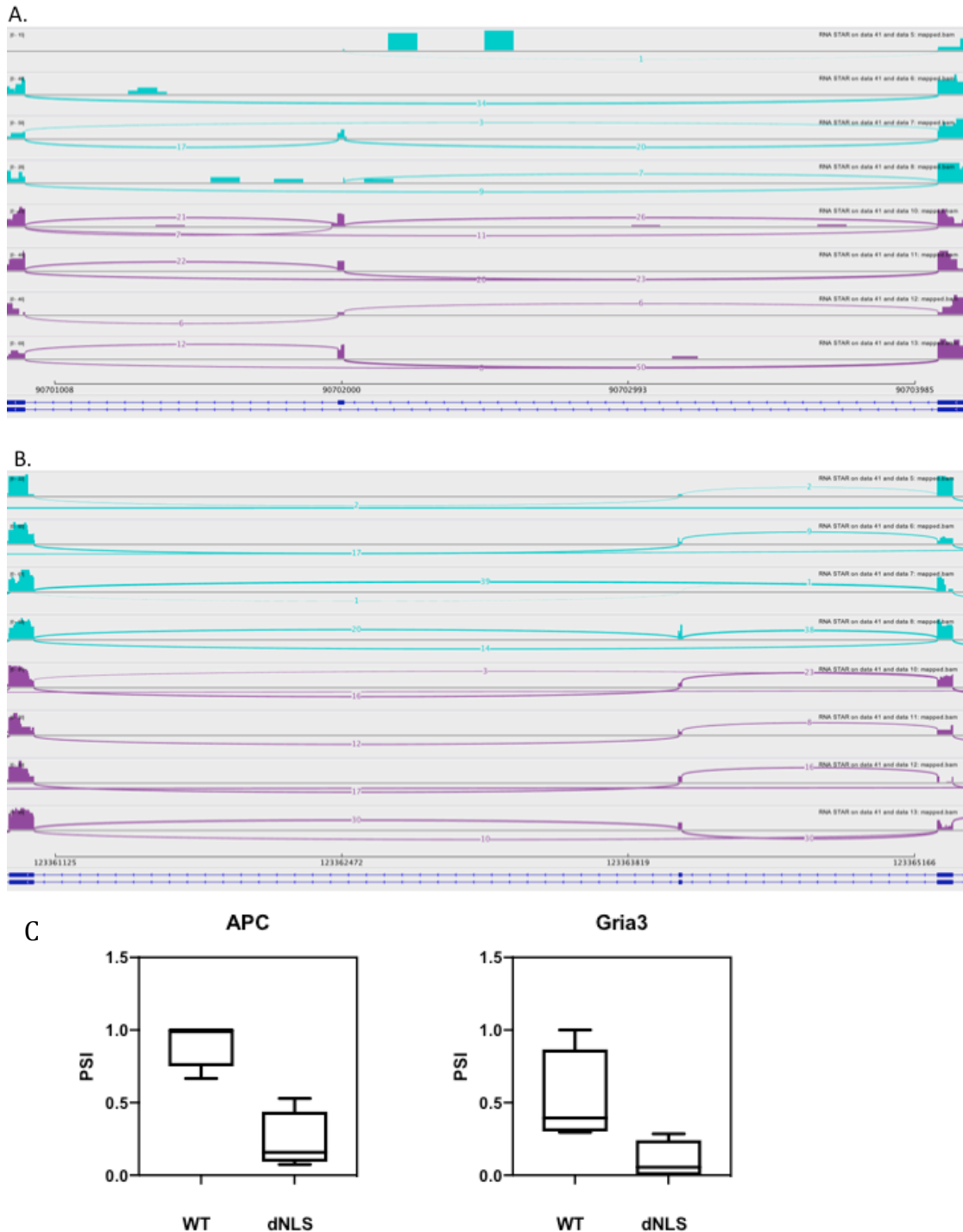


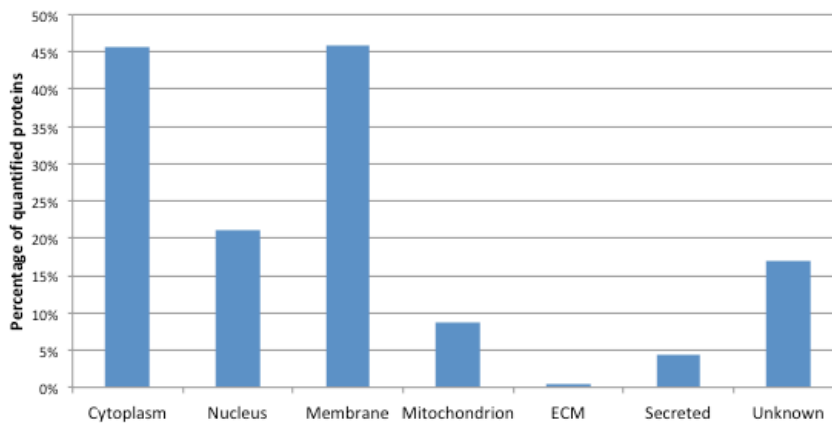
Figure 31: Alternatively spliced isoforms in HET vs. WT FUS-RNPs.

Sashimi plots showing **A.** increased exon 7 inclusion in *Nrxn1* and **B.** increased exon 89 inclusion in *Macf1* in *Fus^{dNLS/+}* mice (purple) relative to wild type (teal) as demonstrated by increased reads above stated exon. Box plots (whiskers showing minimum and maximum) showing **C.** decreased exon 2 inclusion in *APC* in the mutant mice **D.** and decreased exon 14 inclusion in *Gria3*.

3.3. Changes in the protein composition of FUS-RNPs in FUS^{ΔNLS/+} mice

In parallel to the RNA sequencing analysis, I also submitted samples for Liquid Chromatography/Mass Spectrometry (LC/MS). Following elution from the beads with Laemmli buffer, the samples were run on SDS-PAGE gels, excised from the gel in 9 fractions and then submitted to LC/MS. One sample from each genotype was excluded, as the peptide measurement was not ideal. Cell compartment analysis revealed that primarily cytosolic and membrane associated proteins were identified, followed by some nuclear proteins. (Figure 32A). Even though the mice are heterozygous for mutant FUS, we were able to identify several significantly changed proteins in mutant vs. wild-type FUS-IPs (Figure 32B).

A.



B.

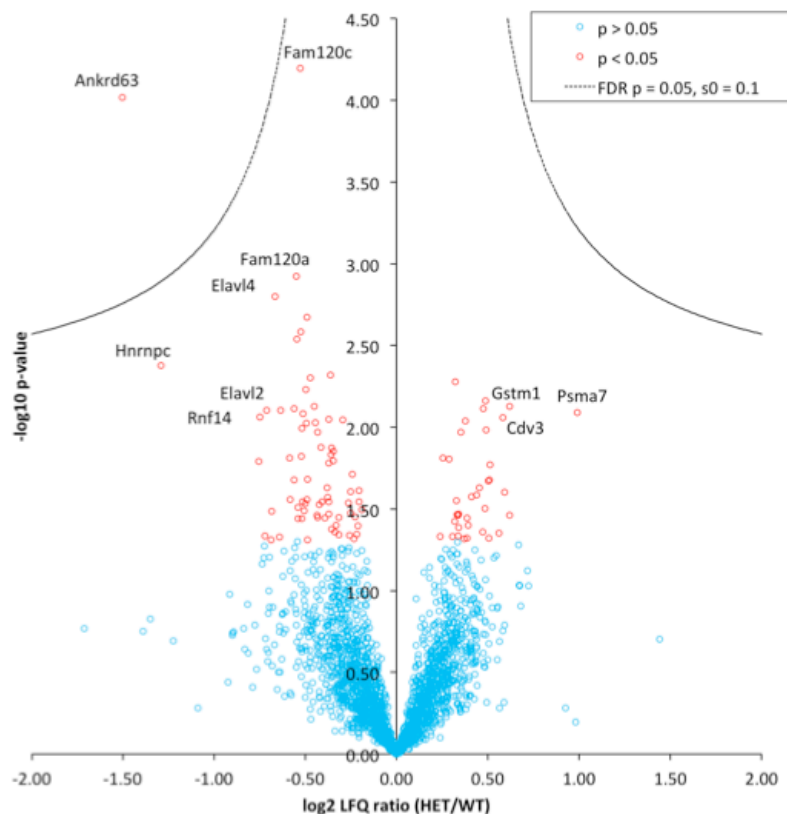
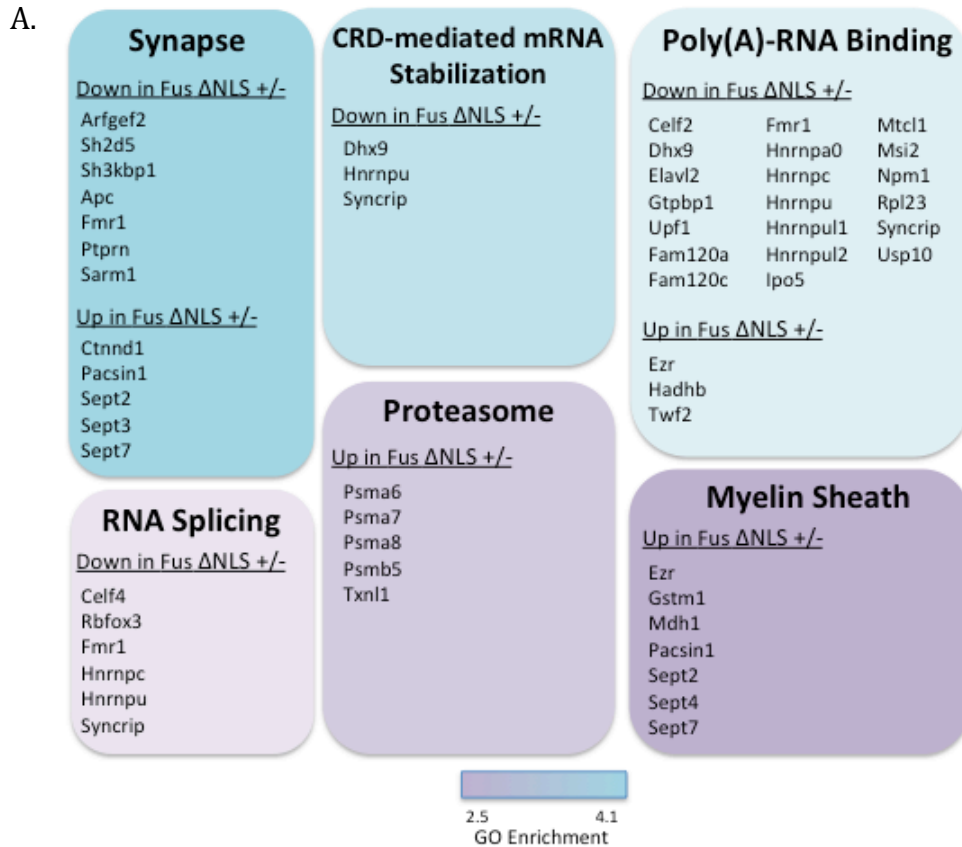


Figure 32: Cell compartment analysis and volcano plot of identified peptides. **A.** Characterization of annotated protein localization in the FUS IP. Proteins annotated to be associated with the cytoplasm and membrane were of the top identified groups. **B.** A volcano plot displaying all changed protein, those in red are significantly different ($p < 0.05$) between wild-type and FUS^{ΔNLS/+} -IPs.

GO analysis revealed several enriched categories among the significantly changed proteins, including proteins involved in synapse, CRD-mediated mRNA Stabilization, poly(A) RNA binding, RNA splicing, proteasome and myelin sheath (Figure 33A). KEGG enrichment showed an enrichment in lysosome and mTOR pathways. The proteins with the larger fold changes, either up or down, are proteins involved in RNA binding, cytoskeleton and proteasome (Figure 33B). An interesting result is that four proteins from the Septin family came up as significantly changed, implying that the interaction between FUS and the septin protein family may be altered in FUS^{ΔNLS/+} mice. As seen in the GO analysis, there was also enrichment in binding of proteins associated with the proteasome in FUS^{ΔNLS/+} mice, indicating an increased association with the proteasome.



B.

Protein	log2 Fold Change	Protein	log2 Fold Change
Ankrd63	-1.50	Sept7	0.47
Hnrnpc	-1.29	Esd	0.48
Dhx9	-0.75	Sept3	0.49
Rnf14	-0.75	Sept4	0.49
Hnrnpul1	-0.72	Psm6	0.49
Elavl2	-0.71	Hagh	0.50
Hnrnpa0	-0.69	Smpd3	0.50
Nexn	-0.68	Crip2	0.51
Elavl4	-0.67	Ddah1	0.51
Celf2	-0.64	Cspg5	0.56
Ttpal	-0.63	Cdv3	0.58
Pla2g6	-0.59	Ahcy	0.59
Arfgef2	-0.58	Gstm1	0.62
Mtcl1	-0.56	Akap7	0.62
Adam9	-0.56	Psm7	0.99

Figure 33: Analysis of protein interactors significantly changed between FUS wild type and FUS ^{Δ NLS/+} IPs. A. GO Enrichment of significantly different proteins found in the FUS IP. B. Largest Log₂-fold changes between wild type and mutant FUS-IPs (among significantly different interactors, all p<0.05)

4. FUS^{ΔNLS/+} target and interactome validation

4.1. Attempts to Establish Primary Neuronal Cultures from FUS^{ΔNLS/+} mice

As one of the goals of the project was to functionally follow up interesting candidates from the RNAseq and MS analysis and more clearly elucidate the functional role which FUS plays in the neuronal cytoplasm, I wanted to establish primary neuronal cell culture from FUS^{ΔNLS/+} mice in our lab. As this technique had not previously been set up in our lab, I first started with wild type mouse cultures.

The mice were imported into our facility in February 2018 and due to breeding problems, it took longer to expand the colony than anticipated. Therefore, I was only able to obtain one viable neuronal culture. In this culture, I stained for FUS with two of our FUS antibodies to confirm the expected cytosolic mislocalization of FUS^{ΔNLS} in the heterozygotic mice and to visualize the various staining patterns each antibody gives (Figure 34).

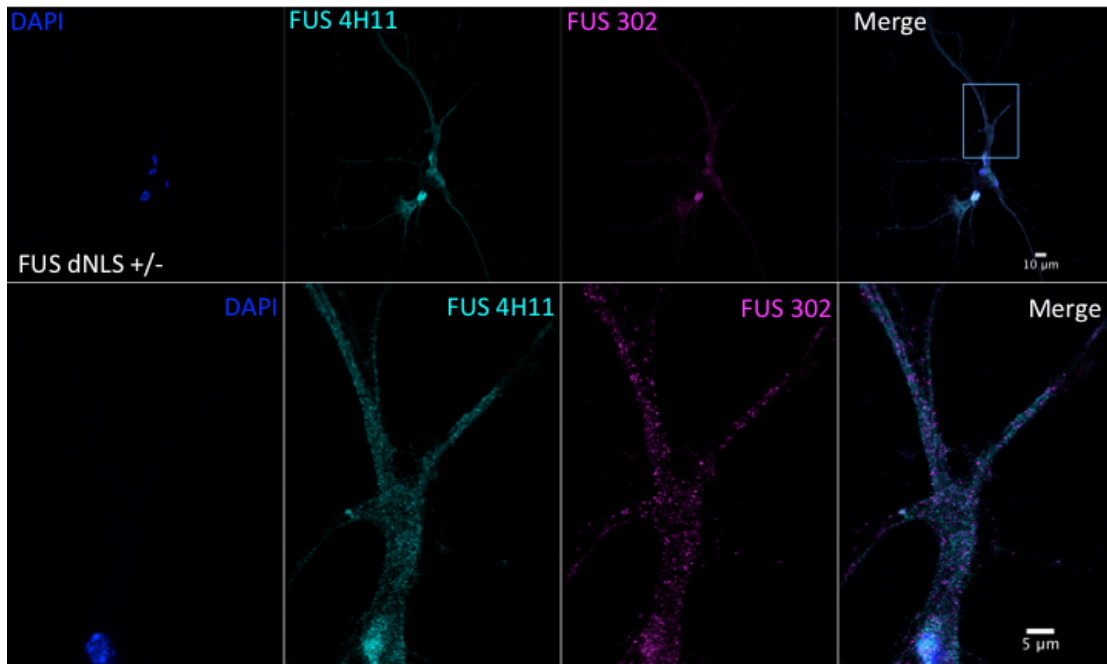
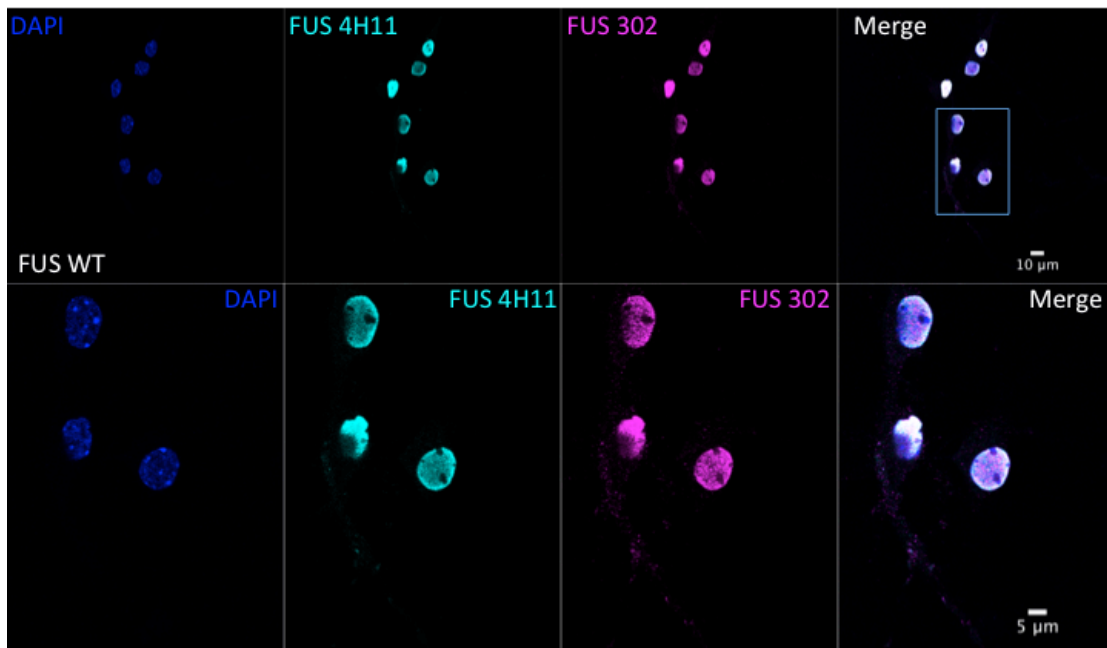


Figure 34: Immunostaining of FUS^{ΔNLS/+} (Fus dNLS +/-) and wild type mice cortical neurons with FUS antibodies. Staining with 4H11 or Bethyl antibody A300-302 yielded approximately the same staining pattern with slightly more cytosolic granular staining with the Bethyl antibody.

4.2 Analyzing candidates from the MS analysis in a FUS WT vs. FUS^{ΔNLS} expressing cell line

4.2.1 FUS and Septin Interactions

As I was not able to regularly obtain neuronal cultures of FUS^{ΔNLS/+} mice, I decided to perform some validation experiments in HeLa cells expressing FUS-WT vs. FUS^{ΔNLS}, in order to follow up on some of the observed changes in the FUS-RNP granule composition in FUS^{ΔNLS/+} mice. I used FUS knockout HeLas (obtained from our collaborator Marc-David Rüpp) and transfected them with either a wild type FUS or a FUS 514X HA-tagged expression plasmid. After either 48 or 72h of expression, I performed immunostaining for FUS and either Septin-2, 7, Caprin2 or HuD to check whether expression of FUS-514X results in an altered localization of any of the candidate proteins (Figures 35 and 36). There was no difference in the localization of Sept2, Sept7, Caprin2 or HuD in cells expressing mislocalized FUS-R514X.

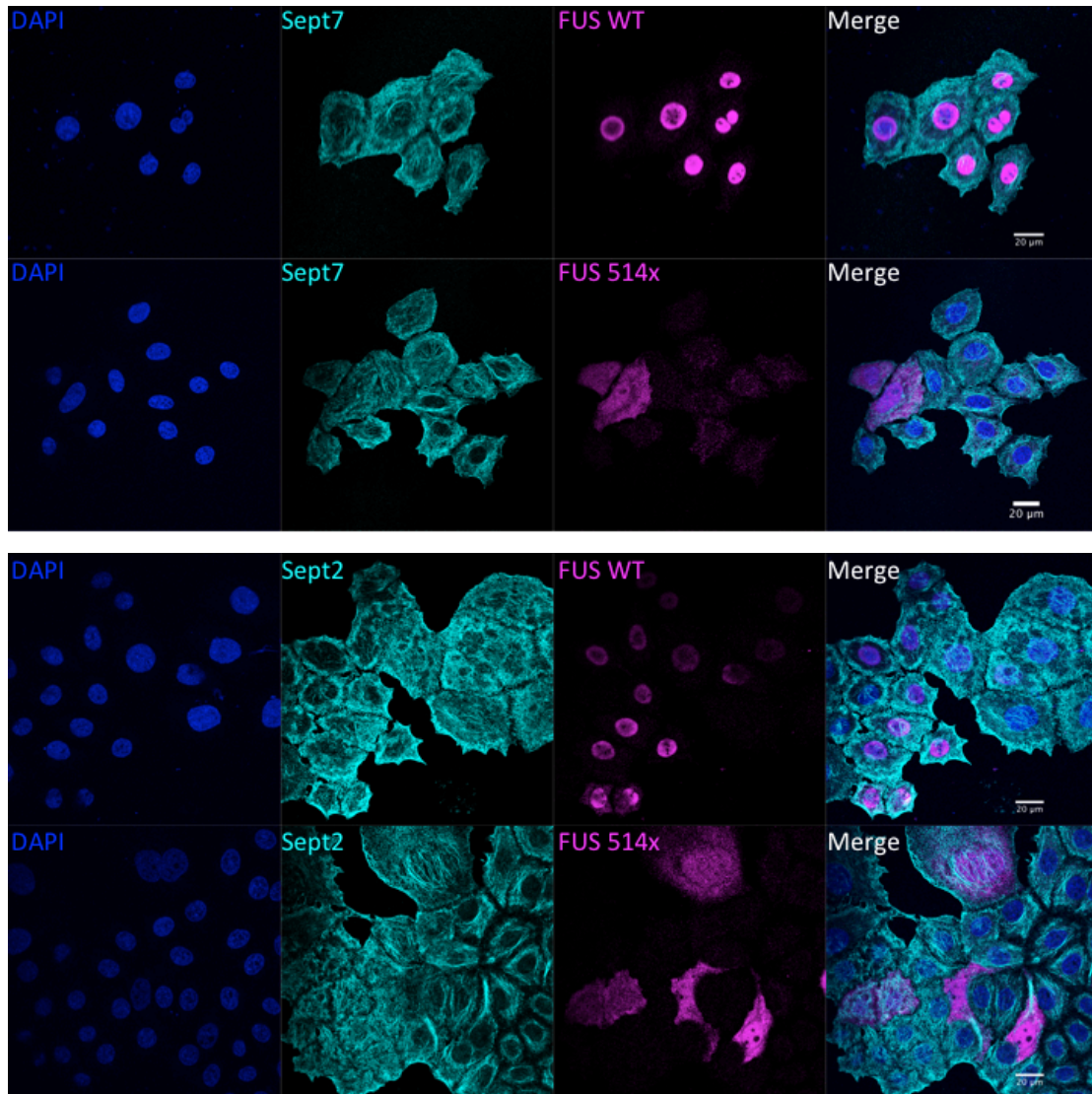


Figure 35: Septin 2 and 7 staining upon expression of either FUS wild type or 514x. Septin 2 and 7 localization remain unchanged with mutant FUS expression.

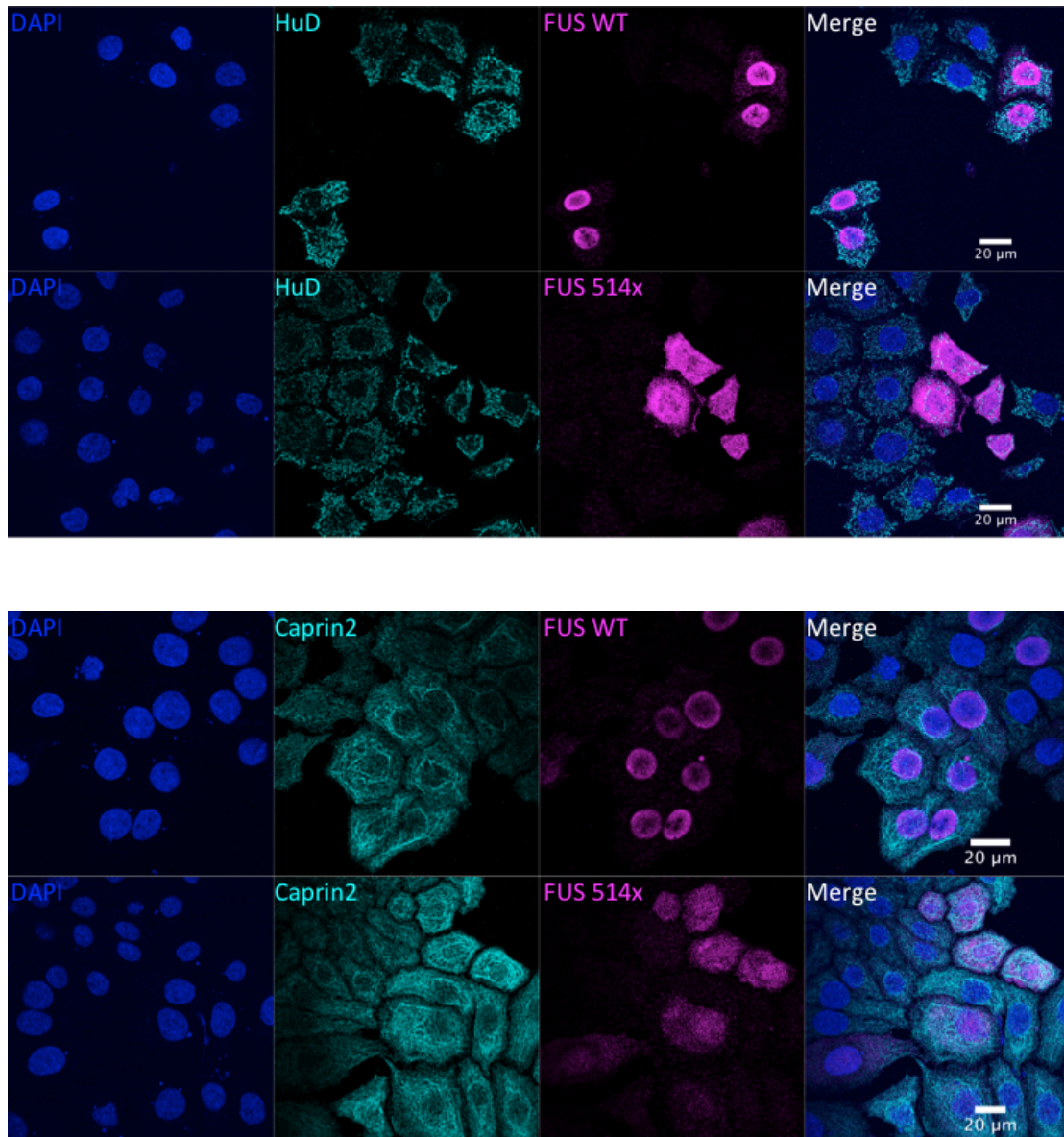


Figure 36: HuD and Caprin2 staining upon expression of either FUS wild type or 514x. HuD (A) and Caprin2 (B) localization remain unchanged with mutant FUS expression.

Additionally, I performed a double transfection of FUS knockout HeLas with FUS (wt or 514x) and Sept2-GFP or Sept7-GFP (gifts from Helge Ewers, Berlin) and again fixed at 48 and 72h post-transfection. This did not yield any changes in localization of the two septins in mutant FUS-expressing cells in comparison to FUS-WT expressing cells (Figure 37).

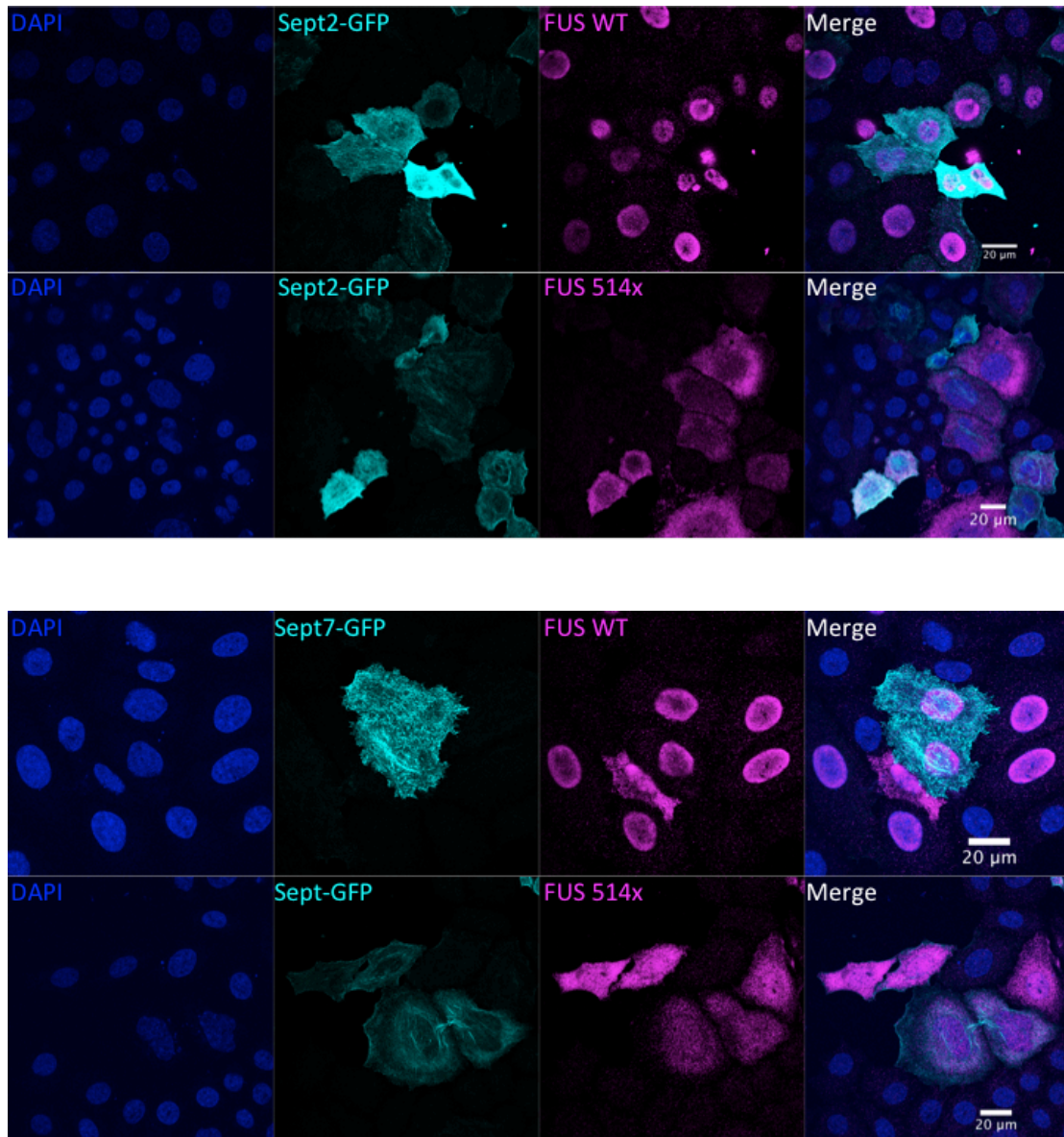


Figure 37: Septin 2 and 7 localization following transfection with Sept2 or 7 and either FUS wild type or 514x. There was no change in localization of either Septin 2 or 7 48 hours following double transfection of either Sept2 or 7 in conjunction with either FUS wild type or 514x.

4.2.2. FUS 514X and recruitment into stress granules following heat shock

Upon heat shock or other types of cellular stress, mutant FUS, but not wild type, has been shown to relocalize into stress granules (Bentmann et al. 2012). Therefore, I was interested to know if FUS 514X also recruits any of the candidate interactors into the stress granules. I transfected HeLa FUS KO cells with either wild type FUS or FUS R514X, and after 48 hours, I heat shocked the cells for 1h at 44°C then stained for Septin 7 and 2, HuD, and HNRNPUL1. Although FUS-R514X was nicely recruited into heat shock-induced stress granules, as visualized by co-staining for the SG marker protein TIA-1, there was no co-recruitment of any of the candidate proteins along with mutant FUS into SGs (Figures 38 and 39).

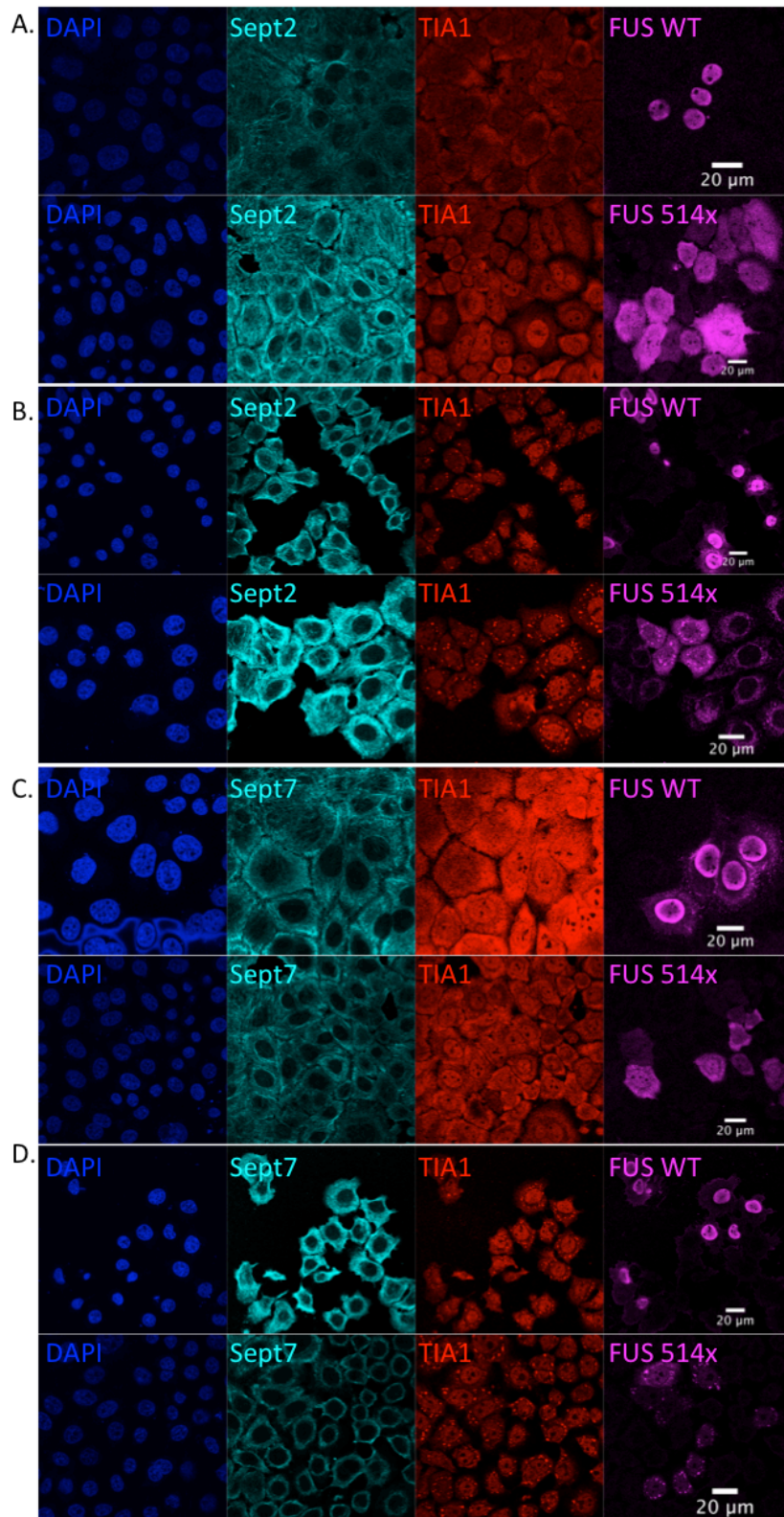


Figure 38: FUS wild type or 514x colocalization with Septins following heatshock. FUS KO HeLas were transfected with either FUS wt or 514x, after 48h they underwent heat shock and were immediately fixed and stained for FUS and **A.** Septin 2 (control) **B.** Septin 2 (heat shock) **C.** Septin 7 (control) **D.** Septin 7 (heat shock).

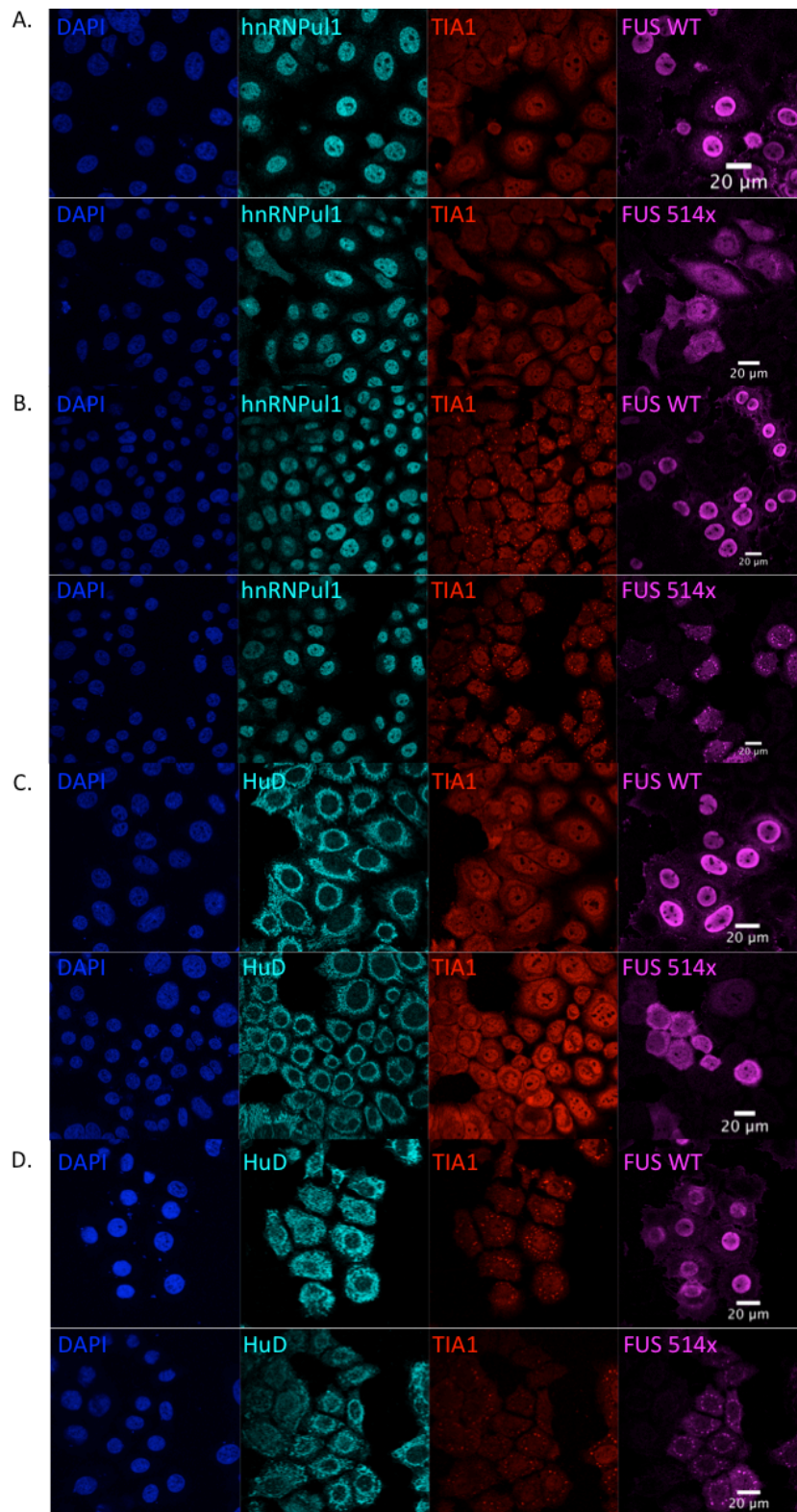


Figure 39: FUS wild type or 514x colocalization with HuD and hnRNPU1 following heatshock. FUS KO HeLas were transfected with either FUS wt or 514x, after 48h they underwent heat shock and were immediately fixed and stained for FUS and **A.** hnRNPU1 (control) **B.** hnRNPU1 (heat shock) **C.** HuD (control) **D.** HuD (heat shock)

4.2.3. Investigation into the interaction between FUS and the Proteasome

As several proteasomal subunits showed increased levels in the FUS-IPs from FUS^{ΔNLS/+} mice (Figure 33), I wanted to test whether there may be a change in proteasome activity in FUS^{ΔNLS/+} expressing cells, e.g. by sequestration of the proteasome or proteasomal subunits by mutant FUS. In order to address this question, I obtained a proteasomal activity reporter, UbG647V-GFP, from the Marc Hipp, MPI Biochemistry, Munich. Upon disruption of the proteasome, this ubiquitin reporter accumulates in the cell and yields higher GFP levels. To measure proteasome activity, I transfected the FUS KO HeLa cells with either FUS WT or R514X along with the proteasome reporter. As a positive control, I treated cells with MG132, a known proteasome inhibitor. After 48h, I fixed the cells, and stained for FUS and analyzed the cells by confocal microscopy (Figure 40). While treatment with MG132 showed a dramatic increase in reporter accumulation, no GFP signal accumulated in FUS WT or FUSR514X-expressing cells. As this experiment was carried out by transient transfection of both FUS and the reporter, it is possible that the timeframe was not long enough observe meaningful changes.

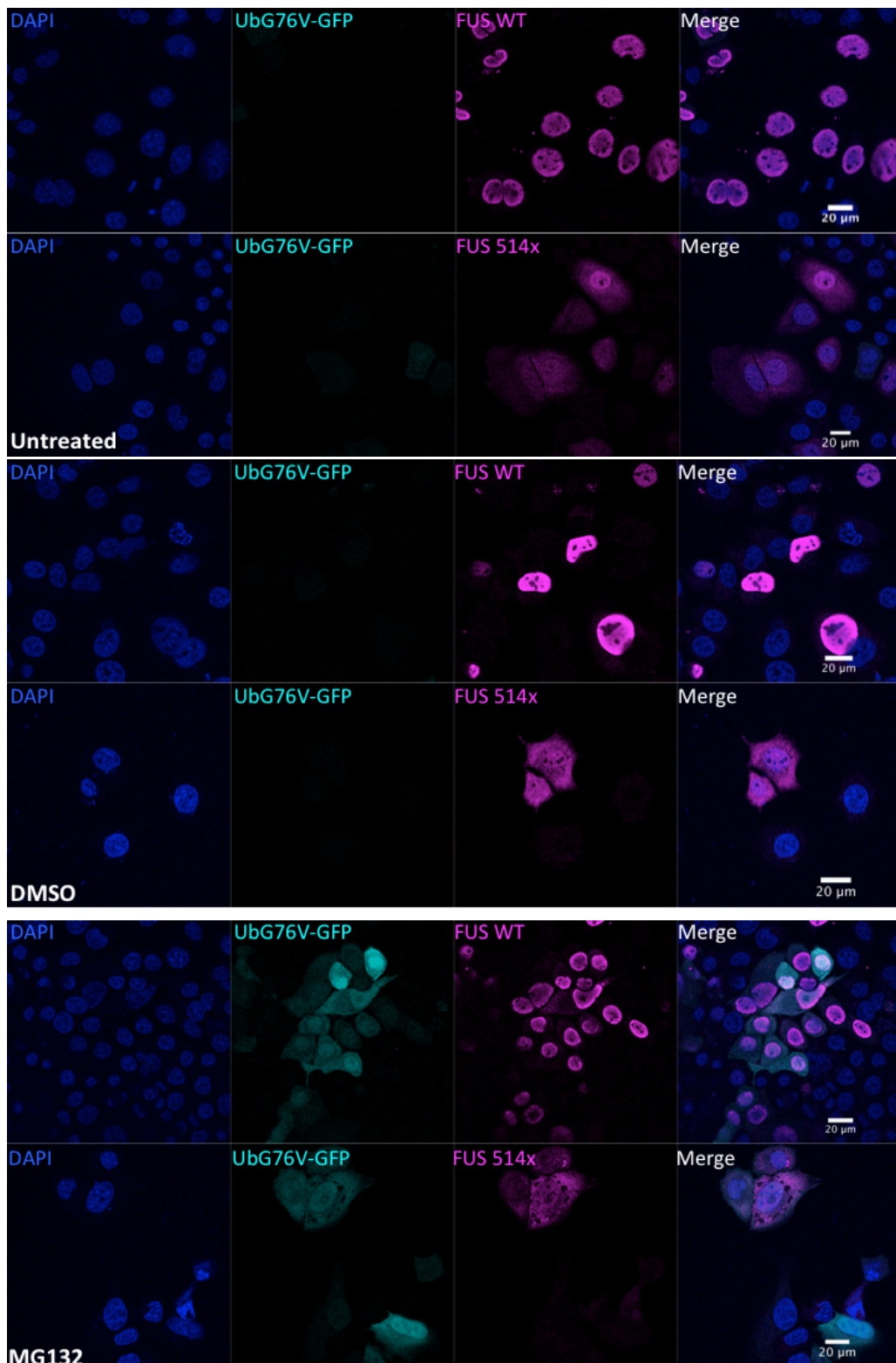


Figure 40: Proteasomal Activity Upon Expression of either FUS WT or 514x. FUS KO HeLa's were transfected with a proteasomal activity reporter, UbG647V-GFP and either FUS WT or FUS 514x. 48h following transfection, cells were either untreated, treated with DMSO or treated with MG132, fixed 5 hours later and stained for FUS.

III. Discussion

1. The FUS RNA and Protein Interactome

As FUS is primarily present in the nucleus, previous work on FUS has largely focused on its nuclear role. It plays an important role in transcription and splicing (Polymenidou et al. 2011; Ishigaki et al. 2012; Lagier-Tourenne et al. 2012; Rogelj et al. 2012; Zhou et al. 2013). More recently groups started to look at Fus outside of the nucleus (Belly et al. 2005; Fujii et al. 2005; Fujii 2005; Udagawa et al. 2015) and have discovered that FUS may be important in mRNA localization, stabilization and possibly translation. Most FUS interaction studies have focused on the entire cell, causing the dataset to be dominated by nuclear interactors (Reber et al. 2016; Hoell et al. 2011; Lagier-Tourenne et al. 2012; S. Sun et al. 2015; Kamelgarn et al. 2016) Thus far the only study focused on cytosolic FUS RNA targets was done by Colombrita and colleagues in 2012, who isolated FUS RNA targets from the cytosol of NSC-34, a motor neuron cell line cells and only for wild type FUS (Colombrita et al. 2012). In this study only wild type FUS was studied. To date no studies of cytosolic protein interactors of FUS have been carried out prior to the work described in this thesis. In order to obtain a more complete picture of the FUS interactome, I used intact mouse cortex to analyze both RNA and protein interactors. I compared the FUS RNA and protein interactome of wild type to an ALS mouse model with cytosolic mislocalization of FUS to reveal disease-related changes.

1.1. Conclusions from RNAseq

1.1.1. Changes in RNA Expression and Splicing in FUS^{ANLS/+} mice

I found very few changes in the overall abundance of RNAs in the cytosolic fraction but several differentially expressed alternative splice isoforms. The FUS IP revealed a large number of changes in both gene and transcript level abundance (Figures 25-27). The lack of gene level expression changes relative to the large amount of transcript level changes in the cytosol could indicate that FUS plays more of a role in alternative splicing, rather than overall expression.

As splicing occurs in the nucleus, this would imply that the nuclear function of FUS is affected in the *Fus*^{ΔNLS/+} mouse line. Interestingly, Dupuis and colleagues show no change in nuclear FUS expression (Scekic-Zahirovic et al. 2017). FUS has been shown to interact via its C-terminus with various SR proteins to regulate splicing (Yang et al. 1998). As the NLS is missing from these mice, perhaps the NLS is functionally important for splicing. Finally, the small amount of cytosolic gene level RNA changes is not particularly surprising as I analyzed a single time point, at a very early stage, heterozygous mouse model. Other groups using mouse lines with an altered FUS C-terminus have performed total cell RNASeq at early timepoints have also shown minimal expression changes (Funikov et al. 2018; Devoy et al. 2017).

1.1.2. Comparison with published RNASeq data from aged *Fus*^{ΔNLS} mouse line

The creators of our mouse model, the Dupuis lab, performed RNAseq on e18.5 homozygous *Fus*^{ΔNLS/+} whole brains (Scekic-Zahirovic et al. 2016) and on the spinal cords of 22-month-old *Fus*^{ΔNLS/+} mice (Scekic-Zahirovic et al. 2017). However, they did not focus on the cytoplasmic fractions and hence did not specifically look for changes to cytosolic RNAs levels. In the aged heterozygous mice, they also did not analyze splicing changes, only RNA level changes.

In the spinal cords of aged *Fus*^{ΔNLS/+} mice, they found several altered RNA transcripts related to myelination, most of them downregulated, implying an oligodendrocytic involvement in motor degeneration. While I did not find GO enrichment in transcripts related to myelination, this difference could be due to the fact that I used cortex and they analyzed spinal cord and because we examined different time points.

Although it is difficult to compare *Fus*^{ΔNLS/ΔNLS} e18.5 brains with cortices of *Fus*^{ΔNLS/+} 50 day old mice, as the former is very much in a developmental state, there is some overlap between the alternative splicing patterns. Between the two datasets, 10 transcripts have significant differential splicing, of those 10, 5 show

changes in alternative splicing of the same exon (Table 3). Excluding Hnrnp2, the splicing changes are in the same direction (both either decreased or increased inclusion in mutant mice). Two interesting transcripts that show altered splicing in Fus ^{ΔNLS/+} mice are Kcnq2 and Ntng1. Kcnq2 encodes for a potassium channel that plays an important role in neuronal excitability. Ntng1, Netrin G1, is a known splicing target of FUS (Orozco and Edbauer 2013). Netrins play an important role in development and Ntng1 is particularly important for axon guidance, synapse formation and maintenance (Yin, Miner, and Sanes 2002). Ntng1 has several splice isoforms and its alternative splicing in response to FUS knockdown has been reported by several groups (Ishigaki et al. 2012; Rogelj et al. 2012; Lagier-Tourenne et al. 2012; Nakaya et al. 2013), some of which report changes in alternative splicing of the same exon (exon 7) as we and the Dupuis group have found. It has been hypothesized that alternative splicing may result in altered ligand affinity. Perhaps the expression of the alternative splice isoform in FUS mutant mice results in changes to synapse maintenance, resulting in altered synaptic activity and possibly increased synaptic vulnerability.

Gene	Inclusion	
	Fus dNLS/-	Fus dNLS/dNLS
Wbp1	Increased	Decreased
Xpa	Increased	Decreased
Ntng1	Decreased	Decreased
Angel2	Increased	Decreased
Hnrnp2	Decreased	Increased
Kcnq2	Decreased	Decreased
Kif21a	Increased	Increased
Tpd52l2	Increased	Decreased
Tpm1	Increased	Increased
Ybx1	Decreased	Decreased

Table 3: Overlap of alternatively spliced transcripts between heterozygous and homozygous Fus ^{ΔNLS} mice. Alternatively spliced transcripts that show an altered splice isoform pattern in both Fus ^{ΔNLS} homozygotic embryos (Dupuis) and the Fus ^{ΔNLS} heterozygotic adult cortices cytosol (this study). In bold are transcripts with changes in the same exon in both datasets.

1.1.3. Involvement of FUS in the nicotinic signaling pathway

In correspondence with the Dupuis lab, we have learned that they have been unable to culture primary neurons derived from *Fus*^{ΔNLS/ΔNLS} embryos, as these neurons die after approximately 8 days in culture (Diana Wiesner, unpublished data). They found that the survival of *Fus*^{ΔNLS/ΔNLS} neurons can be rescued with nicotine. Because of this finding, they treated *FUS*^{ΔNLS/+} mice with nicotine. Surprisingly, the mice were completely resistant to the effects of nicotine relative to wild type littermates. We therefore scrutinized our RNASeq data for any clues that may explain defects in the nicotinic pathway. We found that *Chrn2* and *Ric3* mRNA levels were decreased in the cytosolic FUS-IP in *Fus*^{ΔNLS/+} mice vs. wild-type mice (*Chrn2*: log2 fold change = 0.56; *Ric3*: log2 fold change = 1.12). *Chrn2* is a type alpha 4 beta 2 nicotinic acetylcholine receptor, and *Ric3* functions as a chaperone to nicotinic acetylcholine receptors (Rempel et al. 1998; Halevi et al. 2002). In our splicing analysis, we found alternative splice isoforms of *Apc*, *Macf1*, *Nrxn1* and *Ptprf* in *Fus*^{ΔNLS} mice vs. wild-type controls. The proteins encoded by these mRNAs could be involved in nicotinic receptor assembly and interestingly, *Nrxn1* is a known splicing target of FUS (Lagier-Tourenne et al. 2012; Nakaya et al. 2013). *Apc* and *Macf1* associate with microtubules and are important for axonal guidance. *Nrxn1* is vital for synaptic transmission and certain polymorphisms have been related to nicotine dependence (Nussbaum et al. 2008). *Ptprf*, also known as LAR, has been implicated in axon guidance, development and maintenance of excitatory synapses and is important for cholinergic neuronal number, size and targeting (Dunah et al. 2005) (Van Lieshout et al. 2001).

In order to follow up on some of these interesting candidates from our RNASeq analysis, one could study whether their mRNA and/or protein levels are changed at synapses of *Fus*^{ΔNLS/+} mice. This could be done by performing synaptosomal preparations, running qPCR on the RNAs and immunoblotting against the proteins. Additionally, using primary neuronal culture and confocal microscopy, one could look at both RNA and protein localization.

1.1.4. RNAs that show differential binding to cytosolic Fus^{ΔNLS/+} vs. FUS-WT

GO analysis showed enrichment in several categories, including Transcription, RNA Binding, Lipid Metabolism, Proteasome, G-protein Signaling and Ion Transport (Figure 25), indicating that mRNAs/proteins from these functional categories may be disturbed in Fus^{ΔNLS/+} mice. Reduced binding to transcripts encoding RNA-binding proteins could indicate that the fate of these mRNAs in the cytoplasm is altered, e.g. in terms of mRNA stability, transport or local translation. This could result in altered levels of the encoded RBPs, or in altered local production of the corresponding RBP, thereby altering cytosolic RNP granule composition and dynamics. For example, Nono mRNA shows decreased binding to Fus in Fus^{ΔNLS} mice compared to wildtype controls (log₂ fold change = -0.93). Interestingly, An et al. recently found in a SH-SY5Y of Fus^{ΔNLS} model that FUS and Nono have reduced interaction, causing dysfunction in paraspeckle formation (An et al. 2019).

FUS may regulate translation, disruption of the NLS in mouse models causes translation to become misregulated, whether the effect is only on axonal protein synthesis or global, is still under debate (López-Erauskin et al. 2018; Kamelgarn et al. 2016). It is therefore possible the binding of FUS to different transcripts results in either impeded or differential translation of these transcripts. Perhaps we are seeing the very early stages of a disruption in translation.

1.1.5. Alternative splicing changes in Fus^{ΔNLS/+} mice cortices

Both the cytosolic input and the immunoprecipitated fraction contained many interesting splicing changes in Fus^{ΔNLS/+} mice compared to wild-type controls, primarily splicing events involving skipped exons (Figures 26 and 29). Splicing changes in the cytosolic fraction were enriched in the GO categories RNA binding, Transcription, Proteasome, Anterograde Transport, Lipid Metabolism and Dephosphorylation (Figure 27). Interestingly, there was also an enrichment in the KEGG pathway RNA degradation. Aside from splicing changes in mRNAs involved in to the nicotinic pathway (discussed above), another individual

candidate of interest is *Ddhd1*, a gene that encodes for phospholipase A1 and is responsible for hydrolyzing phosphatidic acid. Mutations in this gene have been associated with juvenile ALS and hereditary spastic paraplegia, possibly due to altered lipid metabolism (C. Wu and Fan 2016; Liguori et al. 2014) . Different isoforms may change substrate specificity. It is possible that a change in substrate specificity of this type could result in altered energy metabolism.

Alternatively spliced transcripts in the FUS IP were enriched in the GO categories Synapse, Microtubule Binding, Transport, Phosphorylation, GEF Activity and Poly (A) RNA Binding (Figure 30) as well as the KEGG pathways Calcium Signaling and Long Term Potentiation. This could indicate that FUS in the cytoplasm is associated with mRNAs that are vital for intracellular transport as well as, synaptic signaling and integrity.

Glutamate receptors are critical for cell signaling and survival. FUS has an intricate relationship with glutamate receptors, stimulation of mGluR5 results in FUS translocation to spines (Fujii et al. 2005) and FUS regulates *GluA1* mRNA stability (Udagawa et al. 2015). *GluA1* mRNA was identified in the FUS IP, but there is no difference in the binding between wild type and mutant. But we do see a difference in the alternative splicing of exon 14 of *Gria3*, another glutamate receptor subunit. Alternative splicing of this exon would result in a change between flip and flop isoforms, which have different receptor desensitization rates (Pei et al. 2009). Altered presence of the flip or flop isoforms in other glutamate receptors has been shown to increase susceptibility to excitotoxicity and alter neuron excitability (Y. H. Park et al. 2016; Lykens et al. 2017).

It would be interesting to follow up whether a change in flip/flop isoforms of *Gria3* are also seen on the protein level and whether this causes changes of either *Gria3* localization or expression levels. If this would be confirmed, one could also examine FUS^{ANLS/+} neuron response to *Gria3* stimulation.

1.1.6. RNASeq Follow Up

The RNASeq results give us specific candidates that show altered FUS interaction. The next step would be to determine what this means. Do the proteins produced from the differentially binding RNAs have aberrant localization or expression levels? This could be addressed by performing immunohistochemistry and either western blot or ELISA on cortices or synaptosomal preparations of the *Fus^{ΔNLS/-}* mice or by immunostaining *Fus^{ΔNLS/-}* primary neurons. If the proteins are mislocalized, this could be due to mislocalization of their mRNA. If mutant *Fus* is causing mislocalization of its target mRNAs, performing FISH on either cultured neuron or brain sections could verify this.

If the encoded proteins show altered levels, what is the underlying mechanism? Is altered FUS binding causing changes to mRNA stability or to translation? Or perhaps mutant FUS is altering proteasomal activity. First, one must determine the best system in which to follow up. My study was performed in 50 day old mouse cortices, while continuing in mice would provide valuable insight, it comes with constraints. Aside from time to age the mice (repeating the experiments at later time points would be extremely valuable) and the difficulty to introduce expression constructs, the cortex is full of many cell types. Therefore, we cannot say that the changes we observe are from neurons and we may be missing cell-specific changes. Performing the initial follow-up experiments in vitro or in dissociated primary neurons would be a good first step to further understand the role of FUS in mutant and wild type conditions. While cultured neurons come from a developing embryo (resulting in a different transcriptome and proteome than adult mice) and can be more difficult to express constructs, they would allow us to look in a neuron, compartment-specific manner at RNA localization and translation. Since they are derived from embryos, we would also be able to compare homozygous neurons and perhaps see more robust RNA regulation changes.

A commonly used method to address mRNA stability involves inhibiting transcription with Actinomycin D and then measuring mRNA levels over time with either qPCR or Northern Blot. This experiment could be tested in either primary neurons or HeLa cells expressing either mutant or wild type FUS. In the case that mutant FUS negatively affects mRNA stability, the mRNA would more rapidly decay over time. The role of FUS in mRNA translation could be addressed either in vitro or in a cell-based assay. One way to do this would be with a reporter assay, such as luciferase. It could be performed in vitro with rabbit reticulocyte lysate, the target of interest plus luciferase and FUS. As FUS functions cooperatively and perhaps in a location-specific manner, an assay in neurons may be better suited to address this question. One could transfect a reporter attached to the 3' UTR of the target of interest, such as luciferase or a SunTag (Yan et al. 2016), into *Fus*^{ΔNLS/+} expressing and wild type neurons. The readout of both assays would show if there is an increase or decrease in translation in the presence of mutant FUS.

1.2. Changes in the cytosolic FUS protein interactome in *Fus*^{ΔNLS/+} mice

Fus^{ΔNLS/+} mice have an altered cytosolic FUS protein interactome. The mechanism by which this arises could be due to several factors. The first of which would be a result of more FUS in the cytoplasm, not only could the availability of more FUS create the opportunity for new aberrant protein interactions but also it increases self-self interaction and phase separation (Patel et al. 2015; Hofweber et al. 2018). Also, interactions which are dependent on the C-terminal NLS could be reduced or lost. The consequences of this altered interactome could result in both of a gain or a loss of mechanism. Some proteins may be abnormally sequestered into mutant FUS granules, no longer able to fulfill their normal function. Additionally, altered RNP granule composition may result in altered mRNA processing.

1.2.1 Comparison to other interactome studies

In 2018, Kamelgarn and colleagues expressed flag-tagged wild type R495X or P525L FUS in N2a cells and then immunoprecipitated FUS (Kamelgarn et al. 2018). They found an increase of translation and mRNA surveillance-related proteins associated with mutant FUS. Our data shows a decrease in FUS interaction in mutant mice in a few ribosomal proteins (Rplp1 and Rpl23). Additionally, they found an increase in UPF1 expression and phosphorylation, signaling an increase in nonsense mediate decay (NMD). Interestingly, UPF1 binding to FUS was decreased in *Fus*^{ΔNLS/+} mice cortices. The discrepancies between the two studies could be explained by the use of different cell types (neuroblastoma cell line vs mouse cortex) or overexpression of flag-tagged FUS vs. physiological expression levels.

Although the fold changes of the interactions with FUS are small, they are some interesting hits. Blokhuis et al. used biotinylation tagging to examine FUS wild type and R521C interactors in N2a cells. Their top disease-related proteins of interest that showed increased aggregation with mutant FUS included several of our top hits (Blokhuis et al. 2016). *Fmrp*, *Upf1*, *HuD* and *Dhx9* had increased colocalization with FUS R521C but were all significantly decreased in binding to FUS in the *Fus*^{ΔNLS/-} cortices. The discrepancy between the increased co-aggregation seen in the Blokhuis data and the decreased co-immunoprecipitation in our data could be explain by either the lack of presence of aggregates in the *Fus*^{ΔNLS/+} cortices or by the missing NLS. Nonetheless, the overlaps in changes of interactors between the two mutants are interesting.

1.2.2. Overlap with unmethylated FUS interactors

FUS is normally asymmetrically dimethylated (ADMA-FUS). In human ALS-FUS cases, normally methylated FUS is found in FUS-positive inclusions, while FTLD-FUS patients have an accumulation of unmethylated and monomethylated FUS (Dormann et al. 2012; Scekcic-Zahirovic et al. 2017; Suárez-Calvet et al. 2016) .

Thus, FUS shows an altered methylation status in FTD-FUS patients and is hypomethylated. Recently, our group has shown that loss of FUS arginine methylation promotes FUS phase separation (Hofweber et al. 2018) and thus is likely to promote FUS aggregation.

To test whether loss of FUS arginine methylation, as seen in FTD-FUS patients, causes other abnormal protein-protein interactions, Mario Hofweber performed a biochemical pulldown with recombinant unmethylated vs. methylated MBP-FUS immobilized on MBP-trap beads and nuclear and cytosolic fractions of adult mouse cortices. After stringent washing, he processed the protein samples on the beads for LC-MS, to identify differential interactors of unmethylated vs. methylated (ADMA-modified) FUS. He identified a large number of interactors that bound more strongly to unmethylated FUS and a small number of proteins that bound more strongly to methylated FUS (unpublished data). These proteins are potentially disease-relevant, as their function might be disturbed in FTD-FUS patients by the aberrant interaction with unmethylated FUS. Therefore, I compared his list of abnormal unme-FUS interactors with my list of altered Fus^{ANLS/-}-protein interactors, as this comparison might identify proteins that normally interact with FUS, but whose interaction is disturbed in both FTD-FUS and ALS-FUS. . The overlap between my list of altered interactors in the Fus^{ANLS/+} IP and his list of proteins that show differential binding to unmethylated FUS yielded 4 proteins: Fam120c, Hnrnpul2, Tnpo2 and Upf1 (Table 4).

Protein	Fus dNLS/-	Unmethylated Fus
Fam120c	-0.53	2.49
Hnrnpul2	-0.69	2.16
Tnpo2	-0.49	2.84
Upf1	-0.38	2

Table 4: Proteins that immunoprecipitate differentially in cortices of Fus^{ANLS/-} mice vs wild type, but also bind differentially to unmethylated vs. methylated FUS. Numbers are log₂-fold changes.

Interestingly, all of these proteins show increased binding to unmethylated FUS relative to methylated, yet, they show a decreased binding to FUS in the *Fus*^{ΔNLS/-} cortices. This could indicate that these four proteins normally interact with FUS, but more strongly when methylation is lost, and less strongly when the C-terminal NLS is missing. Since one of the methylated RGG repeat domains is directly next to the PY-NLS at the C-terminal end of FUS (Figure 2), it seems possible that these proteins interact with FUS via the C-terminal RGG3-PY domain and that these interactions are altered upon loss of RGG3 methylation and NLS deletion. These four hits could be followed up by looking for colocalization using immunostaining in either a cell line or primary neurons.

1.2.3. Fus and the proteasome

Ubiquitinated inclusions are a hallmark pathology of ALS and FTD. Protein quality control is maintained by two different systems, the ubiquitin-proteasome system (UPS) and the autophagy-lysosome system. One group disrupted the proteasome system by knocking out a component of the 26s proteasome in motor neurons. Disruption of the UPS in motor neurons resulted in an ALS-like phenotype in mice (Tashiro et al. 2012). In 2015, Wang and colleagues overexpressed either FUS wild type or P525L in HEK 293 cells, immunoprecipitated FUS and evaluated the differential interactome of mutant vs. wild type FUS. They found two proteasome-related proteins to have increased binding to FUS P525L, UBA1 and PSMD12 (T. Wang et al. 2015). Although both of these proteins were present in our cytosolic FUS-IPs, there is no difference in binding between wild type and mutant. However, our RNASeq showed an increase in *Psme4*, *Psmd6*, *Psme4* mRNA in mutant FUS IP relative to wild type (Figure 25). Several mRNAs that encode for proteasomal components (Figure 27) have alternative splice isoforms present in the cytosol in the cortices of *FUS*^{ΔNLS/+} mice. Finally, LC-MS showed differential binding of several proteasomal components. Proteasomal subunits *Psma6*, *Psma7/8*, *Psmb5* and *Txnl1* all showed increased interaction with FUS under mutant conditions (Figure 33).

The results of the RNASeq and MS suggest that FUS may regulate proteasomal activity both on the RNA and protein level. Is FUS regulating proteasomal mRNA localization and/or translation? And secondly, is mutant FUS either sequestering proteasomal subunits, inhibiting proteasomal activity, or is the proteasome trying to clear away mutant FUS? In order to address the second question, I transfected FUS KO HeLa's with either FUS wild type or FUS 514x in combination with a proteasomal activity reporter. While I did not observe a difference between FUS wild type and 514x, which could have multiple reasons, e.g. that the proteasomal binding differences were cortex-specific or age-dependent, as we observed them in 50 day old mouse cortices. Additionally, 48-72 hours of mutant FUS expression may simply not be enough time to cause changes in the UPS.

In order to fully explore the possibility of disruptions to the UPS, more experiments would be need to be conducted. The Hipp lab, which generously shared the construct with us, has a stable cell line expressing the proteasome reporter, which could be used more accurately measure proteasomal activity (using flow cytometry), although transfection of FUS constructs into these cell lines would results in overexpression of FUS and not accurately reflect the situation we have in the $Fus^{\Delta NLS/+}$ vs. wt mice. A preferred option would be to transfect cultured the $FUS^{\Delta NLS/+}$ and wild type neurons with the proteasome activity reporter, as this would allow us to study proteasomal activity under conditions of stable $Fus^{\Delta NLS/+}$ vs. FUS-wt expression. Unfortunately, I was unable to derive primary neuronal cultures from the mice due to breeding issues (see results, section 4.1).

As some proteasomal mRNAs differentially interact with mutant FUS, this may alter their subcellular localization and therefore translation. Aside from investigating proteasomal activity, one could also look at the localization of proteasomal components with immunohistochemistry of cortical brain sections or cultured neurons.

1.2.4. FUS and the Septins

Septins are cytoskeletal GTPases that can form into heteromeric complexes, filaments and rings. Interacting with actin, microtubules and phospholipids, not only are septins important protein scaffolds, they are important for dendritic spine arborization (Mostowy and Cossart 2012; Kaplan et al. 2017). Recently, Ewers et al. demonstrated that Sept7 restricts membrane protein flow across dendritic spine necks, acting as a diffusion barrier. In particular, they showed that presence of Sept7 reduces GluA2 subunit-containing AMPAR diffusion into spines (Ewers et al. 2014). Our data show an increase in the binding of Fus to Sept2, 3, 4 and 7 (Figure 34). Additionally, through correspondence with the Ewers lab, we have learned that they found wild type FUS as an abundant protein in a Sept7 immunoprecipitation (unpublished results, Helge Ewers, Berlin). This suggests that FUS might, under physiological conditions, interact with Septins and play a role in the diffusion barrier at dendritic spine necks. This raises many interesting questions: What is the role of the Septin-FUS interaction? Does Sept7 also function as a diffusion barrier for FUS-containing RNP granules? FUS has been found in complex with NMDA receptor complexes (Husi et al. 2000) and found within spine heads (Belly et al. 2005), so it will be interesting to test whether this localization is affected by Septins. Finally, what are the functional consequences of the stronger interaction of mutant FUS with Septin, does it affect the function of Septins as a diffusion barrier at the spine neck? Or is mutant FUS somehow getting stuck on the diffusion barrier at the base of the dendritic spine and unable to properly to deliver its target mRNAs into the spine?

These questions would be best addressed in neuronal cultures where a role of Sept7 as a diffusion barrier at dendritic spine necks has been described (Ewers et al. 2014). Unfortunately, since we were not able to derive enough primary neuronal cultures from FUS^{ΔNLS}/- mice due to breeding problems, we attempted to study Septins in HeLa cells, where Septins are also expressed and regulate microtubule stability (Kremer, Haystead, and Macara 2005) . We did not see any change in Sept2 or 7 localization after 48h of wild-type vs. mutant FUS

expression and no co-recruitment of Septins with mutant FUS into stress granules (Figures 36, 38 and 39). To further explore the FUS-Septin interaction, one could perform biochemical experiments, e.g. co-IPs of FUS or Septins, to validate that mutant FUS interacts more strongly than FUS- WT with Septins. Another possibility would be to look into changes to microtubules, as Septins were shown to be important for microtubule stability (Kremer, Haystead, and Macara 2005). Finally, it would be ideal to study the FUS-Septin interaction in primary neurons or brain slices from the FUS^{ΔNLS/+} mice, e.g. by testing whether Sept7 and Sept2 are mislocalized or whether an impairment of diffusion into dendritic spine is seen in FUS mutant neurons. .

Glutamate receptor regulation is also an integral FUS role. FUS regulates GluA1 mRNA stability (Udagawa et al. 2015), Fus^{ΔNLS} binds preferentially to an alternative splice form of Gria3 and finally Fus^{ΔNLS} shows increased association to several members of the septin family, including Sept7. Sept7 forms a diffusion barrier at dendritic spine necks, thereby regulating GluA2 spine expression (Ewers et al. 2014).

2. Conclusion

Not unexpectedly, our results point to defects of several systems in young, early-symptomatic Fus^{ΔNLS/+} mice: RNA metabolism, transcription, synaptic transport, signaling and proteostasis. In conjunction with the preliminary results from our collaborators in the Dupuis lab, several mRNA and protein expression changes seem to point to involvement of the cholinergic system. Two other potentially affected systems might be the proteasome and the septin cytoskeleton. Ubiquitinated inclusions found in ALS and FTD, as well as the disruption of proteasome activity leading to an ALS-like phenotype (Tashiro et al. 2012) make proteasomal degradation a promising candidate pathway. As the mice used in this study are just beginning to manifest symptoms, it would be interesting to follow-up with additional time points, perhaps these transcriptomic and proteomic changes will be more pronounced and are the starting point for neurodegeneration.

IV. EXPERIMENTAL PROCEDURES

1. Mouse breeding and genotyping

Mice were generated by the Dupuis Lab (as described in (Scekic-Zahirovic et al. 2016)). The mouse colony was maintained by crossing male $Fus^{\Delta NLS/+}$ mice with wild type C57BL/6J female mice. Timed matings for cortical neuron preparation were performed using $Fus^{\Delta NLS/+}$ mice and either wild type or $Fus^{\Delta NLS/+}$ female offspring from the aforementioned breeding scheme. Genotyping of the mice was performed using ear tissue; the DNA was extracted and amplified using the Extract -N-Amp PCR Kit (Sigma). Individual mouse embryos were genotyped using the cerebellum. The primer sequences used to amplify the *Fus* locus are listed in Table 5 and the detailed PCR protocol in Table 6. Following amplification, PCR products underwent 2% agarose gel electrophoresis. The expected amplicon sizes are 160 base pair for wild type and 240 base pair for mutant.

<u>Primer</u>	<u>Primer Sequence</u>
FUSdNLS-Forward	GAT-TTG-AAG-TGG-GTA-GAT-AGT-GCA-GG
FUSdNLS-Reverse	CCT-TTC-CAC-ACT-TTA-GTT-TAG-TCA-CAG

Table 5: Primer Sequences for $Fus^{\Delta NLS}$ genotyping.

<u>Temperature</u>	<u>Time (mm:ss)</u>	<u>Cycles</u>
95°C	03:00	1
95°C	01:00	34
62°C	01:00	34
72°C	01:00	34
72°C	10.00	1

Table 6: PCR protocol for amplification of the *Fus* wild type and $Fus^{\Delta NLS}$ locus.

2. Subcellular Fractionation of Adult Mouse Cortices

Mice were euthanized and cortices were extracted and fresh frozen in liquid nitrogen and stored at -80°C until processing. Cortices were removed from the -80°C and immediately chopped with a razor blade on a glass petri dish over ice and then placed into a 2 mL dounce homogenator containing ice cold hypotonic buffer (10 mM HEPES pH7.9, 10 mM KCl, 1.5 mM MgCl₂ and protease inhibitor mix (Sigma)). Cortices were gently and briefly dounced by moving the pestle up and down slowly 7-10 times (until all visible tissue was solubilized) and then allowed to rest for 10 minutes on ice. Samples were then transferred to an eppendorf tube and vortexed several times. Following vortexing, the samples were centrifuged at 3,000 x g for 5 minutes at 4°C. The supernatant was removed to another tube. The pellet (nuclear fraction) was washed one time with hypotonic buffer and resuspended in hypertonic buffer (10 mM HEPES pH 7.9, 10 mM KCl, 1.5 mM MgCl₂, 150 mM NaCl, 0.5% NP-40, protease inhibitor (Sigma)). The supernatant was centrifuged at 14,000 x g for 5 minutes, the supernatant from this spin was then collected as the cytosolic fraction. Samples were either stored at -80°C until later use or immediately used for FUS immunoprecipitation (IP). In the finalized protocol, NaCl to a final concentration of 150 mM was added to the cytosolic fractions before IP

3. FUS Immunoprecipitation (IP)

The first trial runs of this procedure used protein A or G sepharose beads (Helmholtz Antibody Core Facility), blocking of the beads with 1 ug/ul BSA (Sigma) and 20 ug/ul yeast tRNA (Invitrogen) and performing the IP in the presence of 10% glycerol. Control IgG (rabbit or mouse IgG, Santa Cruz , cat. #sc-2027 and sc-2025) tests used 4 ug of either rabbit or mouse IgG per IP. The final immunoprecipitation (IP) procedure excludes these steps and was as follows:

For each IP sample, 50 μ l Protein G-linked Dynabeads (Thermo Fisher, cat. # 1007D) were washed two times with phosphate buffered saline (PBS). 4 μ g of mouse anti-Fus Antibody (Santa Cruz, 4H11) was incubated with the beads for 1.5 h on a rotating wheel at 4°C. Afterwards, beads were first washed two times with PBS and then with 0.1 M Borate buffer pH 9. The antibody was then covalently conjugated to the beads by adding 5.2 mg/ml dimethyl pimelidate (DMP, Sigma) in 0.1 M Borate buffer pH 9 for 30 minutes at room temperature with occasional agitation, this step was repeated one time. The antibody-conjugated beads were then washed two times with 50 mM glycine pH 2.5 and stored in PBS at 4°C until use.

For pre-clearing the cytosolic fraction, unbound Dynabeads were washed two times with IP buffer (hypotonic buffer plus 150 mM NaCl) and then incubated with the cytosolic fraction for 1h at 4°C on a rotating wheel. The pre-cleared cytosolic fraction was removed and then incubated with of the antibody-conjugated beads for 1.5 h at 4°C while rotating. Afterwards, the beads were washed 3 times with IP Buffer. During the final wash step, samples were split in half and then either eluted with room temperature Tri Reagent RNA Isolation Reagent (Sigma) (incubation for 10 min at room temperature and then the supernatant transferred to a new tube) or by boiling for 5 min in 2x Laemmli buffer. Samples were stored at -80°C until submission to the appropriate facility.

4. RNAseq library preparation and RNA Sequencing analysis

RNA in Trizol (Tri Reagent, Sigma) was submitted to the Laboratory for Functional Genome Analysis (LAFUGA) at the Gene Center Munich. There, RNA was isolated using Direct-zol RNA Miniprep Kit (Zymo) and RNA quality was determined using Nanodrop ND-1000 (ThermoFisher Scientific) and 2100 Bioanalyzer (RNA 6000 Nano, Agilent). cDNA library preparation was completed with Encore® Complete RNA-Seq Library Multiplex DR Systems Kit (NuGEN) and multiplexed sequencing was performed on the HiSeq 1500 (Illumina) using 100 bp single end reads.

RNA Sequencing Analysis was performed by Dr. Tobias Straub of the Biomedical Center at LMU (on a collaborative basis). Sequencing reads were aligned to the mm10 genome using STAR aligner, for transcript level analysis, the transcript levels were quantified using Rsem. Following normalization to the cytosolic input, differential expression was calculated. For alternative splicing, following alignment to the genome, Rmats was used to calculate differential splicing events. Gene Ontology and KEGG Analysis were performed using DAVID (<https://david.ncifcrf.gov/summary.jsp>).

5. Mass spectrometry

All IP samples were submitted to the laboratory of Prof. Stefan Lichtenthaler for sample preparation and MS analysis by Dr. Stephan Müller (on a collaborative basis).

5.1 Sample preparation for mass spectrometry

In the first FUS IP experiments, samples in Laemmli buffer were separated on a 10% SDS PAGE. The gels were cut into six or eight fractions and subjected to in-gel digestion. In gel digestion and peptide purification were performed as previously described (Shevchenko et al. 2006). Briefly, proteins residing in the gel were denatured with 10 mM dithiothreitol (DTT) in 100 mM ammonium bicarbonate (ABC), reduced with 55 mM iodoacetamide (IAA) in 100 mM ABC and proteolytic digestion was performed at 37°C overnight using 150 ng trypsin per fraction. 40% acetonitrile (ACN) supplemented with 0.1% formic acid was used to extract the peptides. Peptides were dried by vacuum centrifugation, and reconstituted in 0.1% formic acid for proteomic analysis.

Some in-gel digestions could not be analyzed properly because of contamination problems. Therefore, we applied another sample preparation method (on-bead digestion) for the final experiment that is better suited to remove contaminations. Samples in Laemmli buffer were subjected to a modified single-pot solid-phase-enhanced sample preparation (SP3) protocol (Hughes et al. 2019). Briefly, 10 µL of a 4 µg/µL bead slurry of Sera-Mag SpeedBeads A and B

(GE Healthcare) were added to the samples. Protein binding to the magnetic beads was achieved by adding acetonitrile (ACN) to a final volume of 70 % (v/v) and mixing at 1200 rpm at 24 °C for 30 min in a Thermomixer (Eppendorf). Magnetic beads were retained in a DynaMag-2 magnetic rack (Thermo Fisher Scientific) and the supernatant was discarded. Cystines were alkylated by adding 25 µL of 80 mM iodoacetamide (Sigma-Aldrich) and incubated at 1200 rpm at 24 °C for 30 min in the dark in a Thermomixer. The reaction was quenched by adding 3 µL of 200 mM DTT (Biozol). Protein binding to the beads was repeated in 70% (v/v) ACN for 30 min. After removing the solvent, beads were washed twice in 200 µL 70% (v/v) ethanol and twice in 180 µL of 100% (v/v) ACN. Next, 250 ng of LysC and 250 ng of trypsin (Promega) were added in 20 µL of 50 mM ammonium bicarbonate (Sigma). The protein digestion was performed for 16 h at room temperature. Samples were acidified with formic acid to a final concentration of 1% (v/v) and placed in the magnetic rack. The supernatants were transferred into fresh 0.5 mL protein lobind tubes (Eppendorf). A volume of 20 µL of 2% (v/v) dimethyl sulfoxide was added to the beads and samples were subjected to sonication for 30 s in a water bath. Tubes were placed in the magnetic rack and the supernatants were transferred to the same tubes. The samples were dried in a vacuum centrifuge and dissolved in 20 µL 0.1% formic acid.

5.2 LC-MS/MS analysis

Samples were analyzed by LC-MS/MS for relative label free protein quantification. A volume of 10 µL per sample was separated on a nanoLC system (EASY-nLC 1200, Thermo Scientific) using an in-house packed C18 column (30 cm x 75 µm ID, ReproSil-Pur 120 C18-AQ, 1.9 µm, Dr. Maisch GmbH) with a binary gradient of water (A) and acetonitrile (B) containing 0.1% formic acid at 50°C column temperature and a flow rate of 250 nl/min (gradient for final experiment: 0 min., 2.4% B; 2 min., 4.8% B; 92 min., 24% B; 112 min., 35.2% B; 121 min., 60% B; gradient for in-gel digested samples: 0 min, 2% B; 3:30 min 5% B; 48:30 min, 25% B; 59:30, 35% B; 64:30, 60% B).

The nanoLC was coupled online via a nanospray flex ion source (Proxeon – part of Thermo Scientific) equipped with a PRSO-V2 column oven (Sonation) to a Q-Exactive (in-gel digestion 1), a Velos Pro Orbitrap (in-gel digestion 2), or a Q-Exactive HF (SP3 digestion) mass spectrometer (Thermo Scientific).

On the Velo Pro Orbitrap mass spectrometer, full MS spectra were acquired in profile mode at a resolution of 60,000 covering a m/z range of 300-1400. The ten most intense peptide ions per full MS scan were chosen for collision induced dissociation (CID) within in the ion trap (isolation width: 2 m/z ; normalized collision energy: 35%; activation q : 0.25; activation time: 10 ms). A dynamic exclusion of 60 s was applied for peptide fragmentation. On the Q-Exactive mass spectrometer, full MS spectra were acquired at a resolution of 70,000. The top 10 peptide ions were chosen for Higher-energy C-trap Dissociation (HCD) with a normalized collision energy of 25% and an isolation width of 2 m/z . Fragment ion spectra were acquired at a resolution of 17,500. A dynamic exclusion of 60 s was used for peptide fragmentation. On the Q-Exactive HF, full MS spectra were acquired at a resolution of 120,000. The top 15 peptide ions were chosen for Higher-energy C-trap Dissociation (HCD) with a normalized collision energy of 26% and an isolation width of 1.6 m/z . Fragment ion spectra were acquired at a resolution of 15,000. A dynamic exclusion of 120 s was used for peptide fragmentation.

5.3 LC-MS/MS data analysis and label free quantification

The raw data was analyzed by the software Maxquant (maxquant.org, Max-Planck Institute Munich) version and 1.5.5.1 (Cox et al. 2014). The MS data was searched against a reviewed canonical fasta database of *Mus musculus* from UniProt (downloads: In-gel Digestion 1: June 08th 2016, 16798 entries In-gel Digestion 2: January 11th 2017, 16843 entries; SP3 digestion: January 17th 2018, 16954 entries). Trypsin was defined as protease. Two missed cleavages were allowed for the database search. The option first search was used to recalibrate the peptide masses within a window of 20 ppm. For the main search peptide mass tolerances were set to 4.5 ppm. The fragment mass tolerances were set to

20 ppm for samples analyzed on Q-Exactive instruments and to 0.5 Da for samples analyzed on the Velos Pro Orbitrap mass spectrometer. Carbamidomethylation of cysteine was defined as static modification. Acetylation of the protein N-term as well as oxidation of methionine were set as variable modifications. The false discovery rate for both peptides and proteins was adjusted to less than 1%. Label free quantification (LFQ) of proteins required at least two ratio counts of razor peptides. Only unique peptides were used for quantification. The option “match between runs” was enabled with a matching time of 1 min. Samples were normalized separately for each batch of biological replicates.

In a test experiment, three different antibodies for Fus (mouse 4H11 and rabbit A300-294 and 11570-1-AP) and two control IgGs (mouse and rabbit IgG) were used for the Fus Co-IP. The LFQ ratios of the different antibodies against the mouse or rabbit IgG controls were calculated for each protein. The three protein LFQ ratios were \log_2 transformed and a one-sample T-test against a μ_0 of zero was applied separately for mouse and rabbit normalized ratios to estimate the significance of the protein abundance differences.

In a second test experiment, mouse 4H11 antibody against Fus and two mouse IgG controls were used in the Co-IP experiment. Therefore, protein LFQ ratios of the two Co-IPs against the related control IgG identify were calculated to identify potential binding partners of FUS.

In the final experiment, the FUS mouse 4H11 antibody was used on wild-type vs. Fus^{ΔNLS/-}-samples, protein LFQ intensities were \log_2 transformed, the mean \log_2 LFQ ratio was calculated and a Student's T-test was applied to identify significant changes between samples of Fus^{ΔNLS/-} and wild type mice.

6. SDS-PAGE and Immunoblotting

Laemmli buffer was added to the samples, which were then run on SDS-PAGE gels, either self-made or pre-cast AnyKD gels (Bio-Rad). Protein was then

transferred to a nitrocellulose membrane (Bio-Rad) by either wet transfer (using a Mini Trans-Blot® Electrophoretic Transfer System (Bio-Rad) or semi-dry transfer (using the Bio-Rad Trans Blot Turbo). The membrane was blocked in Tris buffered saline with Tween-20 (TBS-T) with 5% milk and then incubated with the specified primary antibody overnight at 4°C or for 1h at RT and after washing (3 times in TBS-T) with a suitable secondary antibody (see Table 6). Blots were imaged using the Licor's Odyssey CLx imaging system. Densitometry measurements were carried out in ImageJ.

7. Optiprep Gradient and High Speed Centrifugation

A 15-30% Optiprep gradient (hypotonic buffer, Optiprep (Sigma), H₂O, 1 mM DTT, protease inhibitor (Roche)) was prepared in polyallomer tubes. Briefly, a 15% and 30% Optiprep solution (in hypotonic buffer with 1 mM DTT and protease inhibitor) were prepared, the 15% solution was gently layered onto the 30% solution. Samples, treated with or without RNase I (Thermo Fisher) for 1h at 37°C, were gently placed on top of the gradient and ultracentrifuged at 197,500 x g for 2.5 h at 4°C and then 1 mL fractions were collected from top to bottom.

To extract proteins from each fraction, a chloroform-methanol precipitation was performed. The samples were centrifuged and the pellet was resuspended in Laemmli and then analyzed by SDS-PAGE and immunoblotting.

For high speed centrifugation, nuclear and cytosolic fractions were either untreated, treated with RNase I (Thermo Fisher) or DNase I (NEB) for 1h at 37°C. Samples were then centrifuged at 20,000 x g for 15 min at 4°C, a fraction of the supernatant and the pellet were collected for SDS-PAGE and Western blot analysis. The remaining supernatant was transferred to a new tube and centrifuged at 100,000 x g for 30 min at 4°C. Supernatant and pellet fractions were then analyzed by SDS-PAGE and Western blot analysis.

8. Cell Culture

HeLa cells and FUS knockout HeLa cells (created as described in Suarez-Calvet 2017) were cultured in Dulbecco's Modified Eagle Medium (DMEM) with Glutamax (Life Technologies) supplemented with 10% fetal calf serum (FCS, Life Technologies) and Gentamycin (10 mg/ml, Invitrogen). SH-SY5Y cells were cultured in DMEM/F12 with Glutamax plus 10% FCS (Life Technologies) and Gentamycin (10 mg/ml, Invitrogen).

All transfections were performed in 24 well plates with Turbofect (Thermo Fisher) with a maximum of 500 ng/well of DNA. Double transfections with FUS and Septin constructs were performed at 2:1 ratio and double transfection with FUS constructs and the proteasome activity reporter, Ub-G76V-GFP, were carried out at a 3:1 ratio. Transfected cells were analyzed 48h days post-transfection.

9. Primary Neuronal Culture

Timed pregnancies of either C57BL/6J wild type x wild type or C57BL/6J *Fus^{ANLS/-}* x wild type were initiated. At e15.5, pregnant females were sacrificed by CO₂ followed by cervical dislocation. Embryos were extracted and cortices were removed into Hank's Balanced Salt Solution (HBSS, Thermo Fisher). The cerebellum was removed for genotyping (as described in section XX). Cortices were then incubated with trypsin (Thermo Fisher) for 10 min at 37°C and then resuspended in Neurobasal medium plus 10% horse serum (Thermo Fisher) and triturated with a fire-blasted pipette (Figure 42). Cells were filtered with a 100 um and then a 70 um filter, counted and plated onto poly-D-lysine coated coverslips. Poly-D-lysine coverslips were prepared by adding 1 mg/mL poly-D-lysine in borate buffer for 1 hour. Coverslip were then rinsed one time with Millipore water and then treated with UV light to sterilize.

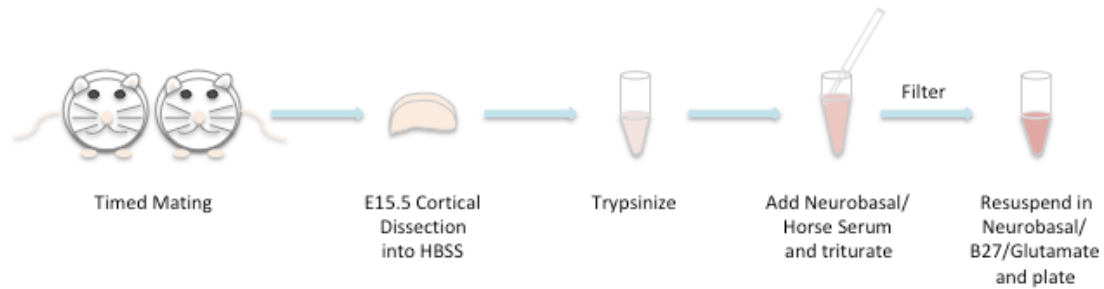


Figure 42: Cortical neuron dissociation workflow. A timed mating between adult mice was set up, embryos were taken at E15.5 and cortices dissected into Hanks Balanced Salt Solution (HBSS). Cortices were trypsinized at 37°C for 10 minutes. and neurobasal medium + 10% horse serum were added for quenching. The cortices were triturated, the neurons passed through a 70 μm filter, centrifuged for 3 minutes at 500 x g and then resuspended in neurobasal medium + B27 supplement+ glutamax. The neurons were cultured up to 10 days with one 50% medium change.

10. Immunostaining

All steps were performed at room temperature. Cell lines were washed one time in PBS then fixed in 4% formaldehyde, neurons in 4% formaldehyde/4% sucrose in PBS for 10 minutes. Permeabilization of the cell lines and neurons was done with 0.2% Triton X-100 or 0.1% Triton X-100 in PBS, respectively. All wash steps were performed in PBS with 0.1% saponin (PBSS). Cells were blocked with PBSS plus 5% donkey serum. Primary and secondary antibodies were diluted in PBSS plus 10% blocking solution and applied for 1h or 30 min, respectively. Coverslips were mounted onto glass slides using ProLong Diamond Antifade Reagent with DAPI (Invitrogen) and dried at room temperature overnight.

11. Fluorescence Microscopy

Confocal microscopy was performed at the Bioimaging core facility of the Biomedical Center with an inverted Leica SP8, equipped with lasers for 405, 488, 552 and 638 nm excitation. Images were acquired using a 63x1.4 oil objective.

Acquired z-stacks were deconvolved using Hyugens Essential Software. Single z-planes were then adjusted for brightness in Fiji.

12. Antibodies

Name	Company
Fus (4H11)	Santa Cruz
Fus (A300-302)	Bethyl
Fus (A300-294)	Bethyl
Fus (19B2)	Ruepp Lab
Fus	Ruepp Lab
Fus (11570-1-AP)	Proteintech
Fus	Abcam
HuD (24992-1-AP)	Proteintech
Caprin2 (20766-1-AP)	Proteintech
Tia1	Santa Cruz
Sept2 (11397-1-AP)	Proteintech
Sept7 (18991)	IBL
HnRNPU1 (10578-1-AP)	Proteintech
Histone H3	Abcam
GAPDH (10F4)	Helmholtz Center Munich Antibody Core Facility
Alexa 488 Donkey anti-rabbit	Invitrogen
Alexa 488 Donkey anti-mouse	Invitrogen
Alexa 555 Donkey anti-rabbit	Invitrogen
Alexa 555 Donkey anti-mouse	Invitrogen
Alexa 647 Donkey anti-mouse	Invitrogen
Alexa 647 Donkey anti-rabbit	Invitrogen
Alexa 647 Donkey anti-goat	Invitrogen
IRDye 680RD Donkey anti-mouse IgG	LI-COR
IRDye 800VW Donkey anti-mouse IgG	LI-COR
IRDye 800VW Donkey anti-rabbit IgG	LI-COR

Table 6: Antibodies used in this thesis.

V. REFERENCES

- Ajrroud-Driss, Senda, and Teepu Siddique. 2014. "Sporadic and Hereditary Amyotrophic Lateral Sclerosis (ALS)." *BBA - Molecular Basis of Disease*, September. Elsevier B.V., 1–6. doi:10.1016/j.bbadis.2014.08.010.
- Anderson, Paul, and Nancy Kedersha. 2006. "RNA Granules.." *The Journal of Cell Biology* 172 (6): 803–8. doi:10.1083/jcb.200512082.
- Anderson, Paul, and Nancy Kedersha. 2008. "Stress Granules: the Tao of RNA Triage.." *Trends in Biochemical Sciences* 33 (3): 141–50. doi:10.1016/j.tibs.2007.12.003.
- Aoki, Naoya, Shinji Higashi, Ito Kawakami, Zen Kobayashi, Masato Hosokawa, Omi Katsuse, Takashi Togo, Yoshio Hirayasu, and Haruhiko Akiyama. 2012. "Localization of Fused in Sarcoma (FUS) Protein to the Post-Synaptic Density in the Brain." *Acta Neuropathologica* 124 (3): 383–94. doi:10.1007/s00401-012-0984-6.
- Armstrong, Gary A B, and Pierre Drapeau. 2013. "Calcium Channel Agonists Protect Against Neuromuscular Dysfunction in a Genetic Model of TDP-43 Mutation in ALS.." *The Journal of Neuroscience : the Official Journal of the Society for Neuroscience* 33 (4). Society for Neuroscience: 1741–52. doi:10.1523/JNEUROSCI.4003-12.2013.
- Arnold, Eveline S, Shuo-Chien Ling, Stephanie C Huelga, Clotilde Lagier-Tourenne, Magdalini Polymenidou, Dara Ditsworth, Holly B Kordasiewicz, et al. 2013. "ALS-Linked TDP-43 Mutations Produce Aberrant RNA Splicing and Adult-Onset Motor Neuron Disease Without Aggregation or Loss of Nuclear TDP-43.." *Proceedings of the National Academy of Sciences of the United States of America* 110 (8). National Acad Sciences: E736–45. doi:10.1073/pnas.1222809110.
- Atlas, Roe, Leah Behar, Evan Elliott, and Irith Ginzburg. 2004. "The Insulin-Like Growth Factor mRNA Binding-Protein IMP-1 and the Ras-Regulatory Protein G3BP Associate with Tau mRNA and HuD Protein in Differentiated P19 Neuronal Cells.." *Journal of Neurochemistry* 89 (3): 613–26. doi:10.1111/j.1471-4159.2004.02371.x.
- Aulas, Anaïs, Guillaume Caron, Christos G Gkogkas, Nguyen-Vi Mohamed, Laurie Destroismaisons, Nahum Sonenberg, Nicole Leclerc, J Alex Parker, and Christine Vande Velde. 2015. "G3BP1 Promotes Stress-Induced RNA Granule Interactions to Preserve Polyadenylated mRNA.." *The Journal of Cell Biology* 209 (1): 73–84. doi:10.1083/jcb.201408092.
- Aulas, Anaïs, Stéphanie Stabile, and Christine Vande Velde. 2012. "Endogenous TDP-43, but Not FUS, Contributes to Stress Granule Assembly via G3BP.." *Molecular Neurodegeneration* 7 (1): 54. doi:10.1186/1750-1326-7-54.
- Baker, Matt, Ian R Mackenzie, Stuart M Pickering-Brown, Jennifer Gass, Rosa Rademakers, Caroline Lindholm, Julie Snowden, et al. 2006. "Mutations in Progranulin Cause Tau-Negative Frontotemporal Dementia Linked to Chromosome 17." *Nature* 442 (7105): 916–19. doi:10.1038/nature05016.
- Baleriola, Jimena, Ying Jean, Carol Troy, and Ulrich Hengst. 2015. "Detection of Axonally Localized mRNAs in Brain Sections Using High-Resolution in Situ Hybridization.." *Journal of Visualized Experiments : JoVE*, no. 100 (June): e52799. doi:10.3791/52799.

- Bang, Jee, Salvatore Spina, and Bruce L Miller. 2015. "Frontotemporal Dementia." *The Lancet* 386 (10004): 1672–82. doi:10.1016/S0140-6736(15)00461-4.
- Baron, Desiree M, Laura J Kaushansky, Catherine L Ward, Reddy Ranjith K Sama, Ru-Ju Chian, Kristin J Boggio, Alexandre J C Quaresma, Jeffrey A Nickerson, and Daryl A Bosco. 2013. "Amyotrophic Lateral Sclerosis-Linked FUS/TLS Alters Stress Granule Assembly and Dynamics.." *Molecular Neurodegeneration* 8 (1): 30. doi:10.1186/1750-1326-8-30.
- Bäumer, D, D Hilton, S M L Paine, M R Turner, J Lowe, K Talbot, and O Ansorge. 2010. "Juvenile ALS with Basophilic Inclusions Is a FUS Proteinopathy with FUS Mutations.." *Neurology* 75 (7): 611–18. doi:10.1212/WNL.0b013e3181ed9cde.
- Belly, Agnès, Françoise Moreau-Gachelin, Rémy Sadoul, and Yves Goldberg. 2005. "Delocalization of the Multifunctional RNA Splicing Factor TLS/FUS in Hippocampal Neurons: Exclusion From the Nucleus and Accumulation in Dendritic Granules and Spine Heads." *Neuroscience Letters* 379 (3): 152–57. doi:10.1016/j.neulet.2004.12.071.
- Benajiba, Lina, Isabelle Le Ber, Agnès Camuzat, Mathieu Lacoste, Catherine Thomas-Anterion, Philippe Couratier, Solenn Legallic, et al. 2009. "TARDBP mutations in Motoneuron Disease with Frontotemporal Lobar Degeneration." *Annals of Neurology* 65 (4): 470–73. doi:10.1002/ana.21612.
- Bensimon, G, L Lacomblez, and V Meininger. 1994. "A Controlled Trial of Riluzole in Amyotrophic Lateral Sclerosis. ALS/Riluzole Study Group.." *The New England Journal of Medicine* 330 (9): 585–91. doi:10.1056/NEJM199403033300901.
- Bentmann, Eva, Manuela Neumann, Sabina Tahirovic, Ramona Rodde, Dorothee Dormann, and Christian Haass. 2012. "Requirements for Stress Granule Recruitment of Fused in Sarcoma (FUS) and TAR DNA-Binding Protein of 43 kDa (TDP-43).." *Journal of Biological Chemistry* 287 (27): 23079–94. doi:10.1074/jbc.M111.328757.
- Blechingberg, Jenny, Yonglun Luo, Lars Bolund, Christian Kroun Damgaard, and Anders Lade Nielsen. 2012. "Gene Expression Responses to FUS, EWS, and TAF15 Reduction and Stress Granule Sequestration Analyses Identifies FET-Protein Non-Redundant Functions.." Edited by Huaibin Cai. *PLoS One* 7 (9): e46251. doi:10.1371/journal.pone.0046251.
- Blokhuis, Anna M, Max Koppers, Ewout J N Groen, Dianne M A van den Heuvel, Stefano Dini Modigliani, Jasper J Anink, Katsumi Fumoto, et al. 2016. "Comparative Interactomics Analysis of Different ALS-Associated Proteins Identifies Converging Molecular Pathways." *Acta Neuropathologica*, May. Springer Berlin Heidelberg, 1–22. doi:10.1007/s00401-016-1575-8.
- Borroni, B, C Bonvicini, A Alberici, E Buratti, C Agosti, S Archetti, A Papetti, et al. 2009. "Mutation Within TARDBP leads to Frontotemporal Dementia Without Motor Neuron Disease." *Human Mutation* 30 (11): E974–83. doi:10.1002/humu.21100.
- Bowden, Hilary A, and Dorothee Dormann. 2016. "Altered mRNP Granule Dynamics in FTLD Pathogenesis." *Journal of Neurochemistry* 138 (June): 112–33. doi:10.1111/jnc.13601.
- Bramham, Clive R, and David G Wells. 2007. "Dendritic mRNA: Transport, Translation and Function.." *Nature Reviews. Neuroscience* 8 (10): 776–89. doi:10.1038/nrn2150.

- Buchan, J Ross, and Roy Parker. 2009. "Eukaryotic Stress Granules: the Ins and Outs of Translation.." *Molecular Cell* 36 (6): 932–41. doi:10.1016/j.molcel.2009.11.020.
- Buchan, J Ross, Andrew P Capaldi, and Roy Parker. 2012. "TOR-Tured Yeast Find a New Way to Stand the Heat.." *Molecular Cell* 47 (2): 155–57. doi:10.1016/j.molcel.2012.07.005.
- Buchan, J Ross, Denise Muhlrads, and Roy Parker. 2008. "P Bodies Promote Stress Granule Assembly in *Saccharomyces Cerevisiae*.." *The Journal of Cell Biology* 183 (3): 441–55. doi:10.1083/jcb.200807043.
- Burke, Kathleen A, Abigail M Janke, Christy L Rhine, and Nicolas L Fawzi. 2015. "Residue-by-Residue View of in&Nbsp;Vitro FUS Granules That Bind the C-Terminal Domain of RNA Polymerase II." *Molecular Cell*, October. Elsevier Inc., 1–12. doi:10.1016/j.molcel.2015.09.006.
- Buxbaum, Adina R, Bin Wu, and Robert H Singer. 2014. "Single B-Actin mRNA Detection in Neurons Reveals a Mechanism for Regulating Its Translatability.." *Science* 343 (6169): 419–22. doi:10.1126/science.1242939.
- Carlisle, Holly J, Pasquale Manzerra, Edoardo Marcora, and Mary B Kennedy. 2008. "SynGAP Regulates Steady-State and Activity-Dependent Phosphorylation of Cofilin.." *The Journal of Neuroscience : the Official Journal of the Society for Neuroscience* 28 (50): 13673–83. doi:10.1523/JNEUROSCI.4695-08.2008.
- Clement, James P, Massimiliano Aceti, Thomas K Creson, Emin D Ozkan, Yulin Shi, Nicholas J Reish, Antoine G Almonte, et al. 2012. "Pathogenic SYNGAP1 Mutations Impair Cognitive Development by Disrupting Maturation of Dendritic Spine Synapses.." *Cell* 151 (4): 709–23. doi:10.1016/j.cell.2012.08.045.
- Colombrita, Claudia, Elisa Onesto, Francesca Megiorni, Antonio Pizzuti, Francisco E Baralle, Emanuele Buratti, Vincenzo Silani, and Antonia Ratti. 2012. "TDP-43 and FUS RNA-Binding Proteins Bind Distinct Sets of Cytoplasmic Messenger RNAs and Differently Regulate Their Post-Transcriptional Fate in Motoneuron-Like Cells.." *Journal of Biological Chemistry* 287 (19): 15635–47. doi:10.1074/jbc.M111.333450.
- Cox, Jürgen, Marco Y Hein, Christian A Lubner, Igor Paron, Nagarjuna Nagaraj, and Matthias Mann. 2014. "Accurate Proteome-Wide Label-Free Quantification by Delayed Normalization and Maximal Peptide Ratio Extraction, Termed MaxLFQ.." *Molecular & Cellular Proteomics : MCP* 13 (9): 2513–26. doi:10.1074/mcp.M113.031591.
- Crozat, A, P Aman, N Mandahl, and D Ron. 1993. "Fusion of CHOP to a Novel RNA-Binding Protein in Human Myxoid Liposarcoma.." *Nature* 363 (6430): 640–44. doi:10.1038/363640a0.
- Cruts, Marc, Ilse Gijselinck, Julie van der Zee, Sebastiaan Engelborghs, Hans Wils, Daniel Pirici, Rosa Rademakers, et al. 2006. "Null Mutations in Progranulin Cause Ubiquitin-Positive Frontotemporal Dementia Linked to Chromosome 17q21." *Nature* 442 (7105): 920–24. doi:10.1038/nature05017.
- DeJesus-Hernandez, Mariely, Ian R Mackenzie, Bradley F Boeve, Adam L Boxer, Matt Baker, Nicola J Rutherford, Alexandra M Nicholson, et al. 2011. "Expanded GGGGCC Hexanucleotide Repeat in Noncoding Region of C9ORF72 Causes Chromosome 9p-Linked FTD and ALS." *Neuron* 72 (2): 245–56. doi:10.1016/j.neuron.2011.09.011.

- Devoy, Anny, Bernadett Kalmar, Michelle Stewart, Heesoon Park, Beverley Burke, Suzanna J Noy, Yushi Redhead, et al. 2017. "Humanized Mutant FUS Drives Progressive Motor Neuron Degeneration Without Aggregation in 'FUSDelta14' Knockin Mice." *Brain : a Journal of Neurology* 140 (11): 2797–2805. doi:10.1093/brain/awx248.
- Dormann, Dorothee, and Christian Haass. 2013. "Fused in Sarcoma (FUS): an Oncogene Goes Awry in Neurodegeneration." *Molecular and Cellular Neuroscience*, April. Elsevier Inc., 1–12. doi:10.1016/j.mcn.2013.03.006.
- Dormann, Dorothee, Ramona Rodde, Dieter Edbauer, Eva Bentmann, Ingeborg Fischer, Alexander Hruscha, Manuel E Than, et al. 2010. "ALS-Associated Fused in Sarcoma (FUS) Mutations Disrupt Transportin-Mediated Nuclear Import." *The EMBO Journal* 29 (16). Nature Publishing Group: 2841–57. doi:10.1038/emboj.2010.143.
- Dormann, Dorothee, Tobias Madl, Chiara F Valori, Eva Bentmann, Sabina Tahirovic, Claudia Abou-Ajram, Elisabeth Kremmer, et al. 2012. "Arginine Methylation Next to the PY-NLS Modulates Transportin Binding and Nuclear Import of FUS." *The EMBO Journal* 31 (22): 4258–75. doi:10.1038/emboj.2012.261.
- Doyle, Michael, and Michael A Kiebler. 2011. "Focus Review Mechanisms of Dendritic mRNA Transport and Its Role in Synaptic Tagging." *The EMBO Journal* 30 (17). Nature Publishing Group: 3540–52. doi:10.1038/emboj.2011.278.
- Dunah, Anthone W, Emily Hueske, Michael Wyszynski, Casper C Hoogenraad, Jacek Jaworski, Daniel T Pak, Alyson Simonetta, Guosong Liu, and Morgan Sheng. 2005. "LAR Receptor Protein Tyrosine Phosphatases in the Development and Maintenance of Excitatory Synapses.." *Nature Neuroscience* 8 (4): 458–67. doi:10.1038/nn1416.
- Erickson, Stacy L, and Jens Lykke-Andersen. 2011. "Cytoplasmic mRNP Granules at a Glance.." *Journal of Cell Science* 124 (Pt 3): 293–97. doi:10.1242/jcs.072140.
- Ewers, Helge, Tomoko Tada, Jennifer D Petersen, Bence Racz, Morgan Sheng, and Daniel Choquet. 2014. "A Septin-Dependent Diffusion Barrier at Dendritic Spine Necks.." Edited by Lin Mei. *PloS One* 9 (12): e113916. doi:10.1371/journal.pone.0113916.
- Fritzsche, Renate, Daniela Karra, Keiryn L Bennett, Foong yee Ang, Jacki E Heraud-Farlow, Marco Tolino, Michael Doyle, et al. 2013. "Interactome of Two Diverse RNA Granules Links mRNA Localization to Translational Repression in Neurons." *Cell Reports* 5 (6). The Authors: 1749–62. doi:10.1016/j.celrep.2013.11.023.
- Fujii, R. 2005. "TLS Facilitates Transport of mRNA Encoding an Actin-Stabilizing Protein to Dendritic Spines." *Journal of Cell Science* 118 (24): 5755–65. doi:10.1242/jcs.02692.
- Fujii, Ritsuko, Shigeo Okabe, Tomoe Urushido, Kiyoshi Inoue, Atsushi Yoshimura, Taro Tachibana, Toru Nishikawa, Geoffrey G Hicks, and Toru Takumi. 2005. "The RNA Binding Protein TLS Is Translocated to Dendritic Spines by mGluR5 Activation and Regulates Spine Morphology." *Current Biology* 15 (6): 587–93. doi:10.1016/j.cub.2005.01.058.
- Fujita, Yukio, Yuji Mizuno, Masamitsu Takatama, and Koichi Okamoto. 2008. "Anterior Horn Cells with Abnormal TDP-43 Immunoreactivities Show

- Fragmentation of the Golgi Apparatus in ALS." *Journal of the Neurological Sciences* 269 (1-2): 30–34. doi:10.1016/j.jns.2007.12.016.
- Funikov, Sergei Y, Alexander P Rezvykh, Pavel V Mazin, Alexey V Morozov, Andrey V Maltsev, Maria M Chicheva, Ekaterina A Vikhareva, Mikhail B Evgen'ev, and Aleksey A Ustyugov. 2018. "FUS(1-359) Transgenic Mice as a Model of ALS: Pathophysiological and Molecular Aspects of the Proteinopathy." *Neurogenetics* 19 (3): 189–204. doi:10.1007/s10048-018-0553-9.
- Ghasemi, Mehdi, and Robert H Brown Jr. 2018. "Genetics of Amyotrophic Lateral Sclerosis." *Cold Spring Harbor Perspectives in Medicine* 8 (5): a024125–38. doi:10.1101/cshperspect.a024125.
- Gilks, Natalie, Nancy Kedersha, Maranatha Ayodele, Lily Shen, Georg Stoecklin, Laura M Dember, and Paul Anderson. 2004. "Stress Granule Assembly Is Mediated by Prion-Like Aggregation of TIA-1." *Molecular Biology of the Cell* 15 (12): 5383–98. doi:10.1091/mbc.e04-08-0715.
- Halevi, Sarah, Jim McKay, Mark Palfreyman, Lina Yassin, Margalit Eshel, Erik Jorgensen, and Millet Treinin. 2002. "The C. Elegans Ric-3 Gene Is Required for Maturation of Nicotinic Acetylcholine Receptors." *The EMBO Journal* 21 (5): 1012–20. doi:10.1093/emboj/21.5.1012.
- Han, Jeong-Ho, Tae-Hoon Yu, Hyun-Hee Ryu, Mi-Hee Jun, Byung-Kwan Ban, Deok-Jin Jang, and Jin-A Lee. 2013. "ALS/FTLD-Linked TDP-43 Regulates Neurite Morphology and Cell Survival in Differentiated Neurons." *Experimental Cell Research* 319 (13): 1998–2005. doi:10.1016/j.yexcr.2013.05.025.
- Hengst, Ulrich, and Samie R Jaffrey. 2007. "Function and Translational Regulation of mRNA in Developing Axons." *Seminars in Cell & Developmental Biology* 18 (2): 209–15. doi:10.1016/j.semcd.2007.01.003.
- Hirokawa, Nobutaka. 2006. "mRNA Transport in Dendrites: RNA Granules, Motors, and Tracks." *The Journal of Neuroscience : the Official Journal of the Society for Neuroscience* 26 (27): 7139–42. doi:10.1523/JNEUROSCI.1821-06.2006.
- Hoell, Jessica I, Erik Larsson, Simon Runge, Jeffrey D Nusbaum, Sujitha Duggimpudi, Thalia A Farazi, Markus Hafner, Arndt Borkhardt, Chris Sander, and Thomas Tuschl. 2011. "RNA Targets of Wild-Type and Mutant FET Family Proteins." *Nature Structural & Molecular Biology* 18 (12): 1428–31. doi:10.1038/nsmb.2163.
- Hofweber, Mario, Saskia Hutten, Benjamin Bourgeois, Emil Spreitzer, Annika Niedner-Boblentz, Martina Schifferer, Marc-David Ruepp, et al. 2018. "Phase Separation of FUS Is Suppressed by Its Nuclear Import Receptor and Arginine Methylation." *Cell* 173 (3). Elsevier Inc.: 706–13. doi:10.1016/j.cell.2018.03.004.
- Holehouse, Alex S, and Rohit V Pappu. 2015. "Protein Polymers: Encoding Phase Transitions." *Nature Materials* 14 (11): 1083–84. doi:10.1038/nmat4459.
- Hughes, Christopher S, Sophie Moggridge, Torsten Müller, Poul H Sorensen, Gregg B Morin, and Jeroen Krijgsveld. 2019. "Single-Pot, Solid-Phase-Enhanced Sample Preparation for Proteomics Experiments." *Nature Protocols* 14 (1): 68–85. doi:10.1038/s41596-018-0082-x.
- Husi, Holger, Macolm A Ward, Jyoti S Choudharz, Walter P Blackstock, and Seth G N Grant. 2000. "Proteomic Analysis of NMDA Receptor-Adhesion Protein

- Signaling Complexes." *Nature Neuroscience* 3 (7): 1–9.
- Hutton, Mike, Corinne L Lendon, Patrizia Rizzu, Matt Baker, Susanne Froelich, Henry Houlden, Stuart Pickering-Brown, et al. 1998. "Association of Missense and 5'-Splice-Site Mutations in Tau with the Inherited Dementia FTDP-17." *Nature* 393 (6686): 702–5. doi:10.1038/31508.
- Hüttelmaier, Stefan, Daniel Zenklusen, Marcell Lederer, Jason Dichtenberg, Mike Lorenz, Xiuhua Meng, Gary J Bassell, John Condeelis, and Robert H Singer. 2005. "Spatial Regulation of Beta-Actin Translation by Src-Dependent Phosphorylation of ZBP1.." *Nature* 438 (7067): 512–15. doi:10.1038/nature04115.
- Ishigaki, Shinsuke, Akio Masuda, Yusuke Fujioka, Yohei Iguchi, Masahisa Katsuno, Akihito Shibata, Fumihiko Urano, Gen Sobue, and Kinji Ohno. 2012. "Position-Dependent FUS-RNA Interactions Regulate Alternative Splicing Events and Transcriptions.." *Scientific Reports* 2 (1): 529. doi:10.1038/srep00529.
- Jaworski, Jacek, Lukas C Kapitein, Susana Montenegro Gouveia, Bjorn R Dortland, Phebe S Wulf, Ilya Grigoriev, Paola Camera, et al. 2009. "Dynamic Microtubules Regulate Dendritic Spine Morphology and Synaptic Plasticity.." *Neuron* 61 (1): 85–100. doi:10.1016/j.neuron.2008.11.013.
- Jeyabalan, Nallathambi, and James P Clement. 2016. "SYNGAP1: Mind the Gap.." *Frontiers in Cellular Neuroscience* 10: 32. doi:10.3389/fncel.2016.00032.
- Kamelgarn, Marisa, Jing Chen, Lisha Kuang, Alexandra Arenas, Jianjun Zhai, Haining Zhu, and Jozsef Gal. 2016. "Proteomic Analysis of FUS Interacting Proteins Provides Insights Into FUS Function and Its Role in ALS.." *Biochimica Et Biophysica Acta* 1862 (10): 2004–14. doi:10.1016/j.bbadis.2016.07.015.
- Kamelgarn, Marisa, Jing Chen, Lisha Kuang, Huan Jin, Edward J Kasarskis, and Haining Zhu. 2018. "ALS Mutations of FUS Suppress Protein Translation and Disrupt the Regulation of Nonsense-Mediated Decay.." *Proceedings of the National Academy of Sciences of the United States of America* 115 (51): E11904–13. doi:10.1073/pnas.1810413115.
- Kanai, Yoshimitsu, Naoshi Dohmae, and Nobutaka Hirokawa. 2004. "Kinesin Transports RNA." *Neuron* 43 (4): 513–25. doi:10.1016/j.neuron.2004.07.022.
- Kaplan, Charlotte, Mayra Steinmann, Natalia A Zapiorkowska, and Helge Ewers. 2017. "Functional Redundancy of Septin Homologs in Dendritic Branching.." *Frontiers in Cell and Developmental Biology* 5: 11. doi:10.3389/fcell.2017.00011.
- Kato, Masato, Tina W Han, Shanhai Xie, Kevin Shi, Xinlin Du, Leeju C Wu, Hamid Mirzaei, et al. 2012. "Cell-Free Formation of RNA Granules: Low Complexity Sequence Domains Form Dynamic Fibers Within Hydrogels.." *Cell* 149 (4): 753–67. doi:10.1016/j.cell.2012.04.017.
- Kedersha, Nancy, Georg Stoecklin, Maranatha Ayodele, Patrick Yacono, Jens Lykke-Andersen, Marvin J Fritzler, Donalyn Scheuner, Randal J Kaufman, David E Golan, and Paul Anderson. 2005. "Stress Granules and Processing Bodies Are Dynamically Linked Sites of mRNP Remodeling.." *The Journal of Cell Biology* 169 (6): 871–84. doi:10.1083/jcb.200502088.
- Kennedy, Matthew J, and Michael D Ehlers. 2006. "Organelles and Trafficking Machinery for Postsynaptic Plasticity.." *Annual Review of Neuroscience* 29 (1): 325–62. doi:10.1146/annurev.neuro.29.051605.112808.

- Khan, Mohammed Repon, Liying Li, Consuelo Pérez-Sánchez, Anita Saraf, Laurence Florens, Brian D Slaughter, Jay R Unruh, and Kausik Si. 2015. "Amyloidogenic Oligomerization Transforms *Drosophila* Orb2 From a Translation Repressor to an Activator.." *Cell* 163 (6): 1468–83. doi:10.1016/j.cell.2015.11.020.
- Kiebler, Michael A, and Gary J Bassell. 2006. "Neuronal RNA Granules: Movers and Makers.." *Neuron* 51 (6): 685–90. doi:10.1016/j.neuron.2006.08.021.
- Kim, J H, D Liao, L F Lau, and R L Huganir. 1998. "SynGAP: a Synaptic RasGAP That Associates with the PSD-95/SAP90 Protein Family.." *Neuron* 20 (4): 683–91.
- Kim, Jee Hae, Hey-Kyoung Lee, Kogo Takamiya, and Richard L Huganir. 2003. "The Role of Synaptic GTPase-Activating Protein in Neuronal Development and Synaptic Plasticity.." *The Journal of Neuroscience : the Official Journal of the Society for Neuroscience* 23 (4): 1119–24.
- Kremer, Brandon E, Timothy Haystead, and Ian G Macara. 2005. "Mammalian Septins Regulate Microtubule Stability Through Interaction with the Microtubule-Binding Protein MAP4.." *Molecular Biology of the Cell* 16 (10): 4648–59. doi:10.1091/mbc.e05-03-0267.
- Krichevsky, A M, and K S Kosik. 2001. "Neuronal RNA Granules: a Link Between RNA Localization and Stimulation-Dependent Translation.." *Neuron* 32 (4): 683–96.
- Kwiatkowski, T J, D A Bosco, A L LeClerc, E Tamrazian, C R Vanderburg, C Russ, A Davis, et al. 2009. "Mutations in the FUS/TLS Gene on Chromosome 16 Cause Familial Amyotrophic Lateral Sclerosis." *Science* 323 (5918): 1205–8. doi:10.1126/science.1166066.
- Lagier-Tourenne, Clotilde, Magdalini Polymenidou, Kasey R Hutt, Anthony Q Vu, Michael Baughn, Stephanie C Huelga, Kevin M Clutario, et al. 2012. "Divergent Roles of ALS-Linked Proteins FUS/TLS and TDP-43 Intersect in Processing Long Pre-mRNAs." *Nature Neuroscience* 15 (11): 1488–97. doi:10.1038/nn.3230.
- Lang, Cynthia, Angel Barco, Leonard Zablow, Eric R Kandel, Steven A Siegelbaum, and Stanislav S Zakharenko. 2004. "Transient Expansion of Synaptically Connected Dendritic Spines Upon Induction of Hippocampal Long-Term Potentiation.." *Proceedings of the National Academy of Sciences* 101 (47): 16665–70. doi:10.1073/pnas.0407581101.
- Lee, Brittany J, Ahmet E Cansizoglu, Katherine E Süel, Thomas H Louis, Zichao Zhang, and Yuh Min Chook. 2006. "Rules for Nuclear Localization Sequence Recognition by Karyopherin β 2." *Cell* 126 (3): 543–58. doi:10.1016/j.cell.2006.05.049.
- Liguori, Rocco, Maria Pia Giannoccaro, Alessia Arnoldi, Andrea Citterio, Caterina Tonon, Raffaele Lodi, Nereo Bresolin, and Maria Teresa Bassi. 2014. "Impairment of Brain and Muscle Energy Metabolism Detected by Magnetic Resonance Spectroscopy in Hereditary Spastic Paraparesis Type 28 Patients with DDHD1 Mutations." *Journal of Neurology* 261 (9): 1789–93. doi:10.1007/s00415-014-7418-4.
- Lin, Yuan, David S W Protter, Michael K Rosen, and Roy Parker. 2015. "Formation and Maturation of Phase-Separated Liquid Droplets by RNA-Binding Proteins.." *Molecular Cell* 60 (2): 208–19. doi:10.1016/j.molcel.2015.08.018.
- Ling, Shuo-Chien, Magdalini Polymenidou, and Don W Cleveland. 2013.

- “Converging Mechanisms in ALS and FTD: Disrupted RNA and Protein Homeostasis.” *Neuron* 79 (3). Elsevier Inc.: 416–38. doi:10.1016/j.neuron.2013.07.033.
- Liu-Yesucevitz, L, A Y Lin, A Ebata, J Y Boon, W Reid, Y F Xu, K Kobrin, G J Murphy, L Petrucelli, and B Wolozin. 2014. “ALS-Linked Mutations Enlarge TDP-43-Enriched Neuronal RNA Granules in the Dendritic Arbor.” *Journal of Neuroscience* 34 (12): 4167–74. doi:10.1523/JNEUROSCI.2350-13.2014.
- Liu-Yesucevitz, Liqun, Aylin Bilgutay, Yong-Jie Zhang, Tara Vanderweyde, Tara Vanderwyde, Allison Citro, Tapan Mehta, et al. 2010. “Tar DNA Binding Protein-43 (TDP-43) Associates with Stress Granules: Analysis of Cultured Cells and Pathological Brain Tissue..” Edited by Ashley I Bush. *PloS One* 5 (10): e13250. doi:10.1371/journal.pone.0013250.
- López-Erauskin, Jone, Takahiro Tadokoro, Michael W Baughn, Brian Myers, Melissa McAlonis-Downes, Carlos Chillón-Marinas, Joshua N Asiaban, et al. 2018. “ALS/FTD-Linked Mutation in FUS Suppresses Intra-Axonal Protein Synthesis and Drives Disease Without Nuclear Loss-of-Function of FUS..” *Neuron* 100 (4): 816–17. doi:10.1016/j.neuron.2018.09.044.
- Lykens, Nicole M, David J Coughlin, Jyoti M Reddi, Gordon J Lutz, and Melanie K Tallent. 2017. “AMPA GluA1-Flip Targeted Oligonucleotide Therapy Reduces Neonatal Seizures and Hyperexcitability..” Edited by Giuseppe Biagini. *PloS One* 12 (2): e0171538. doi:10.1371/journal.pone.0171538.
- Mallardo, Massimo, Anke Deitinghoff, Juliane Müller, Bernhard Goetze, Paolo Macchi, Christopher Peters, and Michael A Kiebler. 2003. “Isolation and Characterization of Staufen-Containing Ribonucleoprotein Particles From Rat Brain..” *Proceedings of the National Academy of Sciences* 100 (4): 2100–2105. doi:10.1073/pnas.0334355100.
- McMahon, A C, M W Barnett, T S O'Leary, P N Stoney, M O Collins, S Papadia, J S Choudhary, et al. 2012. “SynGAP Isoforms Exert Opposing Effects on Synaptic Strength..” *Nature Communications* 3 (1): 900. doi:10.1038/ncomms1900.
- Meyerowitz, Jodi, Sarah J Parker, Laura J Vella, Dominic Ch Ng, Katherine A Price, Jeffrey R Liddell, Aphrodite Caragounis, et al. 2011. “C-Jun N-Terminal Kinase Controls TDP-43 Accumulation in Stress Granules Induced by Oxidative Stress..” *Molecular Neurodegeneration* 6 (1): 57. doi:10.1186/1750-1326-6-57.
- Mignot, Cyril, Celina von Stülpnagel, Caroline Nava, Dorothée Ville, Damien Sanlaville, Gaetan Lesca, Agnès Rastetter, et al. 2016. “Genetic and Neurodevelopmental Spectrum of SYNGAP1-Associated Intellectual Disability and Epilepsy..” *Journal of Medical Genetics* 53 (8): 511–22. doi:10.1136/jmedgenet-2015-103451.
- Mitchell, Sarah F, and Roy Parker. 2014. “Principles and Properties of Eukaryotic mRNPs..” *Molecular Cell* 54 (4): 547–58. doi:10.1016/j.molcel.2014.04.033.
- Molliex, Amandine, Jamshid Temirov, Jihun Lee, Maura Coughlin, Anderson P Kanagaraj, Hong Joo Kim, Tanja Mittag, and J Paul Taylor. 2015. “Phase Separation by Low Complexity Domains Promotes Stress Granule Assembly and Drives Pathological Fibrillization..” *Cell* 163 (1): 123–33. doi:10.1016/j.cell.2015.09.015.
- Moore, Melissa J, and Nick J Proudfoot. 2009. “Pre-mRNA Processing Reaches Back to Transcription and Ahead to Translation.” *Cell* 136 (4). Elsevier Inc.: 688–700. doi:10.1016/j.cell.2009.02.001.

- Mostowy, Serge, and Pascale Cossart. 2012. "Septins: the Fourth Component of the Cytoskeleton.." *Nature Publishing Group* 13 (3): 183–94. doi:10.1038/nrm3284.
- Murakami, Tetsuro, Seema Qamar, Julie Qiaojin Lin, Gabriele S Kaminski Schierle, Eric Rees, Akinori Miyashita, Ana R Costa, et al. 2015. "ALS/FTD Mutation-Induced Phase Transition of FUS Liquid Droplets and Reversible Hydrogels Into Irreversible Hydrogels Impairs RNP Granule Function." *Neuron*, October. The Authors, 1–14. doi:10.1016/j.neuron.2015.10.030.
- Nakaya, Tadashi, Panagiotis Alexiou, Manolis Maragkakis, Alexandra Chang, and Zissimos Mourelatos. 2013. "FUS Regulates Genes Coding for RNA-Binding Proteins in Neurons by Binding to Their Highly Conserved Introns.." *Rna* 19 (4): 498–509. doi:10.1261/rna.037804.112.
- Narayanan, Ramesh K, Marie Mangelsdorf, Ajay Panwar, Tim J Butler, Peter G Noakes, and Robyn H Wallace. 2013. "Identification of RNA Bound to the TDP-43 Ribonucleoprotein Complex in the Adult Mouse Brain.." *Amyotrophic Lateral Sclerosis & Frontotemporal Degeneration* 14 (4): 252–60. doi:10.3109/21678421.2012.734520.
- Neumann, M, D M Sampathu, L K Kwong, A C Truax, M C Micsenyi, T T Chou, J Bruce, et al. 2006. "Ubiquitinated TDP-43 in Frontotemporal Lobar Degeneration and Amyotrophic Lateral Sclerosis." *Science* 314 (5796): 130–33. doi:10.1126/science.1134108.
- Neumann, M, R Rademakers, S Roeber, M Baker, H A Kretzschmar, and I R A Mackenzie. 2009. "A New Subtype of Frontotemporal Lobar Degeneration with FUS Pathology." *Brain : a Journal of Neurology* 132 (11): 2922–31. doi:10.1093/brain/awp214.
- Nguyen, Hung Phuoc, Christine van Broeckhoven, and Julie van der Zee. 2018. "ALS Genes in the Genomic Era and Their Implications for FTD." *Trends in Genetics*, March. Elsevier Ltd, 1–20. doi:10.1016/j.tig.2018.03.001.
- Nussbaum, Justin, Qing Xu, Thomas J Payne, Jennie Z Ma, Weihua Huang, Joel Gelernter, and Ming D Li. 2008. "Significant Association of the Neurexin-1 Gene (NRXN1) with Nicotine Dependence in European- and African-American Smokers.." *Human Molecular Genetics* 17 (11): 1569–77. doi:10.1093/hmg/ddn044.
- Orozco, Denise, and Dieter Edbauer. 2013. "FUS-Mediated Alternative Splicing in the Nervous System: Consequences for ALS and FTLD.." *Journal of Molecular Medicine (Berlin, Germany)* 91 (12): 1343–54. doi:10.1007/s00109-013-1077-2.
- Ostareck-Lederer, Antje, Dirk H Ostareck, Christophe Cans, Gitte Neubauer, Karol Bomsztyk, Giulio Superti-Furga, and Matthias W Hentze. 2002. "C-Src-Mediated Phosphorylation of hnRNP K Drives Translational Activation of Specifically Silenced mRNAs.." *Molecular and Cellular Biology* 22 (13): 4535–43.
- Pak, ChangHui, Tamas Danko, Yingsha Zhang, Jason Aoto, Garret Anderson, Stephan Maxeiner, Fei Yi, Marius Wernig, and Thomas C Südhof. 2015. "Human Neuropsychiatric Disease Modeling Using Conditional Deletion Reveals Synaptic Transmission Defects Caused by Heterozygous Mutations in NRXN1." *Stem Cell*, August. Elsevier Ltd, 1–14. doi:10.1016/j.stem.2015.07.017.
- Park, Hye Yoon, Hyungsik Lim, Young J Yoon, Antonia Follenzi, Chiso Nwokafor,

- Melissa Lopez-Jones, Xiuhua Meng, and Robert H Singer. 2014. "Visualization of Dynamics of Single Endogenous mRNA Labeled in Live Mouse.." *Science* 343 (6169): 422–24. doi:10.1126/science.1239200.
- Park, Yong H, Heather V Broyles, Shaoqing He, Nolan R McGrady, Linya Li, and Thomas Yorio. 2016. "Involvement of AMPA Receptor and Its Flip and Flop Isoforms in Retinal Ganglion Cell Death Following Oxygen/Glucose Deprivation.." *Investigative Ophthalmology & Visual Science* 57 (2): 508–26. doi:10.1167/iovs.15-18481.
- Patel, Avinash, Hyun O Lee, Louise Jawerth, Shovamayee Maharana, Marcus Jahnel, Marco Y Hein, Stoyno Stoynov, et al. 2015. "A Liquid-to-Solid Phase Transition of the ALS Protein FUS Accelerated by Disease Mutation." *Cell* 162 (5). Elsevier Inc.: 1066–77. doi:10.1016/j.cell.2015.07.047.
- Pei, Weimin, Zhen Huang, Congzhou Wang, Yan Han, Jae Seon Park, and Li Niu. 2009. "Flip and Flop: a Molecular Determinant for AMPA Receptor Channel Opening †." *Biochemistry* 48 (17): 3767–77. doi:10.1021/bi8015907.
- Polymenidou, Magdalini, Clotilde Lagier-Tourenne, Kasey R Hutt, Stephanie C Huelga, Jacqueline Moran, Tiffany Y Liang, Shuo-Chien Ling, et al. 2011. "Long Pre-mRNA Depletion and RNA Missplicing Contribute to Neuronal Vulnerability From Loss of TDP-43." *Nature Publishing Group* 14 (4). Nature Publishing Group: 459–68. doi:10.1038/nn.2779.
- Puthanveetil, Sathyanarayanan V, Francisco J Monje, Maria Concetta Miniaci, Yun-Beom Choi, Kevin A Karl, Eugene Khandros, Mary Ann Gawinowicz, Michael P Sheetz, and Eric R Kandel. 2008. "A New Component in Synaptic Plasticity: Upregulation of Kinesin in the Neurons of the Gill-Withdrawal Reflex.." *Cell* 135 (5): 960–73. doi:10.1016/j.cell.2008.11.003.
- Rabbits, T H, A Forster, R Larson, and P Nathan. 1993. "Fusion of the Dominant Negative Transcription Regulator CHOP with a Novel Gene FUS by Translocation T(12;16) in Malignant Liposarcoma.." *Nature Genetics* 4 (2): 175–80. doi:10.1038/ng0693-175.
- Rademakers, Rosa, Manuela Neumann, and Ian R Mackenzie. 2012. "Advances in Understanding the Molecular Basis of Frontotemporal Dementia." *Nature Reviews Neurology* 8 (8): 423–34. doi:10.1038/nrneurol.2012.117.
- Reber, Stefan, Jolanda Stettler, Giuseppe Filosa, Martino Colombo, Daniel Jutzi, Silvia C Lenzken, Christoph Schweingruber, et al. 2016. "Minor Intron Splicing Is Regulated by FUS and Affected by ALS-Associated FUS Mutants.." *The EMBO Journal* 35 (14): 1504–21. doi:10.15252/embj.201593791.
- Rempel, N, S Heyers, H Engels, E Sleegers, and O K Steinlein. 1998. "The Structures of the Human Neuronal Nicotinic Acetylcholine Receptor Beta2- and Alpha3-Subunit Genes (CHRNA3 and CHRNB2).." *Human Genetics* 103 (6): 645–53.
- Renton, Alan E, Elisa Majounie, Adrian Waite, Javier Simón-Sánchez, Sara Rollinson, J Raphael Gibbs, Jennifer C Schymick, et al. 2011. "A Hexanucleotide Repeat Expansion in C9ORF72 Is the Cause of Chromosome 9p21-Linked ALS-FTD." *Neuron* 72 (2): 257–68. doi:10.1016/j.neuron.2011.09.010.
- Ringholz, G M, S H Appel, M Bradshaw, N A Cooke, D M Mosnik, and P E Schulz. 2005. "Prevalence and Patterns of Cognitive Impairment in Sporadic ALS.." *Neurology* 65 (4): 586–90. doi:10.1212/01.wnl.0000172911.39167.b6.
- Rogelj, Boris, Laura E Easton, Gireesh K Bogu, Lawrence W Stanton, Gregor Rot,

- Tomaž Curk, Blaž Zupan, et al. 2012. "Widespread Binding of FUS Along Nascent RNA Regulates Alternative Splicing in the Brain.." *Scientific Reports* 2 (1): 603. doi:10.1038/srep00603.
- Rosen, D R, T Siddique, D Patterson, D A Figlewicz, P Sapp, A Hentati, D Donaldson, J Goto, J P O'Regan, and H X Deng. 1993. "Mutations in Cu/Zn Superoxide Dismutase Gene Are Associated with Familial Amyotrophic Lateral Sclerosis.." *Nature* 362 (6415): 59–62. doi:10.1038/362059a0.
- Sama, Reddy Ranjith K, Catherine L Ward, Laura J Kaushansky, Nathan Lemay, Shinsuke Ishigaki, Fumihiko Urano, and Daryl A Bosco. 2013. "FUS/TLS Assembles Into Stress Granules and Is a Prosurvival Factor During Hyperosmolar Stress.." *Journal of Cellular Physiology* 228 (11): 2222–31. doi:10.1002/jcp.24395.
- Scekic-Zahirovic, Jelena, Hajer El Oussini, Sina Mersmann, Kevin Drenner, Marina Wagner, Ying Sun, Kira Allmeroth, et al. 2017. "Motor Neuron Intrinsic and Extrinsic Mechanisms Contribute to the Pathogenesis of FUS-Associated Amyotrophic Lateral Sclerosis.." *Acta Neuropathologica* 133 (6): 887–906. doi:10.1007/s00401-017-1687-9.
- Scekic-Zahirovic, Jelena, Oliver Sendscheid, Hajer El Oussini, Mélanie Jambeau, Ying Sun, Sina Mersmann, Marina Wagner, et al. 2016. "Toxic Gain of Function From Mutant FUS Protein Is Crucial to Trigger Cell Autonomous Motor Neuron Loss.." *The EMBO Journal* 35 (10): 1077–97. doi:10.15252/embj.201592559.
- Schoen, Michael, Jochen M Reichel, Maria Demestre, Stefan Putz, Dhruva Deshpande, Christian Proepper, Stefan Liebau, et al. 2015. "Super-Resolution Microscopy Reveals Presynaptic Localization of the ALS/FTD Related Protein FUS in Hippocampal Neurons.." *Frontiers in Cellular Neuroscience* 9 (107): 496. doi:10.3389/fncel.2015.00496.
- Sephton, C F, A A Tang, A Kulkarni, J West, M Brooks, J J Stubblefield, Y Liu, et al. 2014. "Activity-Dependent FUS Dysregulation Disrupts Synaptic Homeostasis." *Proceedings of the National Academy of Sciences* 111 (44): E4769–78. doi:10.1073/pnas.1406162111.
- Sharma, Aarti, Alexander K Lyashchenko, Lei Lu, Sara Ebrahimi Nasrabady, Margot Elmaleh, Monica Mendelsohn, Adriana Nemes, Juan Carlos Tapia, George Z Mentis, and Neil A Shneider. 2016. "ALS-Associated Mutant FUS Induces Selective Motor Neuron Degeneration Through Toxic Gain of Function.." *Nature Communications* 7 (1): 10465. doi:10.1038/ncomms10465.
- Shevchenko, Andrej, Henrik Tomas, Jan Havlis, Jesper V Olsen, and Matthias Mann. 2006. "In-Gel Digestion for Mass Spectrometric Characterization of Proteins and Proteomes.." *Nature Protocols* 1 (6): 2856–60. doi:10.1038/nprot.2006.468.
- Shin, Yongdae, and Clifford P Brangwynne. 2017. "Liquid Phase Condensation in Cell Physiology and Disease.." *Science* 357 (6357): eaaf4382. doi:10.1126/science.aaf4382.
- Si, Kausik, Yun-Beom Choi, Erica White-Grindley, Amitabha Majumdar, and Eric R Kandel. 2010. "Aplysia CPEB Can Form Prion-Like Multimers in Sensory Neurons That Contribute to Long-Term Facilitation.." *Cell* 140 (3): 421–35. doi:10.1016/j.cell.2010.01.008.
- Sommer, B, K Keinänen, T A Verdoorn, W Wisden, N Burnashev, A Herb, M

- Köhler, T Takagi, B Sakmann, and P H Seeburg. 1990. "Flip and Flop: a Cell-Specific Functional Switch in Glutamate-Operated Channels of the CNS.." *Science* 249 (4976): 1580–85.
- Suárez-Calvet, Marc, Manuela Neumann, Thomas Arzberger, Claudia Abou-Ajram, Eva Funk, Hannelore Hartmann, Dieter Edbauer, et al. 2016. "Monomethylated and Unmethylated FUS Exhibit Increased Binding to Transportin and Distinguish FTLD-FUS From ALS-FUS.." *Acta Neuropathologica* 131 (4): 587–604. doi:10.1007/s00401-016-1544-2.
- Sun, Shuying, Shuo-Chien Ling, Jinsong Qiu, Claudio P Albuquerque, Yu Zhou, Seiya Tokunaga, Hairi Li, et al. 2015. "ALS-Causative Mutations in FUS/TLS Confer Gain and Loss of Function by Altered Association with SMN and U1-snRNP." *Nature Communications* 6 (January). Nature Publishing Group: 1–14. doi:10.1038/ncomms7171.
- Sun, Zhihui, Zamia Diaz, Xiaodong Fang, Michael P Hart, Alessandra Chesi, James Shorter, and Aaron D Gitler. 2011. "Molecular Determinants and Genetic Modifiers of Aggregation and Toxicity for the ALS Disease Protein FUS/TLS." Edited by Jonathan S Weissman. *PLoS Biology* 9 (4): e1000614–26. doi:10.1371/journal.pbio.1000614.
- Takahara, Terunao, and Tatsuya Maeda. 2012. "Transient Sequestration of TORC1 Into Stress Granules During Heat Stress.." *Molecular Cell* 47 (2): 242–52. doi:10.1016/j.molcel.2012.05.019.
- Takei, Koji, Kazutoshi Watanabe, Satoshi Yuki, Makoto Akimoto, Takeshi Sakata, and Joseph Palumbo. 2017. "Edaravone and Its Clinical Development for Amyotrophic Lateral Sclerosis." *Amyotrophic Lateral Sclerosis & Frontotemporal Degeneration* 18 (sup1): 5–10. doi:10.1080/21678421.2017.1353101.
- Tan, Adelene Y, Todd R Riley, Tristan Coady, Harmen J Bussemaker, and James L Manley. 2012. "TLS/FUS (Translocated in Liposarcoma/Fused in Sarcoma) Regulates Target Gene Transcription via Single-Stranded DNA Response Elements.." *Proceedings of the National Academy of Sciences of the United States of America* 109 (16): 6030–35. doi:10.1073/pnas.1203028109.
- Tashiro, Yoshitaka, Makoto Urushitani, Haruhisa Inoue, Masato Koike, Yasuo Uchiyama, Masaaki Komatsu, Keiji Tanaka, et al. 2012. "Motor Neuron-Specific Disruption of Proteasomes, but Not Autophagy, Replicates Amyotrophic Lateral Sclerosis.." *Journal of Biological Chemistry* 287 (51): 42984–94. doi:10.1074/jbc.M112.417600.
- Taylor, J Paul, Robert H Brown, and Don W Cleveland. 2016. "Decoding ALS: From Genes to Mechanism." *Nature* 539 (7628): 197–206. doi:10.1038/nature20413.
- Temburni, M K. 2004. "Neuronal Nicotinic Synapse Assembly Requires the Adenomatous Polyposis Coli Tumor Suppressor Protein." *Journal of Neuroscience* 24 (30): 6776–84. doi:10.1523/JNEUROSCI.1826-04.2004.
- Thomas, María G, Leandro J Martinez Tosar, Mariela Loschi, Juana M Pasquini, Jorge Correale, Stefan Kindler, and Graciela L Boccaccio. 2005. "Staufen Recruitment Into Stress Granules Does Not Affect Early mRNA Transport in Oligodendrocytes.." *Molecular Biology of the Cell* 16 (1): 405–20. doi:10.1091/mbc.e04-06-0516.
- Tompa, Peter, Norman E Davey, Toby J Gibson, and M Madan Babu. 2014. "A Million Peptide Motifs for the Molecular Biologist.." *Molecular Cell* 55 (2):

- 161–69. doi:10.1016/j.molcel.2014.05.032.
- Tushev, Georgi, Caspar Glock, Maximilian Heumüller, Anne Bieber, Marko Jovanovic, and Erin M Schuman. 2018. “Alternative 3' UTRs Modify the Localization, Regulatory Potential, Stability, and Plasticity of mRNAs in Neuronal Compartments..” *Neuron* 98 (3): 495–96. doi:10.1016/j.neuron.2018.03.030.
- Udagawa, Tsuyoshi, Yusuke Fujioka, Motoki Tanaka, Daiyu Honda, Satoshi Yokoi, Yuichi Riku, Daisuke Ibi, et al. 2015. “FUS Regulates AMPA Receptor Function and FTL/ALS-Associated Behaviour via GluA1 mRNA Stabilization.” *Nature Communications* 6 (May). Nature Publishing Group: 1–13. doi:10.1038/ncomms8098.
- van Blitterswijk, Marka, Bianca Mullen, Aleksandra Wojtas, Michael G Heckman, Nancy N Diehl, Matthew C Baker, Mariely DeJesus-Hernandez, et al. 2014. “Genetic Modifiers in Carriers of Repeat Expansions in the C9ORF72 Gene..” *Molecular Neurodegeneration* 9 (1): 38. doi:10.1186/1750-1326-9-38.
- van Es MD, Michael A, Prof Orla Hardiman MD, Prof Adriano Chio MD, Prof Ammar Al-Chalabi MD, Prof R Jeroen Pasterkamp PhD, Prof Jan H Veldink MD, and Prof Leonard H van den Berg MD. 2017. “Amyotrophic Lateral Sclerosis.” *The Lancet* 390 (10107). Elsevier Ltd: 2084–98. doi:10.1016/S0140-6736(17)31287-4.
- van Langenhove, Tim, Julie van der Zee, and Christine van Broeckhoven. 2011. “The Molecular Basis of the Frontotemporal Lobar Degeneration–Amyotrophic Lateral Sclerosis Spectrum.” *Annals of Medicine* 44 (8): 817–28. doi:10.3109/07853890.2012.665471.
- Van Lieshout, E M, I Van der Heijden, W J Hendriks, and C E Van der Zee. 2001. “A Decrease in Size and Number of Basal Forebrain Cholinergic Neurons Is Paralleled by Diminished Hippocampal Cholinergic Innervation in Mice Lacking Leukocyte Common Antigen-Related Protein Tyrosine Phosphatase Activity..” *Neuroscience* 102 (4): 833–41.
- Vance, Caroline, Boris Rogelj, Tibor Hortobagyi, Kurt J De Vos, Agnes Lumi Nishimura, Jemeen Sreedharan, Xun Hu, et al. 2009. “Mutations in FUS, an RNA Processing Protein, Cause Familial Amyotrophic Lateral Sclerosis Type 6..” *Science* 323 (5918): 1208–11. doi:10.1126/science.1165942.
- Vance, Caroline, Emma L Scotter, Agnes L Nishimura, Claire Troakes, Jacqueline C Mitchell, Claudia Kathe, Hazel Urwin, et al. 2013. “ALS Mutant FUS Disrupts Nuclear Localization and Sequesters Wild-Type FUS Within Cytoplasmic Stress Granules..” *Human Molecular Genetics* 22 (13): 2676–88. doi:10.1093/hmg/ddt117.
- Vanderweyde, Tara, Haung Yu, Megan Varnum, Liqun Liu-Yesucevitz, Allison Citro, Tsuneya Ikezu, Karen Duff, and Benjamin Wolozin. 2012. “Contrasting Pathology of the Stress Granule Proteins TIA-1 and G3BP in Tauopathies..” *The Journal of Neuroscience : the Official Journal of the Society for Neuroscience* 32 (24): 8270–83. doi:10.1523/JNEUROSCI.1592-12.2012.
- Vessey, John P, Angelo Vaccani, Yunli Xie, Ralf Dahm, Daniela Karra, Michael A Kiebler, and Paolo Macchi. 2006. “Dendritic Localization of the Translational Repressor Pumilio 2 and Its Contribution to Dendritic Stress Granules..” *The Journal of Neuroscience : the Official Journal of the Society for Neuroscience* 26 (24): 6496–6508. doi:10.1523/JNEUROSCI.0649-06.2006.
- Walker, Adam K, Kai Y Soo, Vinod Sundaramoorthy, Sonam Parakh, Yi Ma, Manal

- A Farg, Robyn H Wallace, et al. 2013. "ALS-Associated TDP-43 Induces Endoplasmic Reticulum Stress, Which Drives Cytoplasmic TDP-43 Accumulation and Stress Granule Formation.." Edited by Weidong Le. *PLoS One* 8 (11): e81170. doi:10.1371/journal.pone.0081170.
- Wang, Chih-Chieh, Richard G Held, and Benjamin J Hall. 2013. "SynGAP Regulates Protein Synthesis and Homeostatic Synaptic Plasticity in Developing Cortical Networks.." Edited by Laurent Groc. *PLoS One* 8 (12): e83941. doi:10.1371/journal.pone.0083941.
- Wang, Jie, Jeong-Mo Choi, Alex S Holehouse, Hyun O Lee, Xiaojie Zhang, Marcus Jahnel, Shovamayee Maharana, et al. 2018. "A Molecular Grammar Governing the Driving Forces for Phase Separation of Prion-Like RNA Binding Proteins.." *Cell* 174 (3): 688–699.e16. doi:10.1016/j.cell.2018.06.006.
- Wang, Ming-Dong, Julian Little, James Gomes, Neil R Cashman, and Daniel Krewski. 2017. "Identification of Risk Factors Associated with Onset and Progression of Amyotrophic Lateral Sclerosis Using Systematic Review and Meta-Analysis.." *Neurotoxicology* 61 (July): 101–30. doi:10.1016/j.neuro.2016.06.015.
- Wang, Tao, Xin Jiang, Gang Chen, and Jin Xu. 2015. "Interaction of Amyotrophic Lateral Sclerosis/Frontotemporal Lobar Degeneration-Associated Fused-in-Sarcoma with Proteins Involved in Metabolic and Protein Degradation Pathways.." *Neurobiology of Aging* 36 (1): 527–35. doi:10.1016/j.neurobiolaging.2014.07.044.
- Weber, Stephanie C, and Clifford P Brangwynne. 2012. "Getting RNA and Protein in Phase.." *Cell* 149 (6): 1188–91. doi:10.1016/j.cell.2012.05.022.
- Wheaton, M W, A R Salamone, D M Mosnik, R O McDonald, S H Appel, H I Schmolck, G M Ringholz, and P E Schulz. 2007. "Cognitive Impairment in Familial ALS.." *Neurology* 69 (14): 1411–17. doi:10.1212/01.wnl.0000277422.11236.2c.
- Wu, Chujun, and Dongsheng Fan. 2016. "A Novel Missense Mutation of the DDHD1 Gene Associated with Juvenile Amyotrophic Lateral Sclerosis." *Frontiers in Aging Neuroscience* 8 (December): 913–15. doi:10.3389/fnagi.2016.00291.
- Yan, Xiaowei, Tim A Hoek, Ronald D Vale, and Marvin E Tanenbaum. 2016. "Dynamics of Translation of Single mRNA Molecules in Vivo.." *Cell* 165 (4): 976–89. doi:10.1016/j.cell.2016.04.034.
- Yang, L, L J Embree, S Tsai, and D D Hickstein. 1998. "Oncoprotein TLS Interacts with Serine-Arginine Proteins Involved in RNA Splicing.." *Journal of Biological Chemistry* 273 (43): 27761–64.
- Yang, Liuqing, Jozsef Gal, Jing Chen, and Haining Zhu. 2014. "Self-Assembled FUS Binds Active Chromatin and Regulates Gene Transcription.." *Proceedings of the National Academy of Sciences of the United States of America* 111 (50): 17809–14. doi:10.1073/pnas.1414004111.
- Yin, Yong, Jeffrey H Miner, and Joshua R Sanes. 2002. "Laminets: Laminin- and Netrin-Related Genes Expressed in Distinct Neuronal Subsets.." *Molecular and Cellular Neuroscience* 19 (3): 344–58. doi:10.1006/mcne.2001.1089.
- Yokoi, Satoshi, Tsuyoshi Udagawa, Yusuke Fujioka, Daiyu Honda, Haruo Okado, Hirohisa Watanabe, Masahisa Katsuno, Shinsuke Ishigaki, and Gen Sobue. 2017. "3'UTR Length-Dependent Control of SynGAP Isoform A2 mRNA by FUS and ELAV-Like Proteins Promotes Dendritic Spine Maturation and

- Cognitive Function.." *Cell Reports* 20 (13): 3071–84.
doi:10.1016/j.celrep.2017.08.100.
- Yoshimura, Atsushi, Ritsuko Fujii, Yasuhito Watanabe, Shigeo Okabe, Kenji Fukui, and Toru Takumi. 2006. "Myosin-Va Facilitates the Accumulation of mRNA/Protein Complex in Dendritic Spines." *Current Biology* 16 (23): 2345–51. doi:10.1016/j.cub.2006.10.024.
- Zhang, G, T A Neubert, and B A Jordan. 2012. "RNA Binding Proteins Accumulate at the Postsynaptic Density with Synaptic Activity." *Journal of Neuroscience* 32 (2): 599–609. doi:10.1523/JNEUROSCI.2463-11.2012.
- Zhou, Yueqin, Songyan Liu, Guodong Liu, Arzu Oztürk, and Geoffrey G Hicks. 2013. "ALS-Associated FUS Mutations Result in Compromised FUS Alternative Splicing and Autoregulation.." Edited by Hamish S Scott. *PLoS Genetics* 9 (10): e1003895. doi:10.1371/journal.pgen.1003895.

VI. ACKNOWLEDGEMENTS

Although many are due a wealth of gratitude for helping me reach this point, there are a few I would like to especially thank.

I would like to thank my advisor, Dorothee Dormann, for her leadership and advice. I would like to thank my committee, Michael Kiebler, Stefan Lichtenthaler and Dieter Edbauer, for helpful advice and mentorship during my time as a student. Saskia Hutten has been a fantastic source of both knowledge and support. Thank you to the Dormann lab members for scientific comradery and members of the Kiebler lab for allowing me to constantly annoy them with questions (and a special shout out to Christine Illig, Sandra Fernandez Moya, Inma Segura and Sabine Thomas).

Thank you to David Housman for his wise advice, interesting conversation and, most of all, for believing in me.

Thanks to the GSN, especially Lena Bittl and Conny Kopp-Scheinflug, for all of their support.

Finally, I would like to thank three very important people in my life, two unwilling and one willing participant in this PhD journey. First, my husband, who has been an amazing support and reminds me where I put my head whenever I have misplaced it. Second, my daughters, Leia and Ayla, whose love, silliness and smiles make the complexities of PhD and motherhood completely worth it.

VIII. DECLARATION OF COPYRIGHT AND CONTRIBUTIONS

Hilary Wunderlich wrote the thesis text, performed most experiments and prepared most of the figures (see section “ Results - Declaration of contributions” for detailed listing of exceptions).

Dorothee Dormann, supervisor and lab head, developed the design of the project and coordinated involved collaborators (e.g. communication with collaborators, exchange of mice and expression vectors), she functions as a representative for contributing collaborators and facilities:

1. Luc Dupuis, Strasbourg, kindly provided the FUS^{ΔNLS/+} mouse model.
2. Stephan Mueller and Stefan Lichtenthaler, DZNE Munich, performed the sample preparation, LC/MS-MS.
3. cDNA library preparation and RNA Sequencing was performed by Laboratory for Functional Genome Analysis (LAFUGA) at the Gene Center Munich.
4. RNA Sequencing Analysis was performed in collaboration with Tobias Straub of the Biomedical Center, LMU.
5. Diana Wiesner (University of Ulm) provided mouse cortices.

Date, Place

Hilary Wunderlich

Date, Place

Dorothee Dormann

